

1 **Temperature-enhanced effects of iron on Southern Ocean phytoplankton**

2

3 Charlotte Eich^{†,1,2,*}, Mathijs van Manen^{†,3}, J. Scott P. McCain^{4,5}, Loay J. Jabre^{4,6}, Willem H. v.d. Poll⁷, Jinyoung
4 Jung⁸, Sven B. E. H. Pont¹, Hung-An Tian³, Indah Ardiningsih³, Gert-Jan Reichart^{3,9}, Erin M. Bertrand⁴, Corina
5 P.D. Brussaard^{1,2,*}, Rob Middag^{3, 10}

6

7 [†]These authors contributed equally to this work.

8 Affiliations:

9 ¹Department of Marine Microbiology and Biogeochemistry, NIOZ Royal Netherlands Institute for Sea Research,
10 1797 SZ 't Horntje, The Netherlands

11 ²Institute for Biodiversity and Ecosystem Dynamics (IBED), University of Amsterdam, 1098 XH Amsterdam,
12 The Netherlands

13 ³Department of Ocean Systems, NIOZ Royal Netherlands Institute for Sea Research, 1797 SZ 't Horntje, The
14 Netherlands

15 ⁴Department of Biology, Dalhousie University, Halifax, Nova Scotia, Canada

16 ⁵Current Address: Department of Biology and Department of Earth, Atmospheric, and Planetary Sciences,
17 Massachusetts Institute of Technology, Cambridge, MA 02142, USA

18 ⁶Current Address: Marine Chemistry & Geochemistry Department, Woods Hole Oceanographic Institution,
19 Woods Hole, MA 02543, USA

20 ⁷CIO Oceans, Energy and Sustainability Research Institute Groningen, Faculty of Science and Engineering,
21 University of Groningen, Nijenborgh 7, Groningen, AG 9747, The Netherlands.

22 ⁸Korea Polar Research Institute, 26, Songdomirae-ro, Yeonsu-gu, Incheon 21990, Republic of Korea

23 ⁹Department of Earth Sciences, Faculty of Geosciences, Utrecht University, Utrecht, the Netherlands

24 ¹⁰Centre for Isotope Research-Oceans, Energy and Sustainability Research Institute Groningen, Faculty of Science
25 and Engineering, University of Groningen, 9712 CP Groningen, The Netherlands

26

27 *Correspondence to: Charlotte Eich (charlotte.eich@nioz.nl) & Corina Brussaard (corina.brussaard@nioz.nl)

28

29 **Short summary**

30 Phytoplankton growth in the Southern Ocean (SO) is often limited by low iron (Fe) concentrations. Sea surface
31 warming impacts Fe availability and can affect phytoplankton growth. We used Fe clean shipboard incubations
32 to test how changes in Fe and temperature affect SO phytoplankton. Their abundances usually increased with Fe
33 addition and temperature increase, with Fe being the major factor. These findings imply potential shifts in
34 ecosystem structure, impacting food webs and elemental cycling.

35

36 **Abstract**

37 Iron (Fe) is a key limiting nutrient for Southern Ocean phytoplankton. Input of Fe into the Southern Ocean is
38 projected to change due to global warming, yet the combined effects of a concurrent increase in temperature with
39 dissolved Fe (dFe) addition on phytoplankton growth and community composition are understudied. To improve
40 our understanding of how Antarctic phytoplankton communities respond to Fe and enhanced temperature, we
41 performed four full factorial onboard bioassays under trace metal clean conditions with phytoplankton
42 communities from different regions of the Weddell and the Amundsen Seas in the Southern Ocean. Treatments
43 consisted of a combined 2 nM Fe addition with 2 °C warming treatment (TF), compared to the single factor
44 treatments of Fe addition at *in-situ* temperature (F), and non-Fe addition at + 2 °C (T) and at *in-situ* temperature
45 (C). Temperature had limited effect by itself but boosted the positive response of the phytoplankton to Fe addition.
46 Photosynthetic efficiency, phytoplankton abundances, and chlorophyll *a* concentrations typically increased
47 (significantly) with Fe addition (F and/or TF treatments) and the phytoplankton community generally shifted from
48 haptophytes to diatoms upon Fe addition. The < 20 µm phytoplankton fraction displayed population-specific
49 growth responses, resulting in a pronounced shift in community composition and size distribution (mainly towards
50 larger-sized phytoplankton) for the F and TF treatment. Such distinct enhanced impact of dFe supply with
51 warming on Antarctic phytoplankton size, growth and composition will likely affect trophic transfer efficiency
52 and ecosystem structure, with potential significance for the biological carbon pump.

53

54 Keywords: Antarctic algae, bioassays, size-fractionation, climate change, trace metals

55 1. Introduction

56 The Southern Ocean plays an important role in regulating the Earth's climate as it is an important sink for CO₂
57 (Takahashi et al., 2012; Friedlingstein et al., 2022; Fisher et al., 2023). Phytoplankton take up CO₂ and convert it
58 to biomass, forming not only the base of the pelagic food web but also driving the biological carbon pump
59 (Buesseler et al., 2020; Huang et al., 2023). During the short austral productive season, however, Antarctic
60 phytoplankton growth often becomes limited by low iron (Fe) availability (e.g., Martin et al., 1990; Boyd, 2002;
61 Ryan-Keogh et al., 2023). Fe is a vital micronutrient for a variety of cellular processes, including photosynthesis
62 (Geider & La Roche, 1994; Schoffman et al., 2016; Kroh & Pilon, 2020) and nitrate assimilation (Schoffman et
63 al., 2016, Milligan and Harrison, 2000). Shortage of Fe results in so called high nutrient, low chlorophyll (HNLC)
64 conditions, where the ratio of macronutrients, especially nitrate, relative to total Chlorophyll *a* (Chl *a*)
65 concentrations is comparably high (Minas & Minas, 1992; Sarmiento et al., 2004; Venables & Moore, 2010;
66 Basterretxea et al., 2023).

67 Trace metal supply in the Southern Ocean follows a strong seasonal cycle where in winter Fe is replenished via
68 deep water-mixing (Tagliabue et al., 2014) or sediment resuspension in coastal areas (Boyd et al., 2012), but this
69 supply is to be quickly depleted again by phytoplankton uptake in the next season. Predicted increases in
70 stratification may weaken Fe supply to surface waters from below (Sallée et al. 2011), however, this is still
71 uncertain as increased stratification might not have a strong effect or might even increase turbulent nutrient fluxes
72 associated with breaking internal waves (van Haren et al., 2020). Additionally, increased stratification effects may
73 be counteracted by a deepening of mixed layer depths (Sallée et al., 2021) and changes in gyre-scale circulations
74 (Misumi et al., 2013). In general, However, Fe limitation for Antarctic phytoplankton is predicted to be at least
75 partially relieved in the future (Bazzani et al., 2023) because of enhanced Fe supply by increased wind driven
76 mixing (due to reduced ice-induced stratification) and sources associated with ice melt, i.e., glaciers (Annett et
77 al., 2015; Sherrell et al., 2015; Van der Merwe et al., 2019; ~~L~~-Seyitmuhammedov et al., 2022, Moreau et al. 2023)
78 icebergs (Raiswell et al., 2008; Shaw et al., 2011; Raiswell et al., 2016; Hopwood et al., 2019) or sea-ice (Lannuzel
79 et al., 2016; Gerringa et al., 2020). In the Amundsen Sea, increased Fe input is likely to occur due to enhanced
80 glacial melt and runoff, particularly during the summer months when melting is most pronounced (e. g., Van
81 Manen et al., 2022). Increases in seawater temperature may affect the availability of Fe for phytoplankton, since
82 temperature affects the oxidation of the bioavailable Fe(II) to Fe(III) (e.g., Millero et al., 1987), however, Aflenzer
83 et al. (2023) did not observe a lower bioavailability of added Fe with increased temperatures. In the Weddell Sea,
84 Fe input may increase through upwelling of Fe-rich deep waters and meltwater from ice shelves, but this is less

85 [certain \(Klunder et al., 2011\). Seasonal variations in sea ice cover and glacial melt will play a significant role in](#)
86 [determining the timing and magnitude of Fe input in these regions.](#) These changes in Fe supply are associated
87 with ongoing climate change that is projected to lead to elevated temperatures and changes in wind patterns as
88 well as associated currents and upwelling (Turner et al., 2005; Moore et al., 2018). Overall, future Southern Ocean
89 conditions will most likely be warmer with potentially elevated Fe concentrations, which can be expected to also
90 affect phytoplankton productivity and community composition (Boyd et al., 2015; Laufkötter et al., 2015,
91 Pinkerton et al., 2021). [Depending on the geographical region and the time in the productive season \(Thomalla et](#)
92 [al., 2023\), global warming is predicted to increase wind-induced mixing or strengthen vertical stratification](#)
93 [\(Bronse laer et al., 2020; De Lavergne et al., 2014; Hillenbrand & Cortese, 2006; Shi et al., 2020\). Phytoplankton](#)
94 [will bloom earlier in the productive season as a result of decreasing sea ice and consequently higher light](#)
95 [\(Krumhardt et al., 2022\), most likely rapidly drawing down available Fe, followed by stratification, and thus](#)
96 [favourable conditions for smaller-sized phytoplankton \(Deppeler & Davidson, 2017; Krumhardt et al., 2022\).](#)
97 [Besides Fe and temperature, there are also other factors, e.g., other bio-essential metals \(Mn, Co, Ni, Cu and Zn\),](#)
98 [where notably Mn has been shown to be \(co-\)limiting in the Southern Ocean \(Wu et al; 2019, Browning et al.,](#)
99 [2021, Balaguer et al.; 2022, Hawco et al.; 2022\). Mn is essential for phytoplankton photosystems \(Raven et al.,](#)
100 [1990\) and a co-factor for enzymes dealing with oxidative stress \(Wolfe-Simon et al., 2005\). Moreover, light is](#)
101 [another major limiting factor for phytoplankton growth in Southern Ocean \(e.g., van Oijen et al.; 2004, Strzepek](#)
102 [et al.; 2019, Vives et al.; 2022, Latour et al.; 2024\).](#)

103 Considering the urgency of warming and the anticipated change in Fe supply, there is a need for studies
104 investigating the combined effects of these two important drivers controlling phytoplankton growth in the
105 Southern Ocean. There are many reports on the effects of Fe addition to Fe-limited phytoplankton from the
106 Southern Ocean (Reviewed by e.g., Yoon et al., 2018; Bazzani et al., 2023) and several on the influence of
107 temperature (Reay et al., 2001; Morán et al., 2006; Boyd et al., 2013), but only few studies examined the combined
108 effects of Fe and temperature on Antarctic phytoplankton (i.e. Rose et al., 2009; Zhu et al., 2016; Andrew et al.,
109 2019; Jabre & Bertrand, 2020; Jabre et al., 2021; Aflenzer et al., 2023). In particular, studies using natural
110 phytoplankton communities are scarce (Rose et al., 2009; Jabre et al., 2021) and concentrated on Ross Sea
111 phytoplankton with relatively large temperature increases (3 to 6 °C). Hence, more insight into how phytoplankton
112 from other regional Antarctic seas respond to the warming projected by the year ~2100 (Meredith et al., 2019) is
113 needed.

114 The Weddell Sea is one of the key areas of dense Antarctic bottom water formation (Fahrbach et al., 2004) and
115 plays an important role in the global thermohaline circulation. The subpolar cyclonic Weddell Gyre circulating in
116 the Weddell Sea basin isolates the centre of the Weddell Sea from marginal Fe sources such as melt or sediments,
117 whilst the currents on the edges of the gyre have the potential to pick up Fe from a variety of sources, such as the
118 seafloor, bathymetry driven mixing with deeper water masses, and sources associated with ice melt (Klunder et
119 al., 2014; Sieber et al., 2021, Tian et al., in prep.). Generally, the Weddell Sea has a relatively low primary
120 productivity, associated with Fe limitation in the centre of gyre (Hoppema et al., 2007; Klunder et al., 2014). In
121 contrast, the west Amundsen Sea and specifically the Amundsen Sea Polynya (ASP) is known as one of the most
122 productive regions in the Southern Ocean in terms of net primary production per net area (Arrigo & van Dijken,
123 2003). Additionally, this region (ASP) is characterised by a fast thinning of ice-sheets, shelf ice and glaciers, with
124 associated input of Fe required to sustain the high levels of primary productivity (e.g. Gerringa et al., 2012; van
125 Manen et al., 2022). Nevertheless, phytoplankton in the ASP could still be stimulated by additional Fe input
126 (Alderkamp et al., 2015).

127 The aim of the current study is to examine the concurrent effects of Fe supply and warming on Antarctic
128 phytoplankton communities from the Weddell Sea and the Amundsen Sea under controlled trace metal clean
129 conditions. Given the naturally low dissolved Fe (dFe) concentrations in the Southern Ocean, trace metal clean
130 conditions are crucial to avoid confounding Fe effects when studying temperature alone (Middag et al., 2023).
131 Our bioassay treatments comprised a full factorial combination of dFe and temperature increases. Our bioassay
132 treatments comprised of Fe addition (F treatment), warming (T treatment), Fe addition and warming (TF
133 treatment) and the control (no Fe addition, no warming; C treatment). The temperature was enhanced by 2 °C,
134 based on forecasts from the IPCC report (Meredith et al., 2019). Whilst the Amundsen Sea has shown a warming
135 trend over the past years already (Gómez-Valdivia et al., 2023; Drijfhout et al., 2024), the surface waters of the
136 Weddell Sea might not increase as much with climate change have not (yet) shown a clear increasing temperature
137 trend, but show underlying waters are warming (Strass et al., 2020), and short-term local temperature increases
138 due to upwelling of warm deep water have been observed (Darelius et al., 2023; Morrison et al., 2023; Teske et
139 al., 2024). The concentration of dFe in the Fe addition treatments (F and TF) was increased by 2 nM. Future Fe
140 concentrations are highly uncertain (Hutchins & Boyd, 2016; Tagliabue et al., 2016; Ryan-Keogh et al., 2023),
141 and not necessarily linked to bioavailability of Fe (Van Manen et al., 2022; Fourquez et al., 2023), but previous
142 experiments in the Southern Ocean have shown that such an addition represents (temporarily) Fe replete
143 conditions (De Baar et al., 2005). Moreover, increased Fe availability in the Southern Ocean could have a far-

144 reaching impact, leading to increased nutrient consumption consequently reducing nutrient transfer to lower
145 latitudes where primary production is fuelled by these nutrients (Primeau et al., 2013; Moore et al., 2018). By
146 integrating biological and trace metal chemistry analyses within large volume (20 L cubitainers), trace metal clean
147 experiments, we aim to provide a clearer understanding of future changes in phytoplankton growth patterns and
148 the implications for the Southern Ocean's role in global climate regulation.

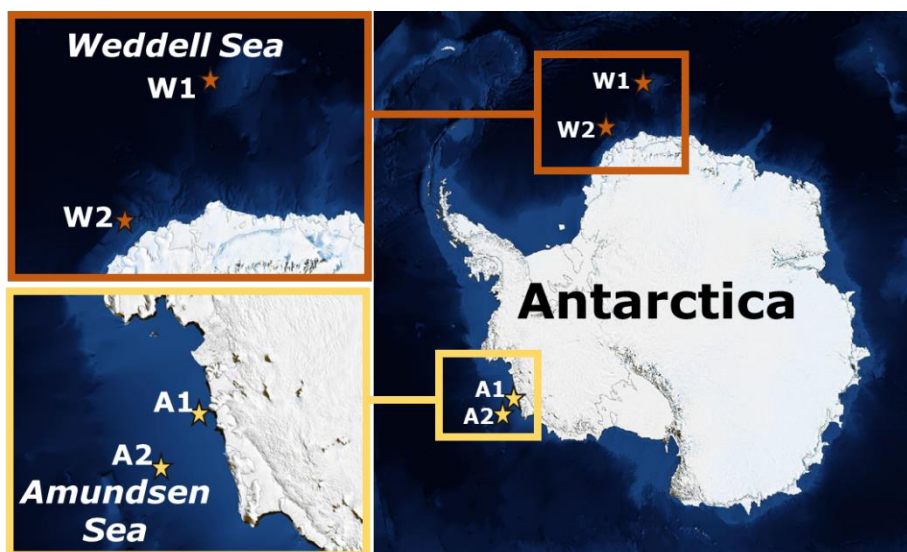
149

150 2. Material and Methods

151 2.1 Location and sampling

152 Natural seawater for the bioassays was collected during research expeditions (Fig. 1) in the Amundsen Sea
153 (bioassays A1 and A2, R/V Araon, ANA08B, 2017/18) and in the Weddell Sea (bioassays W1 and W2, R/V
154 Polarstern, Alfred-Wegener-Institut Helmholtz-Zentrum für Polar- und Meeresforschung (2017), PS117,
155 2018/19) in austral summer (December – February).

156



157

158 **Figure 1:** Location of the four bioassay experiments: Bioassays A1 and A2 were performed in the Amundsen Sea and
159 W1 and W2 in the Weddell Sea (Image obtained from NASA Worldview).

160

161 Seawater was sampled at the autofluorescence maximum (36 m for A2 and 20 m for both W1 and W2), except
162 for bioassay A1, which did not show an autofluorescence maximum and was sampled at the mid-mixed layer
163 depth (15 m). Water for each bioassay was collected in a single deployment of NIOZ's Titan ultraclean CTD
164 sampling system for trace metals (De Baar et al., 2008), mounted with pristine large volume samplers (Rijkenberg
165 et al., 2015). To prevent light shock for the phytoplankton, the original [Polyvinylidene fluoride \(PVDF\)](#) Pristine

166 samplers were replaced by a light-proof poly-propylene version. Salinity (conductivity), temperature,
 167 fluorescence, depth (pressure) and oxygen were measured with a CTD (Seabird SBE 911+) mounted on the trace
 168 metal clean sampling system (De Baar et al., 2008). To avoid contamination, further processing was performed
 169 under trace metal clean, dimmed light conditions and at 2 °C in a cleanroom environment inside a modified high-
 170 cube shipping container which fits the Titan sampling system. During transport on deck, cubitainers were covered
 171 with black light-proof bags to avoid light stress.

172 Water for Amundsen Sea bioassay A1 was sampled from the middle of the ~~Amundsen Sea Polynya (ASP)~~ ASP
 173 and for bioassays A2 in the marginal sea ice zone just outside of the ASP. Both W1 and W2 were performed with
 174 water from the eastern Weddell Sea. The Amundsen Sea bioassays A1 and A2 ran for 6 days (25 to 31 January
 175 and 31 January to 6 February 2018, respectively), whilst the Weddell Sea bioassays W1 and W2 ran for 8 days
 176 (28 December 2018 to 5 January and 9 to 17 January 2019, respectively, see Fig. S1 for regional Chlorophyll a
 177 concentrations at the start of bioassay incubations and Fig. S2 for station depth profiles). Amundsen Sea bioassays
 178 were thus initiated towards the end of the reported bloom period (Arrigo et al. 2012), whilst Weddell Sea bioassays
 179 were initiated during the start of the bloom period (von Berg et al., 2020). See Table 1 for *in situ* environmental
 180 conditions at sampling depth (at the start of the bioassays). The *in situ* temperature was below zero for all
 181 bioassays, with lowest values for A2 and W2 (-1.6 °C and -1.4 °C, respectively, compared to -0.6 °C and -0.3 °C
 182 for A1 and W1). The daily average irradiance at sampling depth on day of sampling was lowest for A1 and A2,
 183 i.e., < 6 μmol quanta m⁻² s⁻¹, compared to 18 and 98 μmol quanta m⁻² s⁻¹ for W1 and W2.

184 ~~**Table 1:** Characteristics of the seawater used for the bioassay experiments. Lat. = latitude, Long. =~~
 185 ~~longitude, Temp = temperature, Si = silicate, PO₄ = phosphate, NO_x = nitrate + nitrite, Fe = iron, Chl a~~
 186 ~~= chlorophyll a, Phyto = total flow cytometry based phytoplankton abundances, F_w/F_{tot} = photosynthetic~~
 187 ~~capacity of the total phytoplankton. The reported irradiance is the average irradiance at the sampling~~
 188 ~~depth on the day of sampling.~~

Bioassay	Station	Lat.	Long.	Temp.	Salinity	Irradiance	Si
-	-	(°S)	(°W)	(°C)	(psu)	(μmol quanta m ⁻² sec ⁻¹)	(μM)
A1	31	73.50	116.50	-0.6	33.99	5.0	84.7
A2	52	72.00	118.42	-1.6	33.89	3.1	78.5

W1	17	65.00	000.00	-0.3	33.90	17.7	58.3
W2	36	70.08	011.08	-1.4	33.82	97.6	27.7
<hr/>							
Bioassay	PO ₄	NO _x	Fe	total-Chl α	<20-μm Chl α	Phyto	F _v /F _m
-	(μM)	(μM)	(nM)	(μg L ⁻¹)	(%)	(x10 ³ mL ⁻¹)	r.u.
<hr/>							
A1	1.8	27.7	0.28	3.0	42	8.4	0.6
A2	2.1	30.9	0.10	0.4	98	7.1	0.6
W1	1.6	24.0	0.05	1.5	24	5.6	0.3
W2	1.9	27.9	0.03	0.6	65	4.4	0.3
<hr/>							

189

190 2.2 Bioassay incubation set-up

191 [Incubations were performed in custom built deck incubators \(see Supplement Bioassay Setup for more](#)
192 [information\)](#). Collapsible 20 L cubitainers (LDPE with PP caps and fitted with PE faucet; Cole-Palmer, Illinois,
193 USA) were used ~~for the bioassay incubations~~. These were soap and HCL (1 M) cleaned prior to the expeditions
194 and stored with full surface contact in 0.024 M HCl (VWR Normatom Ultrapur, Avantor, Radnor, USA) for at
195 least two months. Before use, cubitainers were rinsed five times with ambient seawater. The natural seawater for
196 the actual incubations was distributed randomly to the total of 12 cubitainers which were then randomly assigned
197 to the different treatments. Trace metal clean conditions were maintained during all sampling and sample
198 handling.

199 The bioassay treatments (performed in triplicate) were: *in-situ* conditions (control, C), + 2 nM dFe (as FeCl₃)
200 addition (F), + 2 °C temperature increase (T), and + 2 nM dFe addition and + 2 °C temperature increase (TF). For
201 the Amundsen Sea bioassays, a natural isotopic composition (natural dFe) was used for the dFe addition, whilst
202 d⁵⁷Fe was used in the Weddell Sea bioassays. This practice was adopted to better differentiate the added Fe from
203 the naturally present Fe, as we noticed that the dFe concentration in Fe amended Amundsen Sea bioassays quickly
204 returned to background concentrations (see section 3.1). Measuring Fe with a natural isotopic composition at these

205 low concentrations is still a challenge and combined with inherent variability between replicates. After several
206 days it became impossible to distinguish the Fe amended and non-amended treatments in Amundsen Sea bioassays
207 based on their natural dFe concentration (see section 3.1). The variation in natural dFe expected between Fe
208 amended and non-amended treatments despite precipitation and uptake, was hidden in the analytical and
209 environmental variability. For Weddell Sea bioassays we thus decided to add ^{57}Fe , a rare (2.12 % abundant vs
210 91.75 % for ^{56}Fe) natural isotope of Fe. Given its low natural abundance, ^{57}Fe is not nearly as sensitive to analytical
211 and replicate variation as such variation is insignificant relative to the addition, allowing better insight in Fe
212 drawdown over the course of the experiments.

213 Average starting concentrations of dFe in the Fe addition treatments ranged from 2.03 to 2.28 nM for both Weddell
214 and Amundsen Sea bioassays. Temperatures in the T and TF treatments were 1.4, 0.4, 1.7 °C and 1 °C, for A1,
215 A2, W1 and W2, respectively (see Table 1 for an overview of starting conditions in all treatments). One replicate
216 of the control treatment in bioassay W1 started leaking during the incubation and was thus not sampled from day
217 4 onwards. For bioassay W2, the *in-situ* temperature of -1.4 °C could not be maintained due to the very sunny
218 weather, resulting in an increase of 0.4°C for all treatments. Final incubation temperatures were -1.0 °C in the
219 control (C) and Fe-only (F) treatment and 1 °C (instead of 0.6 °C) in the T and TF treatments. This temperature
220 adjustment was done slowly over the course of 24 h on the second day of the incubation. More details about the
221 set-up can be found in the supplemental data (Fig. S13, supplement Bioassay Setup). Over the course of the
222 incubation period, temperatures were kept constant, with a maximum temperature fluctuation of ± 0.3 °C.

223 For Amundsen Sea bioassays, light levels were chosen to mimic *in-situ* conditions, but noting the low light
224 conditions during these incubations (ca. 3 % of in-air photoactive radiation, PAR; i.e. average 3.4 and 1.5 μmol
225 quanta $\text{m}^{-2} \text{s}^{-1}$ for A1 and A2 over the course of incubation), we opted for non-limiting light conditions (Bertrand
226 et al., 2011) for the (later performed) bioassays of the Weddell Sea (ca. 12 % of in-air PAR; i.e. average 69 and
227 100 μmol quanta $\text{m}^{-2} \text{s}^{-1}$ for W1 and W2 over the course of incubation). The percentages and values reported refer
228 to approximate light conditions within cubitainers. - Light levels were adapted using neutral density screens.

229 Samples for dissolved and particulate metals, Chl *a*, pigment-based taxonomic analyses, and particulate organic
230 carbon (POC), nitrogen (PON) and phosphate (POP) were taken before filling of the cubitainers at the start of the
231 bioassay incubations (t_0), and at the end of the incubations after 6 (Amundsen Sea) or 8 (Weddell Sea) days
232 (difference in duration due to logistical constraints). Samples for phytoplankton photosynthetic efficiency (F_v/F_m)
233 and phytoplankton abundances were taken at least every other day. Macronutrients were measured on board at
234 least every other day to screen for potential macronutrient limitation.

235
236
237
238
239
240
241
242
243
244
245
246
247
248
249
250
251
252
253
254
255
256
257
258
259
260
261
262

2.3 Setup verification

To test for potential Fe contamination, three cubitainers were filled with ultrapure (UP) water and handled and subsampled using the same methods and frequency as the treatments. Subsamples for dFe analysis were taken at the start (0.08 ± 0.04 nM) and after three (0.07 ± 0.04 nM) and six (0.06 ± 0.04 nM) days. Concentrations of dFe stayed consistently low, suggesting minimal or no contamination. We also tested whether added dFe stayed in solution or adsorbed to the cubitainer walls and found a slow gradual decrease over the first few days in dFe concentrations after addition to UP water that we attribute to precipitation and wall adsorption (Table S1). During our experiments, the concentrations of added dFe decreased more rapidly, whereas the dFe concentrations in the non-Fe treatments, as well as the non-added form of dFe in Fe treatments ($d^{57}\text{Fe}$ for Amundsen and natural dFe for Weddell Sea bioassays), stayed low and relatively constant over time. Since phytoplankton grew in all treatments, the faster decrease of added dFe was likely due to uptake and sorption onto (biogenic) particles rather than precipitation to the cubitainer walls. Low traceable amounts of $d^{57}\text{Fe}$ during the second half of the incubations in W1 and W2 suggested that the initial decrease in dFe concentrations did not correspond to permanent removal from the bioavailable Fe pool (e.g. due to absorption; Jensen et al., 2020) but instead buffered the dissolved pool (as suggested for natural settings with exchange between the (labile) pFe and dFe pools; Van Manen et al., 2022), or that most of the added dFe was taken up by phytoplankton as rapid luxury uptake during the first days of an experiment (Lampe et al., 2018).

2.4 Macronutrients

During the Amundsen Sea bioassays, dissolved macronutrients were measured onboard following Jeon et al. (2021), according to the Joint Global Ocean Flux Study (JGOFS) protocols (Gordon et al., 1993) using a four-channel Auto-Analyzer (QuAAtro, Seal Analytical, Norderstedt, Germany). Measurement precisions were ± 0.02 , ± 0.28 and ± 0.14 μM for phosphate, ~~silicic acid~~ silicate, and nitrogen (nitrate + nitrite), respectively (Jeon et al., 2021). For Weddell Sea bioassays, samples for nitrate, nitrite, phosphate, and ~~silicate silicic acid~~ were measured following the method described by Gerringa et al. (2019). Measurements precisions were ± 0.01 , ± 0.31 and ± 0.04 μM for phosphate, ~~silicates~~ silicic acid, and nitrogen (nitrate + nitrite), respectively.

263 2.5 Dissolved and particulate metals

264 Cubitainers were subsampled for dFe as well as other dissolved trace metals (dMn, dCo, dCu, dNi, dZn, dCd)
265 using a 0.2 µm Sartobron-300 filter cartridge (Sartorius AG, Göttingen, DE) for bioassay A1 and A2 and pre-acid
266 cleaned 0.2 µm Acropak filter cartridges (Cytiva, Marlborough, USA) for W1 and W2. Filters were fitted to an
267 UP-cleaned vented PE faucet attached to the cubitainer with HCl acid (1.5 M) cleaned silicon tubing. Filtered
268 samples were taken by applying pressure to the cubitainer. Different filters were used for Fe replete and deplete
269 treatments, and filters were replaced between experiments. The dissolved trace metal samples were collected in
270 acid cleaned 125 mL LDPE bottles following GEOTRACES protocols (Cutter et al., 2017) and directly acidified
271 by adding ultra-pure HCl (Baseline®HCl; Seastar Chemicals Inc, Sidney, CA), resulting in a concentration of
272 0.024 M with a final pH of ~1.8. Samples were stored until analysis at NIOZ. Trace metal samples were prepared
273 and analysed following van Manen et al. (2022) and references within. In short, trace metal samples were
274 preconcentrated using a SeaFAST pre-concentration system (ESI). Blank contributions from sample handling,
275 pre-concentration, and analysis steps were determined by analysing acidified MQ water (~1.8 pH) prepared in the
276 same way as real samples.

277 For particulate trace metals (pFe, pMn, pCo, pCu, pZn, pCd, pAl) and POP, 25 mm poly-ether-sulfone (PES) disc
278 filters (0.45 µm Pall Supor, Port Washington, USA) and polypropylene filter holders (Advantec, Cole-Parmer,
279 Vernon Hills, USA) were used, following the protocol adapted by Van Manen et al. (2022) with one additional
280 step: samples were soaked for at least 30 minutes in oxalate-EDTA (respectively 0.75M and 5.5M) in a 10L carboy
281 (VWR Collection; Avantor, Radnor, USA) to remove all trace metals outside or adsorbed to phytoplankton cell
282 walls (modified after Hassler & Schoemann, 2009) and subsequently filtered. The EDTA oxalic acid wash used
283 on particulate samples prior to filtration should effectively remove surface-bound metals, also minimizing the
284 authigenic Fe fraction. Due to time limitations, samples for particulate metals were only taken during experiment
285 A1, W1 and W2. After filtration, which happened at the end of the experiments, filters were stored frozen at -20
286 °C until analysis. In the NIOZ lab, filters were treated with two successive digestion steps to determine the total
287 particulate fraction. All vials used in the digestion procedures were rigorously cleaned with HF and HCl
288 beforehand and rinsed with UP water. Filters were subjected to a leach consisting of 1.8 mL of 4.35M (25 %) two
289 times sub-boiled distilled acetic acid and 0.02M (2 %) hydroxylamine hydrochloride (99.999 % trace metal basis,
290 Sigma-Aldrich, Saint-Louis, USA). Subsequently, filters were digested following the total digestion protocol
291 developed by Cullen & Sherrell (1999) and modified by Planquette & Sherrell (2012). A volume of 2 mL of 3 ×
292 sub-boiled distilled 8.0 M (50 %) HNO₃ (VWR Chemicals – AnalaR NORMAPUR, Avantor, Radnor, USA) and

293 2.9 M (10 %) HF (Merck – Supelco, Kenilworth, USA) was added. The vials were closed tightly and refluxed for
294 4 h at 110 °C. The solution was then transferred to a secondary Teflon vial and were then heated to near dryness
295 at 110 °C. A 1 mL volume –of 8.0 M (50 %) 3× sub-boiled distilled HNO₃ (VWR Chemicals– AnalaR
296 NORMAPUR, Avantor, Radnor, USA) and 15 % H₂O₂ (Merck – Suprapur, Kenilworth, USA) was added to the
297 dried vial contents. The vials were refluxed for 1 h at 110 °C and subsequently cooled to room temperature.
298 Addition of reagents and refluxing were repeated once. After this repetition, the vials were heated to near dryness
299 at 110 °C. The samples were re-dissolved in 2 mL 1.5 % 3× sub-boiled distilled HNO₃ with 10 ppb Rh as internal
300 standard and transferred to 2 mL Cryovials® (VWR, Avantor, Radnor, USA) for storage and analysis.

301 The lithogenic fraction and concentration of pFe and other particulate metals discussed was determined by
302 assessing the ratio between the particulate metal of interest and particulate aluminium (pAl), assuming all pAl
303 originates from crustal material using the approach described in more detail in van Manen et al (2022). For
304 example, we are using the observed pFe/pAl ratio in the samples and the known crustal ratio of 0.21 mol mol⁻¹
305 (Taylor and McLennan, 1985) to calculate the lithogenic pFe fraction and concentration.

306

307 **2.6 ICP-MS trace metal measurements and particulate organic phosphorous**

308 Dissolved trace metal samples were pre-concentrated using a SeaFAST pre-concentration system (ESI) using two
309 loops of 10 mL and were eluted into 350 µL elution acid (1.5 M Teflon distilled HNO₃ with rhodium as internal
310 standard) which gives a pre-concentration factor of 57.14 (see van Manen et al., 2022). Dissolved trace metal
311 samples, blanks (~~Supplementary T~~Table S2), and references (Table S3) were analysed by ICP-MS (Thermo
312 Scientific Sector Field High-Resolution Element 2, Thermo Fisher-Scientific, Waltham, USA). Blank values were
313 much lower than the analysed samples, and reference results were in good agreement with certified values.

314 For the particulate samples, including POP, the procedure blanks without a filter were treated identically to the
315 samples, except for the steps involving filter handling and the removing of the filter from the filter holders.
316 Therefore, the vial blank is included in this reagent blank. Filter blanks consisted of unused acid cleaned PES disc
317 filters (Table S4).

318 Accuracy and precision of the digestions were assessed by Certified Reference Materials (CRMs). There is no
319 CRM available for marine suspended particulate matter, therefore accuracy could only be approximated by
320 analysis of other available CRMs. PACS-2 and MESS-3 (marine sediments, National Research Council of
321 Canada) were analysed. For each CRM, 10-30 mg were digested, whilst recommended sample weights are 250
322 mg for PACS-2 and MESS-3. The lower sample weights in this study were chosen to be representative of actual

323 marine particulate suspended matter concentrations (similar to Ohnemus et al., 2014). PACS-2 and MESS-3 were
324 only subjected to the total digestion (Table S5). The CRMs were in good agreement with the certified values.

325

326 **2.7 Particulate organic carbon and nitrogen**

327 For POC and PON sampling, 1 L of unfiltered seawater was collected from each cubitainer and stored in dark
328 bottles (Nalgene, Rochester, USA) at 1 °C until further processing (within 4 h after sampling). Filtrations were
329 then performed using combusted (4 h at 500 °C; Verardo et al., 1990) 0.3 µm 25 mm GF75 filters (Whatman,
330 Cytiva, Maidstone UK) and under modest under pressure (max. 200 mbar). Filters were folded once, packed in
331 aluminium foil, and stored frozen (-20 °C) until analysis. The POC and PON concentrations were measured using
332 a Thermo-Interscience Flash EA1112 Series Elemental Analyzer (Thermo Scientific, Waltham, USA) with excess
333 oxygen, at 900 °C and a detection limit of 100 ppm and a precision of 0.3 % (Verardo et al., 1990). Before analysis,
334 GF75 filters were folded and packed into a tin cup. The instrument blank is included by the analyser calibration.
335 Carbon and nitrogen content of samples and blanks were computed according to the results of the standard
336 measurements, and the blank was subtracted from the sample. Acetanilide (C₈H₉NO) with 71.09 % C and 10.36
337 % N (ThermoQuest, Milan, Italy) was measured as standard material, and silty and sandy soil standards from
338 Elemental Microanalysis were measured as an internal reference.

339

340 **2.8 Phytoplankton photosynthetic efficiency**

341 F_v/F_m was determined in a Water-K quartz cuvette (3.5 mL) using pulse amplitude modulated fluorometry (Heinz
342 Walz WATER-PAM, with Red LEDWATER-ED cuvette version S/N EDEE0196, Walz GmbH, Effeltrich,
343 Germany). Samples were kept in 50 mL Greiner tubes (Thermo Fisher-Scientific, Waltham, USA) in the cold
344 (stored in a cool box on ice) and in the dark for dark-adaptation (15 min up to occasionally 4 h). Acclimation
345 times of up to 4 h did not affect photosynthetic efficiency of different phytoplankton (L. Peperzak, personal
346 communication; Eich et al., 2021). The measuring light frequency used was set to level 5 (25 Hz) with an intensity
347 of 8, the SAT-pulse width was set to 0.8 seconds and the far-red pulse width was set to 10 seconds, with intensities
348 of 10 and 6, each. The cuvette was rinsed with ultra-pure (UP) water between samples, which was removed by
349 shaking the cuvette and placing it upside down on lint-free paper towels to remove any remaining droplets (testing
350 technical replicates did not show a significant effect of UP rinsing, non-parametric Kruskal-Wallis ANOVA, p =
351 0.95). and ~~†~~ The relative fluorescence yield (F_t) values were kept between 100 and 1000 by adjusting the PM-gain.
352 Blanking was done for each station and/or bioassay using 0.2 µm filtered seawater (Cullen & Davis 2003) from

353 the respective stations and repeated after PM-gain adjustment when needed. The following formula was used to
354 obtain the photosynthetic efficiency: $F_v/F_m = (F_m - F_0)/F_m$, with F_0 being the minimum fluorescence, and F_m being
355 the maximum fluorescence.

356

357 **2.9 Chlorophyll a concentration and pigment-based taxonomic analyses**

358 Samples (0.54 - 2.65 L) for Chl *a* concentrations and pigment-based community composition were filtered within
359 30 min of subsampling (kept on ice and in the dark) on GF/F glass fibre filters (25 mm diameter, Whatman,
360 Cytiva, Marlborough, USA) using a vacuum pump (max. 200 mbar), until filters showed clear colouring. Samples
361 were taken for total as well as a < 20 µm fraction for better compatibility with phytoplankton community
362 measurements by flow cytometry. For the < 20 µm fraction, natural seawater was reverse sieved through a 20 µm
363 mesh before filtration onto a GF/F filter. Due to low sample volume availability at bioassay A2, the same amount
364 of water from all replicates was combined for both total and < 20 µm Chl *a* samples, resulting in one averaged
365 value for each treatment. Filters were folded once and double wrapped in aluminium foil, flash-frozen in liquid
366 nitrogen and stored at -80 °C until further analysis in the home lab. Pigments were dissolved in 90 % acetone from
367 the freeze-dried filters according to Van Leeuwe et al. (2006) and high-performance liquid chromatography
368 (HPLC) pigment separation was performed (Zobrax-Eclipse XDB-C8 column, 3.5 µm particle size) according to
369 Van Heukelem & Thomas (2001). Detection of pigments was based on both the retention time and diode array
370 spectroscopy of standards (346 nm, Waters 996), quantification was based on calibration curves using those
371 standards (DHI LAB standards). Phytoplankton community composition was determined using CHEMTAX
372 version 1.95 (Mackey et al., 1996), following Selz et al. (2018). For the final pigment ratios, see Table [S766](#).

373

374 **2.10 Phytoplankton and bacterial cell-abundances (< 20 µm)**

375 Phytoplankton cell abundances (< 20 µm) were obtained using a 488 nm Argon laser benchtop Beckton-Dickinson
376 FACSCalibur (BD Biosciences, Franklin Lakes, USA) flow cytometer with the trigger set on red Chl *a*
377 autofluorescence (Marie et al., 1999). The phytoplankton samples from the Amundsen Sea bioassays were
378 measured fresh within 30 min of sampling (stored on ice); the Weddell Sea bioassay phytoplankton samples were
379 fixed for 15 – 30 min with 100 µL formaldehyde-hexamine (18 % v/v:10 % v/v) at 4 °C, flash-frozen in liquid
380 nitrogen and stored at -80 °C until analysis in the home lab. Phytoplankton populations were differentiated based
381 on their red autofluorescence and side scatter, using FCS express 5 (De Novo Software, Pasadena, CA, USA).
382 Freshly counted samples resulted in comparable gating as the fixed samples (tested for Amundsen Sea samples).

383 A total of 25 populations were distinguished (Table S7), whereby not all populations occurred in both seas and
384 all bioassays. Average cell diameters were determined by size-fractionation, i.e., serial gravity filtration through
385 20, 10, 8, 5, 3, 2, 1, 0.8 and 0.6 μm PC filters (Whatman, Cytiva, USA, Marlborough, MA) using a reusable filter
386 holder (Whatman, Cytiva, Marlborough, USA) and a plastic syringe. The number of cells retained by each filter
387 per discriminated population were plotted against the respective filter size. The average cell diameters were
388 defined as the size where 50 % of the original number of cells were retained, based on the fit of a sigmoidal plot
389 (Veldhuis & Kraay, 2004). Phyto 5, 6, 7, 11, 12 and 14 were cryptophytes that were identified by their orange
390 phycoerythrin autofluorescence. Based on earlier work (Biggs et al., 2019), we consider phytoplankton
391 populations Phyto 20 and 22 to 25 to be diatoms and Phyto 8 to be *Phaeocystis antarctica* by comparing the red
392 autofluorescence and side scatter pattern of the respective phytoplankton groups. The latter was confirmed during
393 the Amundsen Sea expedition when we selectively collected *Phaeocystis* colonies and analysed them fresh
394 onboard after gentle shaking (to break up the colonies). Phytoplankton carbon was estimated based on cell volume
395 of phytoplankton, assuming spherical cells, and using $237 \text{ fg C } \mu\text{m}^{-3}$ for picophytoplankton populations Phyto 1
396 to 6 and $196.5 \text{ fg C } \mu\text{m}^{-3}$ for nanophytoplankton populations Phyto 7 to 25 (Garrison et al., 2000; Worden et al.,
397 2004). Phytoplankton net growth rates were calculated using exponential trendlines. For total abundances, the full
398 incubation period was taken into account (i.e., day 1 - 6 for Amundsen Sea and day 2 - 8 for Weddell Sea
399 bioassays). Starting abundances were taken prior to filling of the cubitainers and hence not taken into account.
400 For the phytoplankton group specific rates only those time points (>3 but most often 4-5 time points) with a
401 consecutive increase in abundances were selected.
402 Samples for bacterial abundances were fixed with EM-grade glutaraldehyde (0.5% final concentration; Sigma-
403 Aldrich, Zwijndrecht, The Netherlands), flash-frozen in liquid nitrogen and stored at -80°C until analysis using
404 flow cytometry (Marie et al.: 1999). Bacterial carbon concentrations were calculated assuming $12.4 \text{ fg C cell}^{-1}$
405 (Fukuda et al.: 1998).

406

407 **2.11 Statistical analyses**

408 All statistical analyses were performed using R (R Core Team, 2021). To detect differences in phytoplankton
409 community composition between treatments, an ANOSIM analysis was performed (vegan library, using Bray-
410 Curtis dissimilarity with 9999 permutations). When a significant difference ($p < 0.05$) was detected, an indicator
411 species analysis (vegan library, function r.g. with 9999 permutations) was used as a follow-up analysis to see
412 which phytoplankton groups differed between treatments. This was done for both flow cytometry-based

413 abundances and pigment-based taxonomic group composition, using relative values, thus normalized against total
414 Chl *a* for pigment-based community composition, and total phytoplankton abundance for both pigment-based and
415 flow cytometry-based phytoplankton groups. For the indicator species analysis, p-values are reported. A Scheirer-
416 Ray-Hare test (non-parametric ANOVA-like test) was performed to determine the significance of Fe-addition and
417 temperature increase, as well as potential interaction effects, on the respective response variable measured. The
418 test was performed for data of the last day of the incubation, since effects were usually strongest then, and some
419 variables were only sampled at the beginning and the end of the experiment (day 6 for A1 and A2, day 8 for W1
420 and W2). We manually calculated eta-squared (η^2 , amount of variance explained, the higher the value, the larger
421 the effect) by dividing the sum of squares of the effect of interest (i.e. iron addition, temperature increase and the
422 interaction between these two) by the total sum of squares. The η^2 is provided when temperature increase, iron
423 addition, and/or the interaction between both tested as significant. Since we wanted to look at the overall effect of
424 Fe addition, temperature increase, and potential interaction effects on total phytoplankton abundances based on
425 flow cytometry, we additionally performed a generalized linear model (GLM), assuming a quasi-poisson
426 distribution in combination with a log-link, including the bioassay as well as the day number as factors without
427 interaction, and including an interaction term for the Fe- and temperature-treatment. For the GLM, the data of all
428 bioassays and all timepoints (excluding day 0) were combined. The formula for the GLM was: total phytoplankton
429 abundances ~ Fe treatment * temperature treatment + bioassay name + day number. Statistical results are only
430 reported for variables where more than 1 replicate was available. We also performed an NMDS analysis based on
431 phytoplankton abundances using the vegan library with Bray-Curtis dissimilarity (seed set to 123). A significance
432 level of $p < 0.05$ was used. Where applicable, the mean \pm standard deviation is reported, unless stated otherwise.

433 All statistical results are reported in the Supplements (Tables S9 – S20).

434

435 **3. Results**

436 3.1 Sample site characteristics

437 The *in-situ* temperature was below zero for all bioassays, with lowest values for Amundsen Sea bioassay A2 and
438 Weddell Sea bioassay W2 (-1.6 °C and -1.4 °C, respectively, compared to -0.6 °C and -0.3 °C for A1 and W1).

439 The daily average irradiance at sampling depth on day of sampling was lowest for A1 and A2, i.e., $< 6 \mu\text{mol}$
440 $\text{quanta m}^{-2} \text{s}^{-1}$, compared to 18 and 98 $\mu\text{mol quanta m}^{-2} \text{s}^{-1}$ for W1 and W2. Dissolved inorganic macronutrient
441 concentrations were relatively comparable between bioassays, except the silicate concentration in W1 being ~ 20
442 μM lower than for the other bioassays (but still far from limiting). Initial dFe concentrations in the Weddell Sea

443 were lower compared to the Amundsen Sea (Table 1), as were dMn concentrations (Fig. 2). Bioassay A1 had the
 444 highest Chl *a* concentrations (sampled within the ASP), followed by W1. Both bioassays also had the highest
 445 share of >20 μm Chl *a*. The Chl *a* concentration of A2 was almost exclusively made up of < 20 μm sized
 446 phytoplankton (98% of total Chl *a*, Table 1). Flow cytometry derived phytoplankton abundances were highest for
 447 the Amundsen bioassays. The photosynthetic efficiency F_v/F_m at the start of the incubations was 2-fold lower for
 448 the Weddell Sea bioassays compared to the Amundsen Sea bioassays (i.e., 0.3 vs 0.6 r.u., respectively). The station
 449 for bioassay W2 was closest to the coast, followed by A1, A2 and W1, however distance to land did not seem to
 450 have a major impact on either phytoplankton community composition, or nutrient concentrations.

451

452 **Table 1:** Characteristics of the seawater used for the bioassay experiments. Lat. = latitude, Long. = longitude, Temp =
 453 temperature, Si = silicate, PO_4 = phosphate, NO_x = nitrate + nitrite, dFe = dissolved iron, Chl *a* = chlorophyll *a*, Phyto = total
 454 flow cytometry based phytoplankton abundances, F_v/F_m = photosynthetic capacity of the total phytoplankton. The reported
 455 irradiance is the average irradiance at the sampling depth on the day of sampling.

Bioassay	Station	Lat.	Long.	Temp.	Salinity	Irradiance	Si
-	-	(°S)	(°W)	(°C)	(psu)	($\mu\text{mol quanta m}^2 \text{sec}^{-1}$)	(μM)
A1	31	73.50	116.50	-0.6	33.99	5.0	77.984.7
A2	52	72.00	118.42	-1.6	33.89	3.1	77.578.5
W1	17	65.00	000.00	-0.3	33.90	17.7	58.3
W2	36	70.08	011.08	-1.4	33.82	97.6	71.827.7

Bioassay	PO_4	NO_x	dFe	total Chl <i>a</i>	< 20 μm Chl <i>a</i>	Phyto	F_v/F_m
-	(μM)	(μM)	(nM)	($\mu\text{g L}^{-1}$)	(%)	($\times 10^3 \text{mL}^{-1}$)	r.u.
A1	1.8	24.327.7	0.28	3.0	42	8.4	0.6
A2	2.0 2.4	28.230.9	0.10	0.4	98	7.1	0.6
W1	1.6	24.0	0.05	1.5	24	5.6	0.3
W2	1.9	27.9	0.03	0.6	65	4.4	0.3

456

457

458 **3.21 Nutrient dynamics**

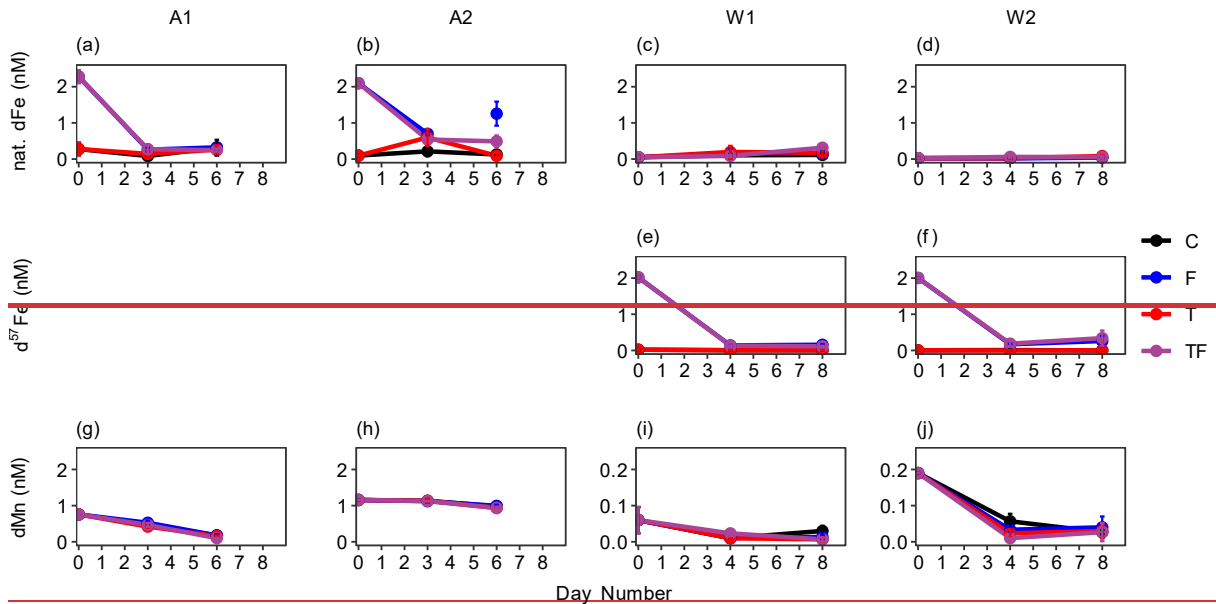
459 Bioassay treatments without Fe addition (C and T) started at naturally low dFe concentrations (0.28 ± 0.16 , 0.10
 460 ± 0.02 , 0.05 ± 0.03 and 0.03 ± 0.01 nM natural dFe for bioassay A1, A2, W1 and W2, respectively), and stayed
 461 within these ranges. The Fe addition treatments (F and TF) showed a rapid (and overall comparable) drawdown

462 of the added Fe (natural Fe for A1 and A2; Fig 2a, b and $d^{57}\text{Fe}$ for W1 and W2; Fig. 2e, f) in all bioassays,
463 regardless of its isotopic composition. The dFe concentrations in F and TF treatments (0.29 ± 0.07 nM) at the end
464 of the bioassays were comparable to concentrations in non-Fe addition treatments (0.28 ± 0.14 nM, [Table S98](#))
465 for the relatively high-Chl *a* bioassay A1. In contrast, bioassay A2 had most dFe left at the end of the incubation
466 (0.80 ± 0.46 nM for F and TF, compared to 0.11 ± 0.04 nM for C and T) which concurs with the low starting Chl
467 *a* concentration and irradiance intensity. However, since the average dFe concentration in Fe amended treatments
468 was lower (0.65 ± 0.10 nM) in the middle of the incubation period (day 3, see Figure 2 b), we cannot rule out
469 potential contamination during sampling as a reason for the higher dFe concentrations, notably in the F treatment.
470 For the Weddell Sea bioassays, $d^{57}\text{Fe}$ in F and TF treatments declined rapidly with low final concentrations (0.14
471 ± 0.03 and 0.31 ± 0.17 nM for W1 and W2, respectively) compared to the non-Fe addition treatments (0.01 ± 0.01
472 nM $d^{57}\text{Fe}$ and below detection limit for W1 and W2, respectively). Other trace metals were also measured, and
473 dissolved manganese (dMn) drawdown did not differ between treatments (Fig. 2g-j). However, the starting
474 concentrations of dMn were low for W1 and W2 (0.06 ± 0.03 and 0.19 , $\text{SD} < 0.01$ nM, compared to 0.76 , $\text{SD} <$
475 0.01 1.16 ± 0.01 nM for A1 and A2, respectively).

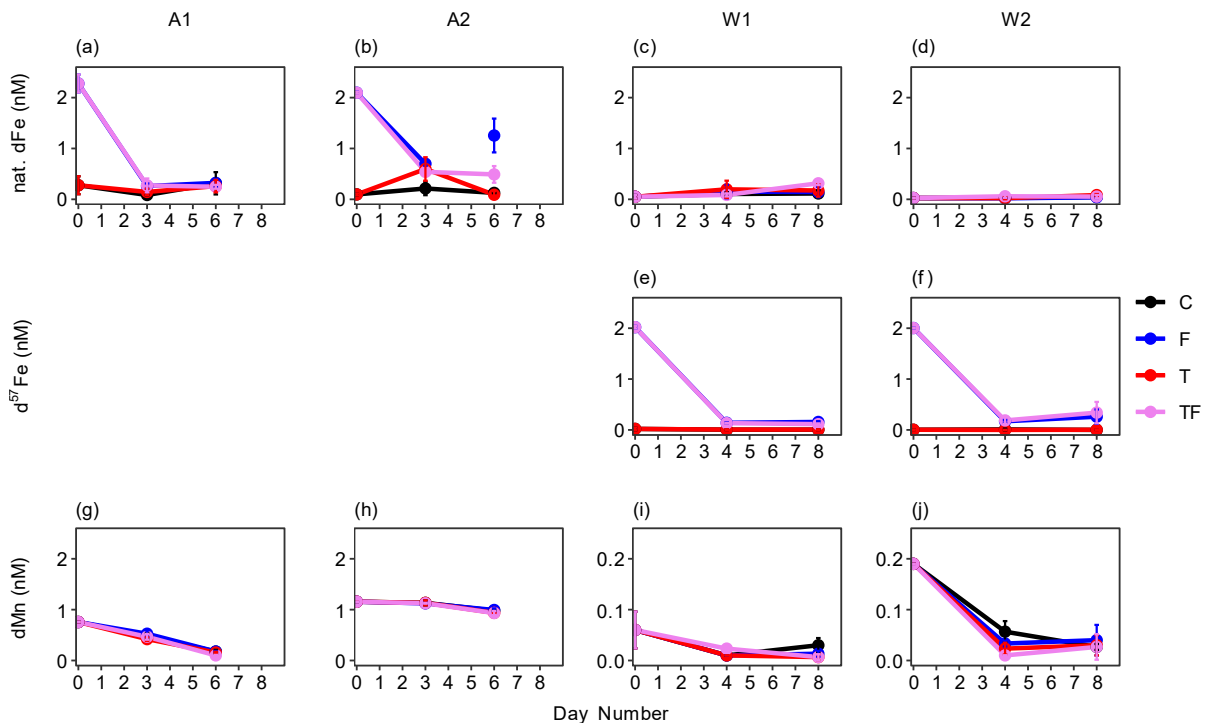
476 The dissolved inorganic macronutrients were not limiting phytoplankton growth during the bioassays. Final
477 concentrations were at least 7.2 , 0.3 and 37 μM in all bioassays for nitrogen, phosphate, and silicate, respectively
478 (Supplement Fig. [S42](#)). Still, there was discernible drawdown of macronutrients by the microbial community
479 during the incubations, except for Amundsen Sea bioassay A2 ([Supplement tables S10, S21](#)). Fe addition (both F
480 and TF treatments) had a significant impact on phosphorous drawdown for bioassays A1, W1 and W2 ($p < 0.05$,
481 η^2 : 0.53 , 0.76 and 0.76 for A1, W1 and W2, respectively; and on average 0.45 μM lower for Fe addition treatments
482 compared to C) and on nitrogen drawdown for bioassays W1 and W2 ($p < 0.004$, $\eta^2 > 0.75$, average of 9.8 μM
483 lower for Fe addition treatments compared to C). The TF treatment showed stronger drawdowns especially for
484 Weddell Sea bioassays W1 and W2 (average 0.7-fold change between TF and F treatments for both phosphorus
485 and nitrogen, respectively), however there was no significant interaction effect between temperature increase and
486 Fe addition. In contrast, silicate acid concentrations at the end of the incubation period were impacted by the
487 increase in temperature for bioassays A1, A2 and W2 ($p < 0.02$, η^2 : 0.76 for A1 and W2 and η^2 : 0.52 for A2 and
488 $p = 0.06$ and η^2 : 0.32 for bioassay W1), with T treatments showing on average a 2.4 μM lower silicate
489 concentration compared to the control. Only bioassay W1 showed an effect of Fe-addition on silicate drawdown
490 ($p = 0.02$, η^2 : 0.52), resulting in the TF treatment showing lowest concentrations on the last day of the incubations
491 (0.8 -fold change compared to the control and 0.9 -fold change compared to both T and F treatment). The ratios of

492 silicate drawdown to nitrogen and to phosphorus were higher in W1 than in W2 (i.e., 1.4 and 18.3 in W1 and 0.7
 493 and 10.5 in W2). Moreover, when dFe was added, the silicate to nitrogen ratio (Si:N), as well as silicate to
 494 phosphorous ratio (Si:P) drawdown was lower in bioassays A1, W1 and W2 compared to non-Fe treatments (0.86
 495 and 1.02 Si:N for Fe and non-Fe treatments and 11.3 and 12.5 Si:P, respectively, [Table S10](#)).

496



497



498

499 **Figure 2:** Average concentrations of natural dissolved Fe (a, b, c, d), $d^{57}Fe$ (e, f) and dMn(g, h, i, j) concentrations for
 500 Amundsen Sea (A1: a, g; A2: b, h) and Weddell Sea (W1: c, e, i; W2: d, f, [g](#)) bioassays. Amundsen Sea bioassays did not
 501 receive ^{57}Fe supplementation. The black line represents the control (C) treatment, the red line the temperature (T) treatment,
 502 the blue line the iron (F) treatment, and the purple line the combined temperature and iron treatment (TF). Error bars
 503 indicates the standard deviation ($n = 2$ or 3 , except for dFe of bioassay A2 TF treatment day 3), when they are not visible it is

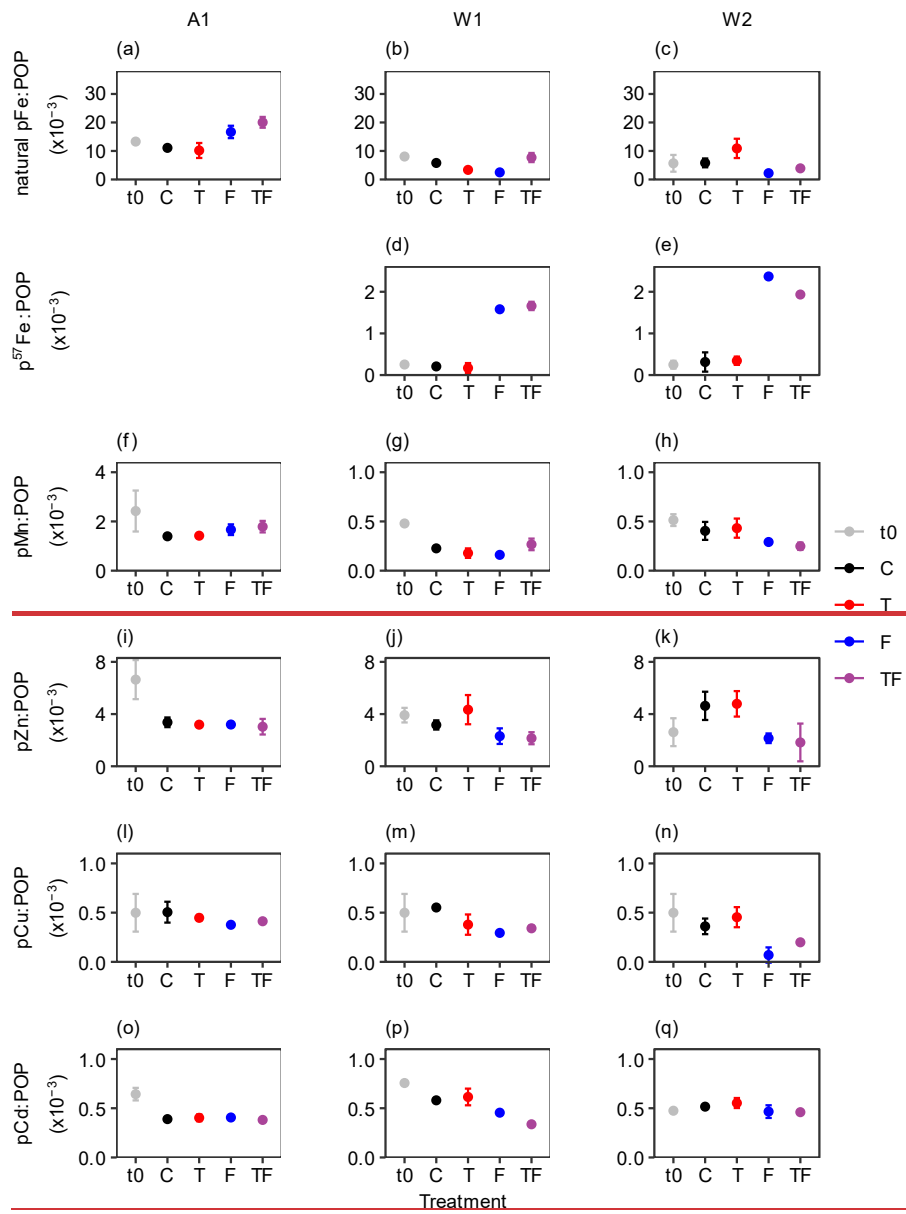
504 smaller than the symbol. Bioassay A2 showed a higher dFe concentration on day 6 compared to day 3, which we cannot
505 exclude to be due to potential contamination and was thus treated as an outlier.

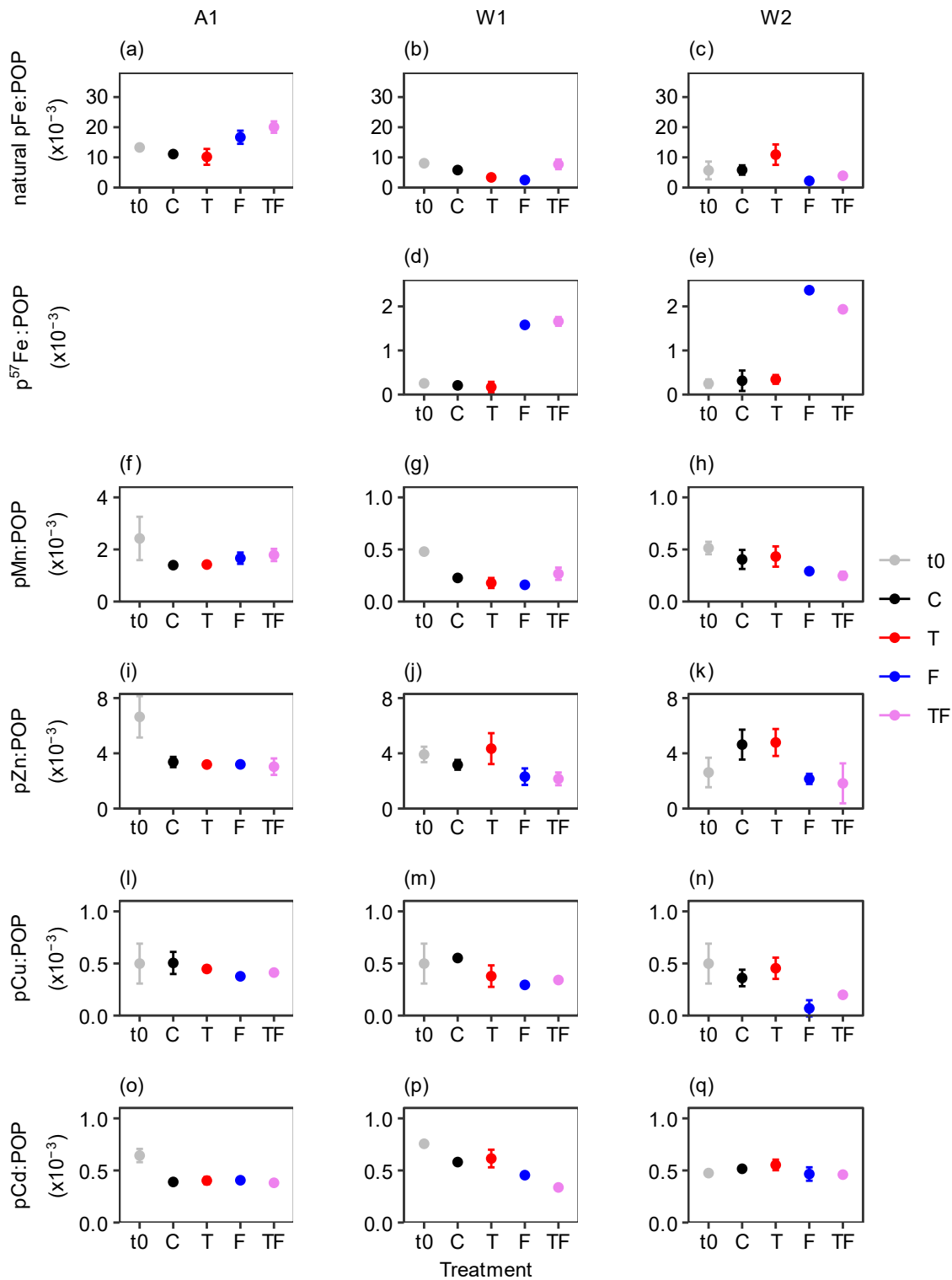
506

507 Particulate Fe concentrations (natural pFe for A1, p⁵⁷Fe for W1 and W2) increased over time for the Fe addition
508 treatments (Table S821 (Metadata), Table S8) in all bioassays examined (excluding A2 as particulate metals were
509 not measured there), and pFe concentrations at the last day of incubations were (positively) impacted by Fe-
510 addition ($p \leq 0.01$, $\eta^2 \geq 0.73$ for A1, W1 and W2, final concentrations were 8.01 ± 0.83 , 1.09 ± 0.10 , 0.89 ± 0.33
511 nM for Fe addition treatments and 4.40 ± 0.21 , 0.08 ± 0.02 , 0.09 , $SD < 0.01$ nM for treatments without Fe addition
512 for A1, W1 and W2, respectively).

513 To examine potential differences in phytoplankton trace metal stoichiometry in response to Fe addition and/or
514 warming, we calculated the ratio of pFe and other trace metals (pMn, pZn, pCd and pCu) to POP concentrations
515 (Fig. 3, Table S821). The initial lithogenic fraction of particulate trace metals was on average 60% in Amundsen
516 Sea compared to 52% in the Weddell Sea. Particulate Al, and hence the estimated lithogenic particle
517 concentrations, remained in the same range between the start and end of the experiments (Table S20) and thus the
518 lithogenic particles provided a consistent background that did not affect observed changes between treatments.

519 Fe-addition significantly increased pFe:POP ratios (natural pFe for A1 and p⁵⁷Fe for W1, W2, Table S11) for all
520 bioassays ($p \leq 0.01$, $\eta^2 \geq 0.73$; average 2.5-fold change for natural pFe:POP (A1) and 13.3-fold change for
521 p⁵⁷Fe:POP in Weddell Sea bioassays for Fe-addition treatments compared to the control). Furthermore, the
522 pMn:POP ratios increased (by 0.33 compared to C) due to Fe-addition in bioassay A1 and decreased (by 0.13
523 compared to C) in W2 ($p < 0.01$ and 0.004 , η^2 : 0.74 and 0.76, respectively). For bioassay W1, neither Fe nor
524 temperature alone had a significant impact on the pMn:POP ratio, however, the combination of both treatments
525 tested significant ($p = 0.01$, η^2 : 0.63), with the TF treatment showing an average 1.4-fold changed ratio compared
526 to all other treatments. Also, the pCd:POP ratio was significantly affected by Fe-addition in W1 and W2 ($p < 0.05$,
527 η^2 : 0.76 and 0.39 for W1 and W2), showing decreased values (by on average 0.12) for Fe-addition treatments
528 compared to the control (Fig. 3 o-q), however no effect was seen for bioassay A1. A similar outcome was observed
529 for pZn:POP ratios ($p \leq 0.01$, η^2 : 0.65 and 0.76 for W1 and W2, respectively, by on average 1.8 compared to C).
530 For pCu:POP ratios, a decrease due to Fe-addition was mainly observed in bioassay A1 and W2 ($p < 0.009$, $\eta^2 \geq$
531 0.73 , by on average 0.16 compared to C), while for bioassay W1, Fe-addition caused a notable, but not statistically
532 significant effect ($p = 0.09$, η^2 : 0.32, Fig. 3, by on average 0.23 compared to C).





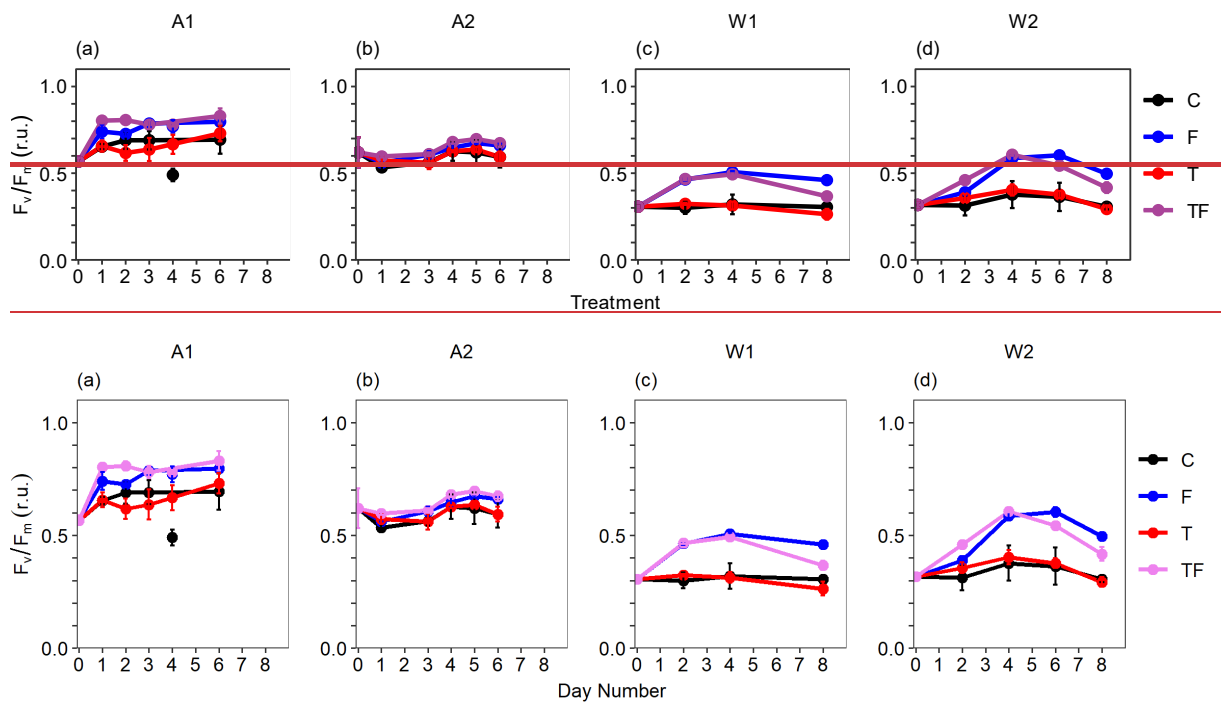
534

535 **Figure 3:** Average ratios (x10⁻³, mM:M) of particulate trace metal to particulate organic phosphorus (POP) for Amundsen
 536 Sea A1 (a, f, h, l, o) and Weddell Sea W1 (b, d, g, j, m, p) and W2 (c, e, h, k, n, q) bioassays. There is no data available for
 537 A2. pFe = natural particulate, p⁵⁷Fe = particulate iron in the ⁵⁷Fe form (not added to Bioassay A1), pMn = particulate
 538 Manganese, pZn = particulate Zinc, pCu = particulate copper, pCd = particulate cadmium. t0 are starting ratios, whilst ratios
 539 for C (control), T (temperature), F (iron) and TF (combination of temperature and iron) were measured on the last day of the
 540 incubations (day 6 and 8 for Amundsen and Weddell Sea bioassays, respectively). Error bars indicates the standard deviation
 541 (n = 2 or 3), except for bioassay A1, T-treatment for all ratios and bioassay W1 C treatment for the pFe:POP ratio, there n =
 542 1. If the error bar is not visible, then it is smaller than the symbol. Please note the different y-axis ranges for manganese to
 543 POP ratios (f-h).

3.32 Photosynthetic efficiency

The photosynthetic efficiency F_v/F_m at the start of the incubations was 2-fold lower for the Weddell Sea bioassays compared to the Amundsen Sea bioassays (i.e., 0.3 vs 0.6 r.u., respectively). Fe addition led to an increase of F_v/F_m for all bioassays (Fig. 4, $p \leq 0.009$; $\eta^2 > 0.68$ for all bioassays, Table S12), with stronger increases in Weddell Sea compared to Amundsen Sea bioassays (average of 1.42- and 1.14-fold change for Fe addition (F and TF) versus control treatments for Weddell and Amundsen Sea bioassays, respectively). Towards the end of the incubations of W1 and W2, F_v/F_m decreased slightly again for the Fe addition treatments (most so for TF, with final F_v/F_m values being still higher than for C and T treatments), coinciding with Fe depletion (Fig. 2).

552



553

554

Figure 4: Temporal dynamics of the photosynthetic efficiency (F_v/F_m , relative units) of the phytoplankton for the Amundsen Sea A1 (Aa), A2 (Ab) and the Weddell Sea W1 (Ac) and W2 (Ad) bioassays. The black line represents the control (C) treatment, the red line the temperature (T) treatment, the blue line the iron (F) treatment, and the purple line the combined temperature and iron (TF) treatment. Averages of triplicates with error bars representing the standard deviation; if not visible it is smaller than the symbol. The control treatment of bioassay A1 showed an outlier for F_v/F_m values on day 4, which was excluded.

561

3.43 POC, Chl a, and phytoplankton taxonomic community composition

Total Chl a concentration at the start of the incubations (Table 1) was highest for the ASP bioassay A1 ($3 \mu\text{g L}^{-1}$) and lowest for bioassay A2 outside the ASP ($0.4 \mu\text{g L}^{-1}$). Of the Weddell Sea bioassays, W1 had the highest Chl a starting concentration (1.5 compared to $0.6 \mu\text{g L}^{-1}$ for W1 and W2). Starting concentrations of total POC in A1

565

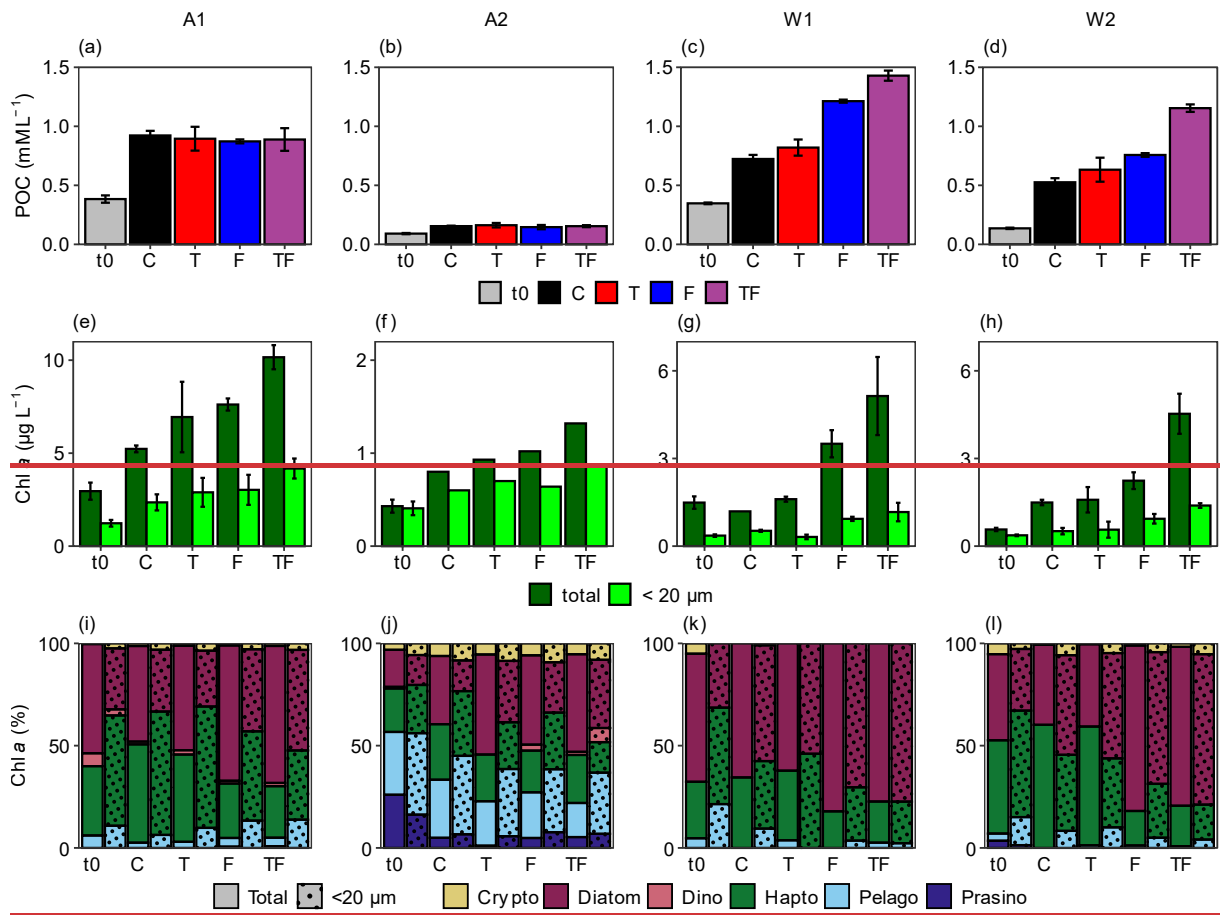
566 and W1 were higher than A2 and W2 (384 and 347 $\mu\text{g L}^{-1}$ compared to 91 and 136 $\mu\text{g L}^{-1}$, respectively). The POC
567 to Chl *a* ratio was lower for A1 (130) than the other bioassays (212-239). Total POC concentrations did not display
568 differences between treatments at the end of the incubations for A1 and A2 (Fig. 5a-d), yet total Chl *a*
569 concentrations exhibited treatment-specific differences for all bioassays (Fig. 5e-h, [Table S13](#)). Only bioassays
570 W1 and W2 showed a significant increase in bacterial abundances with Fe addition (final abundance 4.7 ± 0.9 ,
571 4.5 ± 0.5 vs 3.1 ± 1.0 and 4.7 ± 0.6 , 5.4 ± 0.2 vs 4.4 ± 0.1 for F, TF vs C treatments in W1 and W2, respectively,
572 Table S12). However, bacteria did not have a major effect (less than 3%) on total POC concentrations. Fe-addition
573 always positively impacted Chl *a* concentrations (p : 0.02, 0.005 and 0.006, η^2 : 0.52, 0.76 and 0.67 for bioassays
574 A1, W1 and W2; not tested for A2 due to $n = 1$ for all Chl *a* samples and W1 C due to $n = 1$), however the effect
575 was stronger in Weddell Sea Bioassays (average of 1.6- and 2.9-fold difference for Amundsen and Weddell Sea
576 with Fe addition compared to C). Amundsen Sea bioassays also showed a slight increase in Chl *a* with increased
577 temperatures. Strongest treatment-specific increases in Chl *a* concentrations were, however, obtained for the TF
578 treatment in all bioassays, resulting in an average of 1.7 μg more Chl *a* L^{-1} compared to the F treatment. POC
579 concentrations in W1 and W2 showed similar treatment responses as total Chl *a* in these bioassays.

580 The TF treatment also caused the strongest increase for the $< 20 \mu\text{m}$ Chl *a* fraction (Fig. 5 e–h) for all bioassays,
581 and Fe-addition generally had a positive impact on $< 20 \mu\text{m}$ Chl *a* concentrations, with effects being strongest in
582 both Weddell Sea bioassay W1 and W2 (increases of 1.2, 0.2, 0.5 and 0.7 $\mu\text{g L}^{-1}$ for A1, A2, W1 and W2 compared
583 to the control, respectively and $p = 0.04$ and 0.006, η^2 : 0.37 and 0.67. A2 and W1 were not tested due to missing
584 replicates). The $< 20 \mu\text{m}$ fraction at the start of the bioassays made up respectively 42, 24 and 65 % of total Chl *a*
585 in A1, W1 and W2, whereas for bioassay A2 95 % of the total Chl *a* concentration was $< 20 \mu\text{m}$. At the end of
586 the bioassays, shares were 42, 25, 35 % and 70 % for A1, W1, W2 and A2, respectively.

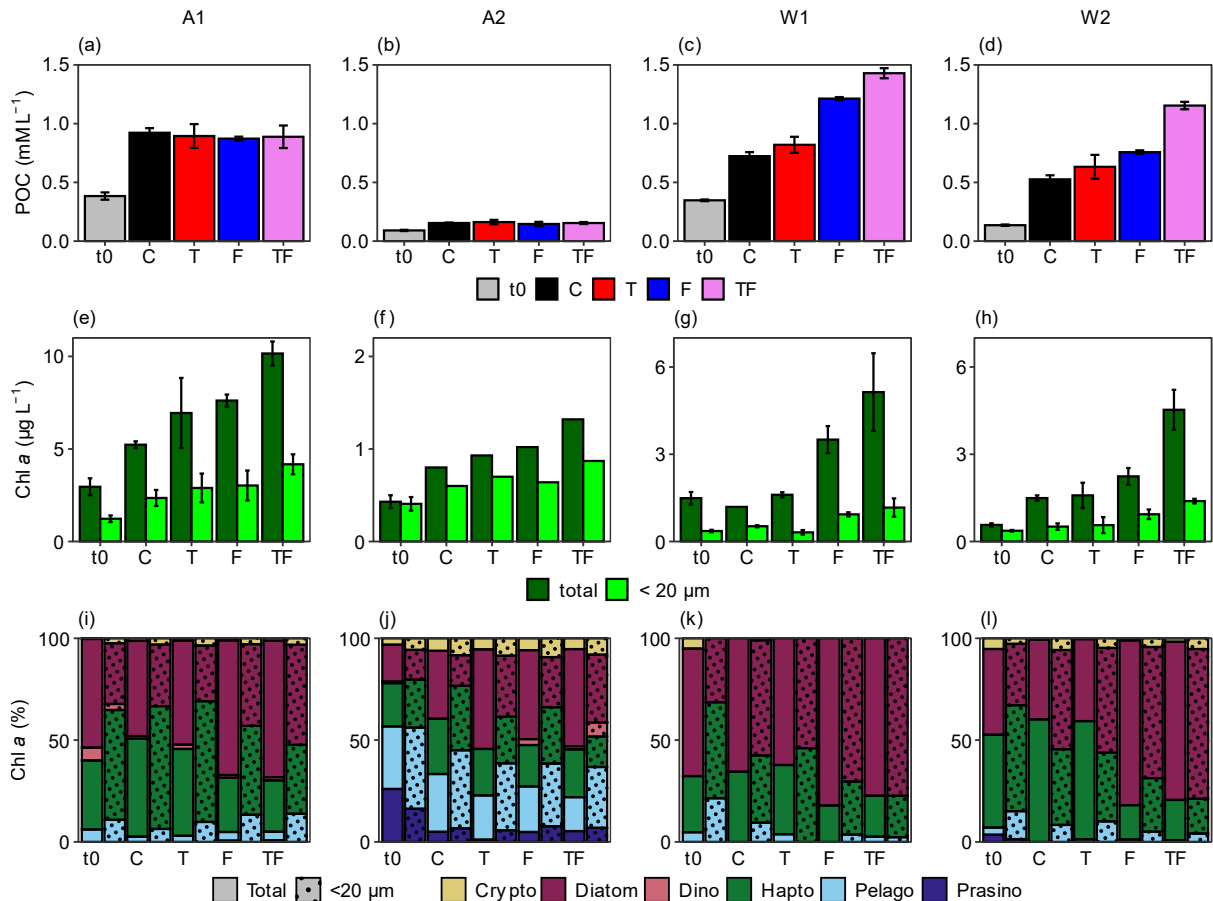
587 Diatoms dominated the phytoplankton community at the start of A1 and W1 (53 and 62 % of total Chl *a*), followed
588 by haptophytes (34 and 27 %; Fig. 5i-l). Bioassay W2 had a comparable share of diatoms and haptophytes (42
589 and 46 % of total Chl *a*), whilst the phytoplankton community of A2 was taxonomically most diverse.

590 Diatoms showed in general a strong response to Fe addition (F and TF treatment) and could be defined as an
591 indicator group for Fe addition treatments in A1 and W2 ($p < 0.005$). Absolute diatom abundances increased as
592 well with Fe-addition, especially for the TF treatment, in bioassays A1 (F and TF treatment, $p = 0.007$) and W2
593 (TF treatment, $p = 0.02$, [Table S821](#)). In bioassay W2, diatoms also showed a higher share for Fe addition
594 treatments in the $< 20 \mu\text{m}$ fraction ($p < 0.05$), with absolute abundances being higher in the TF treatment for
595 bioassays A1, W1 and W2 ($p < 0.04$), and bioassay W1 also showing higher abundances at the F treatment ($p =$

596 0.04). The contribution of haptophytes declined (in response to the diatom increase, also in W1 where the diatom
 597 response was not significant, $p < 0.007$), however their absolute concentration (in $\mu\text{g Chl } a \text{ L}^{-1}$; Table S821) did
 598 not decline except for the F-treatment in bioassay W2 ($p = 0.01$). Both the share ($p = 0.01$) and absolute
 599 concentration ($p = 0.04$) of pelagophytes increased with Fe addition in the $< 20 \mu\text{m}$ fraction of bioassay A1.
 600 Cryptophyte abundances increased in the total fraction of the TF treatment for A1 and W2 ($p = 0.02$ and 0.01 ,
 601 respectively), and the $< 20 \mu\text{m}$ fraction in W1 ($p = 0.02$), however their share did not change with treatments.



602



603

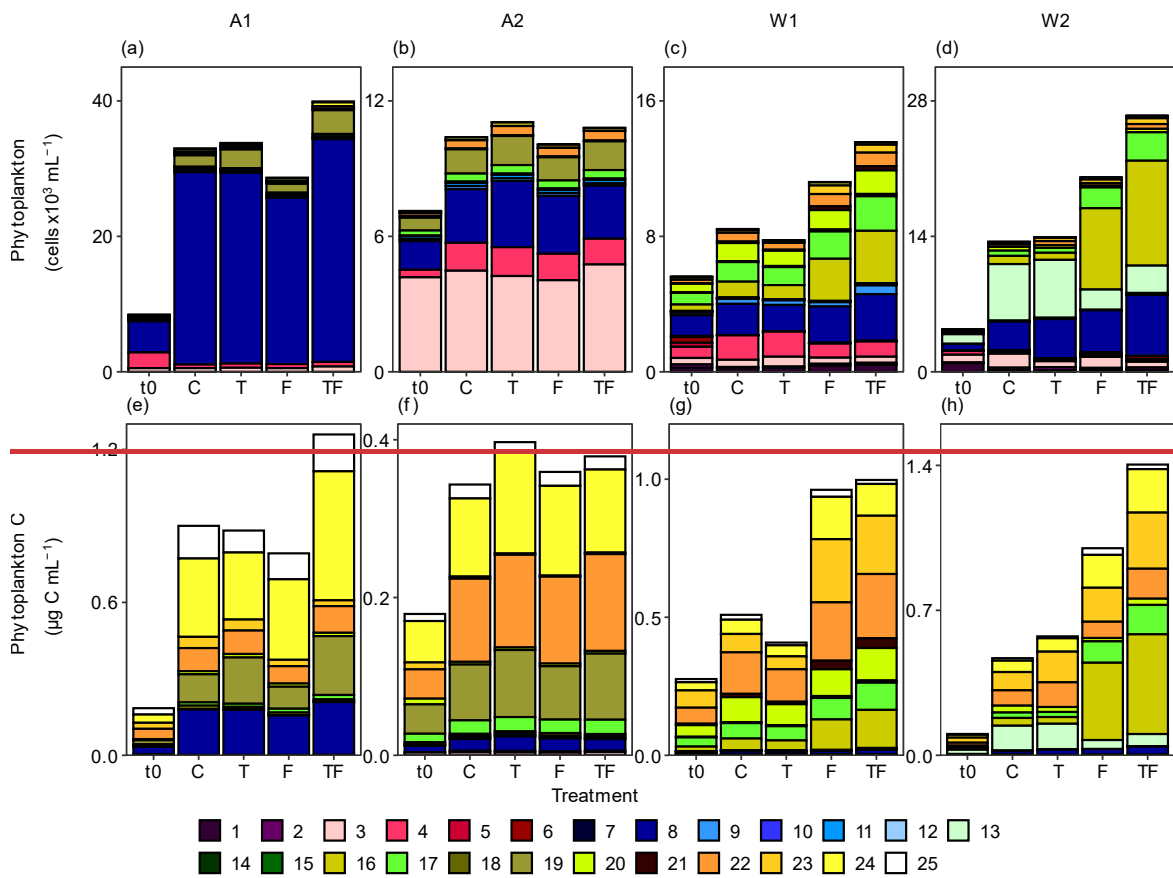
604 **Figure 5:** Average concentrations of particulate organic carbon (POC, a-d), total and < 20 μm (dotted columns) Chl *a* (e-h),
 605 and the taxonomic composition of the phytoplankton community (i-l, % of total Chl *a*) for the Amundsen Sea A1 (a, e, i)
 606 and A2 (b, f, j), and the Weddell Sea W1 (c, g, k) and W2 (d, h, l) bioassays. Error bars represent the standard deviation (n =
 607 3 except when no error bar is shown, then n = 1). t0 = starting conditions, C = control, T = temperature treatment, F = iron
 608 addition treatment, TF = temperature and iron addition treatment. For i-l, Crypto, Dino, Hapto, Pelago and Chloro stands for
 609 cryptophytes, dinophytes, haptophytes, pelagophytes and chlorophytes, respectively. Solid bars represent the total and
 610 shaded bars the < 20 μm fraction community composition. Note the difference in y-axis for the Chl *a* panels e-h.

611

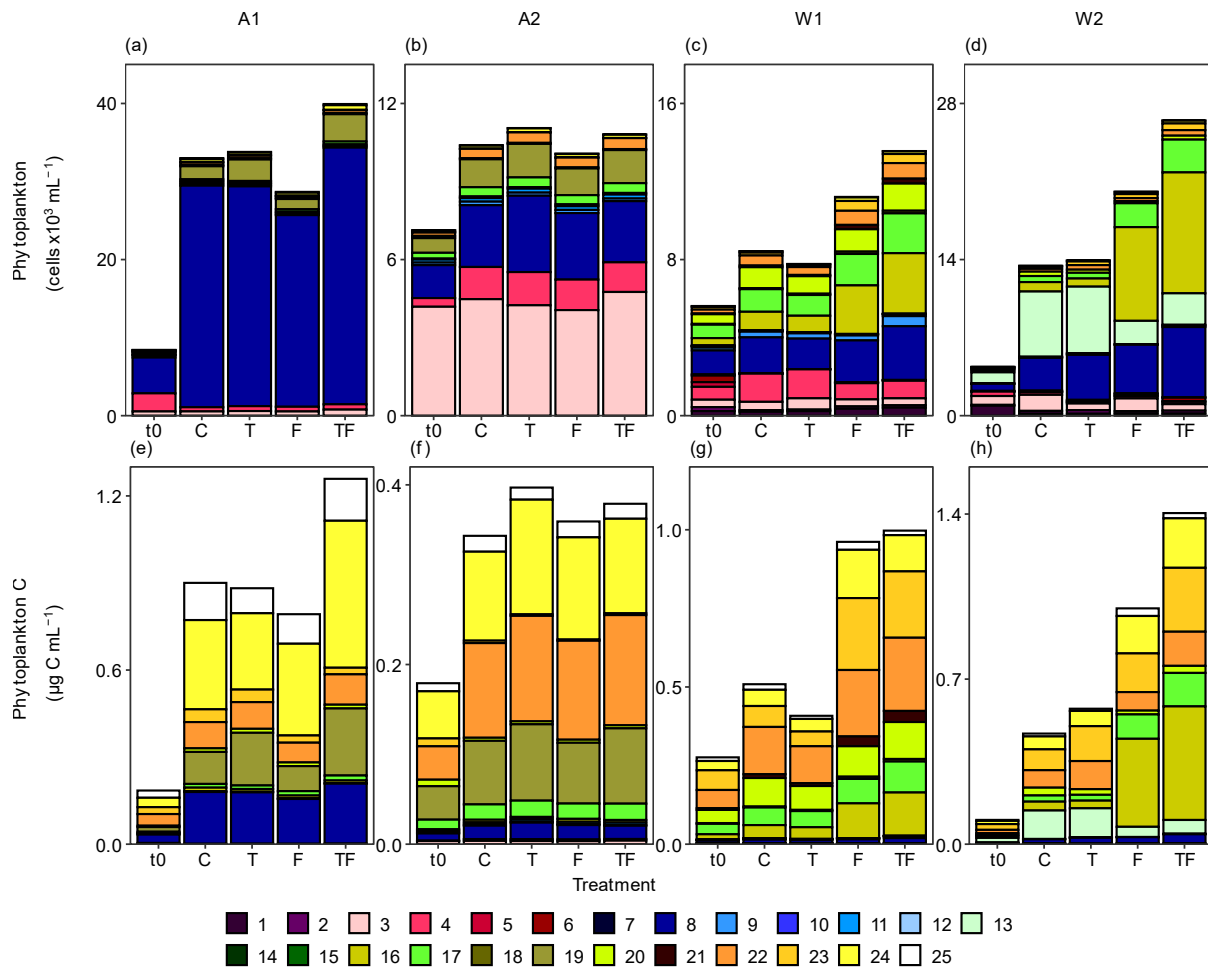
612 3.54 Phytoplankton abundances

613 The total abundances of < 20 μm phytoplankton (Fig. 6, Fig. S35, Table S821) increased with time for all
 614 bioassays and the treatment-specific dynamics largely mimicked the responses observed for the < 20 μm Chl *a*
 615 fraction (Fig. 5e-h, Table S12). Bioassay A1 had overall the highest phytoplankton abundances (up to 40,000 ±
 616 4,000 cells mL⁻¹ for the TF treatment; Fig. 6a) and was dominated by *Phaeocystis antarctica* Phyto 8 (highest
 617 abundances of 37,053 mL⁻¹ were observed in the TF treatment; Table S821). Phyto 19 increased specifically in
 618 abundance and share (Fig. 6a, Table S14) specifically in the temperature treatments, with net growth rates of 0.40
 619 ± 0.08 d⁻¹ and 0.52 ± 0.005 d⁻¹ for the T and TF treatments (compared to 0.35 ± 0.11 d⁻¹ and 0.30 ± 0.09 d⁻¹ for
 620 C and F treatments, p < 0.04, Table S15) and final abundances of 2,800 and 3,500 cells mL⁻¹ for T and TF (
 621 compared to 1,700 and 1,300 mL⁻¹ for C and F, p < 0.01). Phyto 3 also showed higher abundance-derived net
 622 growth rates with warming (0.33 ± 0.13 and 0.32 ± 0.002 vs 0.26 ± 0.06 d⁻¹ for the T, TF and C treatment,

623 respectively), but with abundances being only significantly higher for the TF treatment (776 ± 37 vs 542 ± 107
 624 cells mL⁻¹ for TF and C treatments). Phyto 24 was positively impacted by Fe addition, particularly the TF treatment
 625 resulted in higher net growth rates and final abundances (i.e., 0.32 ± 0.09 vs 0.15 ± 0.06 d⁻¹, and 595 ± 62 vs 361
 626 ± 9 cells mL⁻¹ for TF compared to the C treatment; $p < 0.05$). for C and TF treatment, respectively ($p < 0.05$).
 627 When converted to cellular carbon based on cell volume using 237 and 196.5 fg C μm^{-3} -as conversion factors for
 628 Pico- and Nanophytoplankton, respectively (Fig. 6e), the strong positive response of the phytoplankton to the TF
 629 treatment was mostly due to this larger-sized Phyto 24 (average diameter of 19 μm , $p = 0.01$, stat: 0.92) and to
 630 smaller extent Phyto 19 ($p < 0.01$).



631



632

633 **Figure 6:** Flow cytometry-based phytoplankton community composition (a-d) and carbon (e-h) at the start (t0) and the end
 634 of the bioassay incubations for the different treatments (average of triplicates) for Amundsen Sea bioassays A1 (a, e), A2 (b,
 635 f), and Weddell Sea bioassays W1 (c, g) and W2 (d, h). t0 = starting conditions, C = control, T = temperature treatment, F =
 636 iron addition treatment, TF = temperature and iron addition treatment. Phytoplankton groups are sorted by size, with Phyto 1
 637 – 6 $\leq 3 \mu\text{m}$, Phyto 7 – 20 $\leq 10 \mu\text{m}$ and Phyto 21 – 25 $\geq 10 \mu\text{m}$. Phyto 5, 6, 7, 11, 12 and 14 are cryptophytes, Phyto 20, 22 –
 638 25 diatoms and Phyto 8 *Phaeocystis antarctica*. Note the different scales.

639

640 Bioassay A2 presented the highest share of picoeukaryotes, especially Phyto 3 (59 % compared to max. 18 % in
 641 the other bioassays, Fig. 6b). Only few ~~No apparent~~ treatment-specific responses were recorded, ~~apart from~~ Phyto
 642 19 ~~that~~ increased somewhat with warming ($p = 0.04$), and Phyto groups 16 and 17 showed increased net growth
 643 rates with Fe addition (0.31 ± 0.22 and 0.23 ± 0.06 vs 0.09 ± 0.16 and 0.31 ± 0.06 , 0.30 ± 0.06 and 0.23 ± 0.06
 644 for the F, TF and C treatments of Phyto 16 and 17, respectively, $p < 0.02$ for both, Table S14, Table S16). The
 645 phytoplankton populations in W1 were distributed more equally (Fig. 6c), with higher abundances of especially
 646 Phyto 16 and 17 for the Fe addition treatments ($p < 0.05$, most pronounced for TF with average abundances of
 647 $3,103 \pm 1,290$ vs 948 ± 218 cells mL^{-1} and $2,041 \pm 572$ vs $1,158 \pm 216$ cells mL^{-1} for Phyto 16 and 17 in the TF vs
 648 C treatments, respectively, Table S14). Their specific net growth rates were up to 2.2-fold higher for the Fe
 649 addition treatments than the control (0.29 ± 0.02 , 0.38 ± 0.10 and 0.20 ± 0.02 , and 0.16 ± 0.02 , 0.21 ± 0.06 and

650 0.09 ± 0.02 d⁻¹ for the F, TF and C treatment of Phyto 16 and 17, Table S17). When expressed in carbon, Phyto
651 16 was still a recognisable indicator species (p = 0.03) but at the same time the larger-sized Phyto 21 (average cell
652 diameter of 10 μm) and diatoms Phyto 22-24 (13-19 μm) showed clear positive responses to Fe addition (Fig. 6g,
653 p < 0.05 for all). Net growth rates were largely comparable for these phytoplankton groups: 0.23 ± 0.02, 0.19 ±
654 0.01, 0.17 ± 0.04, 0.20 ± 0.05d⁻¹ for Phyto 21-24 in the F treatment (and similar net growth rates in the TF
655 treatment) compared to 0.09 ± 0.07, 0.14 ± 0.03, 0.04 ± 0.04, 0.12 ± 0.02 in the C treatment, respectively (p <
656 0.03). Bioassay W2 also showed a distinct shift in favour of Phyto 16 and Phyto 17 (away from Phyto 13) with
657 Fe addition, already early in time (Table S821), both for abundances and cellular carbon (Fig. 46d, h, p < 0.01 for
658 all, Table S14). The F treatment net growth rates of Phyto 16, 17 and Phyto 13 were 0.42 ± 0.02, 0.34 ± 0.03 and
659 0.21 ± 0.09 d⁻¹ (again with similar growth in the TF treatments) compared to 0.20 ± 0.03, 0.17 ± 0.04 and 0.37 ±
660 0.02 d⁻¹ in the C treatment (p < 0.03, Table S18). Diatoms 23 and 24 also responded positively to Fe addition with
661 ~2-fold higher net growth rates than the control (Fig. 6h, p < 0.01). Phyto 23 net growth rates were 0.37 ± 0.06
662 and 0.39 ± 0.04 d⁻¹ for F and TF compared to 0.19 ± 0.06 d⁻¹ for the C treatment (p = 0.004), and Phyto 24 net
663 growth rates were 0.38 ± 0.08 and 0.32 ± 0.05 for F and TF treatments vs 0.22 ± 0.09 for the C treatment. Diatom
664 24 responded positively to Fe addition (F and TF, Fig. 16h, p < 0.01), similar as for bioassay W1, and diatom
665 Phyto 23 showed higher abundances for the TF treatment (p = 0.04) Phyto 19 was the only phytoplankton
666 population that showed a consistent selective positive response (in share) to warming (and not to Fe addition) in
667 the Amundsen Sea bioassays. Diatom Phyto 22 increased with temperature in bioassay W2 (p ≤ 0.01). We refer
668 to Table S821 for less pronounced responses of the other phytoplankton populations. Overall, the response by the
669 larger phytoplankton populations is also illustrated by the higher average cellular biovolumes in the F and TF
670 treatments of W1 and W2 (Fig. S64). The Amundsen Sea bioassays did not show a treatment-specific increase in
671 phytoplankton biovolume. Fe-addition had a significant effect on total phytoplankton abundances for Weddell
672 Sea bioassays (p < 0.02, η²: 0.596 and 0.74 for W1 and W2, with Fe addition leading to an average 1.6-fold change
673 compared to C). The GLM we performed (explained deviance: 86 %), indicates an interaction effect of Fe-addition
674 and warming (p = 0.03 for the interaction, exponentiated coefficient (ec): 1.13), i.e. Fe-addition of 2 nM in
675 combination with a 2 °C temperature increase led to an overall increase in algal abundances of about 28 %. Fe-
676 addition (ec: 1.03), temperature increase (ec: 1.11), bioassay and day number (p < 0.001 for all, for other statistical
677 parameters, see Table S920) were also significant explanatory factors. The NMDS analysis of the Weddell Sea
678 bioassays (Fig. S57c, d) demonstrated clear distinction between the Fe addition treatments and the non-addition
679 treatments after the second day of the incubations. For bioassay W1, the TF and T treatments clustered on the last

680 day of incubation separately from the F and C treatments, respectively. For bioassay W2, the T treatment also
681 separated on the last day while the TF and F treatments remained closer together. Bioassays A1 and A2 did not
682 display obvious clustering by treatment, other than time (i.e., separation after day 2).

683

684 4. Discussion

685 4.1 Trace metal and macronutrient dynamics

686 The pFe concentrations showed the expected significant increase in the Fe addition treatments for both Amundsen
687 (natural dFe added) and the Weddell Sea bioassays (d⁵⁷Fe added) at both temperatures, indicating that the added
688 dFe was indeed taken up and incorporated in the phytoplankton cells. Additionally, in bioassay W2 the final p⁵⁷Fe
689 in the TF treatment was higher than in the F treatment (1.12 ± 0.11 nM compared to 0.66 ± 0.20 nM),
690 demonstrating enhanced Fe uptake with higher temperatures.

691 The higher starting concentrations of dFe in the Amundsen Sea, compared to the Weddell Sea, can be attributed
692 to the Fe input from basal melt (Rignot et al., 2013). Conversely, the naturally low dFe concentrations in the
693 Weddell Sea underscore the area's limited Fe input (e.g., de Baar et al., 1990; Klunder et al., 2011).

694 Fe is needed in nitrate assimilation and as such uptake of nitrate is coupled to the Fe nutritional status (Schoffman
695 et al., 2016, [Milligan and Harrison, 2000](#)). Similarly, diatom cellular silicate to nitrogen ratios are known to
696 increase in response to Fe stress (Meyerink et al., 2017). Highest drawdown of the macronutrients typically

697 occurred in the TF treatment, which also showed the largest phytoplankton accumulation ([Table S20, Table S21](#)).

698 However, whilst dissolved inorganic phosphate and nitrogen drawdown was mostly affected by Fe addition,
699 silicate drawdown in bioassays A1 and W2 was more impacted by temperature. Despite a lower Chl *a*

700 concentration (both total and < 20 μm) and phytoplankton abundance for the T than the TF treatment in these

701 bioassays, the silicate drawdown was comparable. Although Fe stress is reported to cause reduced cellular Chl *a*

702 concentrations compared to Fe replete conditions (Greene et al., 1992), it is an unlikely cause as the total

703 phytoplankton abundances displayed similar differences between the T and TF treatment compared to < 20 μm

704 Chl *a* concentrations. Instead, higher temperature may have stimulated Si uptake, as reported for the diatom

705 *Pseudonitzschia seriata* at temperatures above 0 °C (Stapleford & Smith, 1996). It might also be that the T

706 treatment experienced higher Fe stress than the control, which is also known to increase Si uptake (Meyerink et

707 al., 2017). However, since phytoplankton abundances, F_v/F_m and Chl *a* concentrations were not higher in T

708 treatments compared to the control, and since phytoplankton requires less Fe at higher temperatures (Jabre &

709 Bertrand, 2020), this is less likely. Bioassay W1 showed the strongest decline in silicate concentrations, with both

710 temperature and Fe affecting silicate drawdown. The relatively high fraction of diatoms (and specifically the large-
711 sized Phyto 20 and 22-24) in bioassay W1 could theoretically have caused the strong silicate drawdown and high
712 ratio of silicate relative to nitrogen (or phosphorus) uptake for all treatments. However, A1 also had high diatom
713 abundances and over the course of the incubations the concentration of diatoms in W2 became comparable to W1.
714 An alternative explanation may be that Mn stress in W1 (0.06 ± 0.04 vs 0.19 ± 0 nM in W1 and W2, respectively)
715 enhanced Si uptake, similar to Fe stress (Hutchins & Bruland, 1998). Increased Si uptake by diatoms under a
716 combined Fe and Mn limitation may possibly enhance protection against grazers (Assmy et al., 2013; Ryderheim
717 et al., 2022) and/or enhance sinking to more nutrient-rich depths (Waite & Nodder, 2001). Considering an
718 increasing awareness of trace metal co-limitation of phytoplankton growth (Wu et al., 2019; Browning et al.,
719 2021; Balaguer et al., 2022; Burns et al., 2023), we recommend further investigation into these potential
720 interactions and their ecological relevance in future studies.

721 Dissolved Mn is known to (co-)limit Southern Ocean phytoplankton growth and community composition together
722 with Fe (Browning et al. 2021, Balaguer et al. 2022). Under such conditions, Fe addition alone positively impacts
723 Chl *a* concentrations, phytoplankton abundances and POC concentrations, but a combination of dFe and dMn
724 addition can lead to higher increases in these variables (Pausch et al. 2019, Browning et al., 2021). Nevertheless,
725 dMn addition effects can often be masked by the effects of Fe addition (Latour et al. 2023), and Fe addition alone
726 can already lead to increases in Chl *a* even in primarily Mn-limited areas (Browning et al., 2021). This fits our
727 results showing increases in Chl *a* concentrations with Fe addition. Also net growth rates based on total
728 phytoplankton abundances showed increases (i.e. 1.5 (0.20 ± 0.05 vs 0.12 ± 0.02 d⁻¹) and 1.4-fold (0.24 ± 0.01
729 vs 0.18 ± 0.01 d⁻¹) higher for Fe-addition treatments (F and TF) compared to the control for bioassays W1 and
730 W2. The lower starting concentrations of dMn in W1 compared to W2 may have contributed to the 2-fold lower
731 phytoplankton net growth rates in W1 compared to W2, independent of the treatment. Our data indicate potential
732 dMn/dFe colimitation in the Weddell Sea already in early summer. Since the requirements for dMn and dFe differ
733 between different phytoplankton groups (Arrigo, 2005; Twining & Baines, 2013; Balaguer et al., 2023), we
734 suggest that the (co-)limitation of dMn and dFe may be affected by phytoplankton community composition.
735 Considering that Mn limitation can be seasonal (Latour et al., 2023), we also urge to study different stages of the
736 phytoplankton bloom period.

737 Although Fe addition (F and TF treatments) led to 1.8 (0.11 ± 0.03 vs 0.06 ± 0.02 d⁻¹) and 1.5 fold (0.23 ± 0.02
738 vs 0.15 ± 0.01 d⁻¹) higher net growth rates (based on total phytoplankton abundances) in W1 and W2 compared
739 to the control. The lower starting concentrations of dMn in W1 compared to W2 may have contributed to the 2-

~~fold lower phytoplankton net growth rates in W1 compared to W2, independent of the treatment. Since Fe addition still led to an increased growth rate even with low dMn concentrations, Fe must have been the main limiting factor.~~

4.2 Micronutrient stoichiometry

The observed pFe:POP ratios increased upon the addition of iron (natural pFe for bioassay A1 and p⁵⁷Fe for bioassays W1 and W2), validating the experimental design and confirming the uptake of added dFe by phytoplankton. For other bio-essential (Mn, Zn, Cu) or bio-active (Cd) metals, the metal:POP ratio is expected to be elevated under Fe stress due to upregulation of non-specific divalent metal transporters under Fe stress (e.g., Kustka et al., 2007; Lane et al., 2008) or the increased uptake of phosphorous relative to metals under Fe replete conditions (growth-dilution; Cullen et al., 2003). Specifically for Mn, this might also be due to a higher cellular Mn requirement under Fe stress (Peers & Price, 2004). The pMn:POP ratios were indeed higher in the C and T treatments compared to the F and TF treatments of W2, but for W1, no consistent effect of Fe was observed (Fig. 3). In contrast, slightly elevated pMn:POP ratios were observed after Fe addition in A1 (F and TF treatments), matching findings by McCain et al. (2021) and Hawco et al. (2022), showing increased Mn demand in environments with high Fe concentrations. This duality in the pMn:POP ratios is not surprising as Mn demand may not only increase under Fe stress, but it should also increase with Fe addition, as both Mn and Fe are required for photosynthesis (Raven 1990, McCain 2021, Hawco et al. 2022). Hence, in an environment with low dMn concentrations, Fe addition can consequently lead to Mn limitation (e.g., Hawco et al., 2022). Dissolved Mn concentrations at the start of bioassay A1 were relatively high, and indeed pMn:POP ratios increased with Fe addition, while concentrations of dMn decreased during the experiment. However, the low (potentially phytoplankton growth limiting) dMn concentrations in Weddell Sea bioassays from the start might have prevented a noticeable positive effect of Fe addition on Mn uptake. The higher biomass and cell abundance after Fe addition in these experiments implies the community had to make due with less Mn per cell than in the treatments without Fe addition (likely resulting in relatively low Mn quota despite elevated demand), potentially explaining why there was an increase in the pMn:POP ratios in the C and T treatments of W2, whereas this was not observed in W1 with even lower dMn starting concentrations. Such variation in apparent Mn demand and quotas likely reflects adaptive changes in nutrient uptake and storage mechanisms under nutrient stress but could also be due to different phytoplankton community compositions and/or environmental conditions. For example, Twining et al. (2004) observed elevated pMn:POP ratios in individual diatom cells under iron deplete conditions, relative to iron replete

770 conditions, whereas the trend was opposite for autotrophic flagellated cells. However, diatoms were dominant in
771 the F and TF treatments in all experiments, suggesting that other factors besides differences in community
772 composition play a role. ~~The starting dMn concentrations differed between the bioassays, whereby the high~~
773 ~~starting concentrations of dMn in A1 could potentially explain the increased pMn:POP ratios in the F and TF~~
774 ~~treatments of this experiment. We speculate that a high availability of both Fe and Mn under the low light~~
775 ~~conditions in A1 could have led to increased Mn uptake for use in photosynthesis.~~ Since dMn levels are thought
776 to increase with Fe input (e.g., due to ice shelf melting; Van Manen et al., 2022), we recommend including dMn
777 in future studies examining the effects of global climate change on phytoplankton growth.

778 Besides Mn, other trace metals are known to have variable ratios with respect to POP under different
779 environmental conditions. For example, cellular Cu requirements increase under Fe limitation (Schoffman et al.,
780 2016), which could explain the higher pCu:POP ratios in the C and T treatments compared to the Fe addition
781 treatments in all bioassays analysed (Fig. 3). Similarly, the pZn:POP ratios were also elevated in the non-Fe
782 treatments in W1 and W2, akin to the pCd:POP ratios especially in W1, suggesting higher uptake of metals under
783 Fe limitation as previously suggested (Cunningham & John, 2017). ~~Future studies linking these stoichiometric~~
784 ~~ratios with molecular measurements (e.g. protein expression patterns) could provide further insight into the~~
785 ~~processes which underpin trace metal uptake and use within phytoplankton communities under change.~~
786 ~~Nevertheless, this study highlights a potential trend of increased uptake of essential and non-essential metals~~
787 ~~(specifically zinc, copper and cadmium) by phytoplankton under Fe deplete conditions.~~ This trend of increased
788 uptake of essential (manganese, zinc, copper) and non-essential metals (cadmium) under dFe limitation
789 underscores the adaptive strategies employed by phytoplankton in navigating nutrient scarcities, emphasizing the
790 complexity of nutrient interactions and their collective impact on phytoplankton ecology under varying
791 environmental conditions (e.g., Cunningham and John, 2017). Due to the importance of nutrient uptake in the
792 Southern Ocean for the stoichiometry of global nutrient distributions, notably at lower latitudes (Sarmiento et al.,
793 2004; Middag et al., 2020), changes in (micro-)nutrient consumption in the Southern Ocean can have global
794 ramifications for both productivity and ecosystem structure (Moore et al., 2018) which should be further explored
795 in future (modelling) studies. Future studies underpinning these stoichiometric ratios with molecular
796 measurements (e.g., protein expression patterns) could provide further insight into the processes underlying trace
797 metal uptake and use within phytoplankton.

798

4.3 Impact of ~~Iron and Temperature~~ F and T treatments on Phytoplankton Dynamics

The Weddell Sea bioassays exhibited stronger Chl *a* accumulation, a stronger increase in F_v/F_m and increased phytoplankton abundances in response to Fe addition than the Amundsen Sea bioassays, which is likely due to the lower dFe concentrations (and hence higher degree of Fe limitation for the phytoplankton typical for the Weddell Sea) at the start of the incubations. Indeed, given that the Weddell Sea bioassays were performed early in the productive season, these results imply more severe Fe limitation in the Weddell Sea whereas any Fe limitation in the Amundsen Sea likely only develops later in the season. Consistent with the lower dFe concentrations was the reduced *in-situ* F_v/F_m of the phytoplankton in W1 and W2, which stayed low for non-Fe addition treatments throughout the experiments, as it is a, compared to Amundsen Sea bioassays, which stayed low for non-Fe addition treatments throughout the experiments. Although we cannot exclude that the lower light availability in A1 and A2 may have caused enhanced F_v/F_m (compared to W1 and W2; From et al., 2014), low F_v/F_m is a common indicator of Fe stress in the Southern Ocean (Greene et al., 1992; Mills et al., 2012; Olson et al., 2000; Jabre and Bertrand, 2020). In addition, the low dMn concentration may have contributed to the low F_v/F_m (Wu et al., 2019). The decrease in F_v/F_m in the F and TF treatments towards the end of the Weddell Sea bioassays seem to indicate that the added Fe had depleted again to limiting conditions or that Mn became (co-)limitating.

The location the seawater for bioassay W1 was taken has similar coordinates as bioassay S54-65 in a study by Viljoen et al. (2018). These authors sampled 3 weeks later (different year) and at a comparable depth (30 m vs 20 m in our study) and found largely similar responses by the phytoplankton to Fe addition, i.e., total Chl *a* increased by $\sim 2 \mu\text{g Chl } a \text{ L}^{-1}$ and diatoms dominated the phytoplankton community. In contrast to W1 but comparable to our other bioassays, total Chl *a* concentration in bioassay S54-65 (Viljoen et al. 2018) increased in the control over the duration of the bioassay. The lack of increase in Chl *a* in the control (and T) treatment of W1 might be explained by a lower *in-situ* dFe for W1, indicating a stronger limitation of dFe. At the same time, POC (and $< 20 \mu\text{m Chl } a$) concentrations did show an increase over time in the control treatment of bioassay W1. Moreover, bioassay W2, with even lower starting concentrations of dFe, showed an increase in Chl *a* over time for the control. Given the lowest dMn concentrations in W1, it might be that dMn and not (only) dFe was limiting the production of reaction centres (Raven et al.; 1990), resulting in Chl *a* concentrations to not increase. Given the increased requirement for Mn under low Fe (Peers & Price; 2004), Fe addition may have relieved Mn limitation in the Fe addition treatments slightly, resulting in the observed increase of Chl *a* in those treatments

828 While for the Weddell Sea bioassays the POC concentrations followed comparable responses to total Chl *a* upon
829 Fe addition (Fig. 5), the POC concentrations in the Amundsen Sea bioassays did not. The relatively low Chl:POC
830 ratios in the Weddell Sea bioassays (average over all treatments 0.003 ± 0.003 vs 0.008 ± 0.002 for the Amundsen
831 Sea bioassays) may indicate stronger Fe limitation, since Fe limited cells are known to have a lower Chl:POC
832 ratio compared to non-limited cells (Moore et al. 2007). Alternatively, acclimation to t~~The lower irradiance during~~
833 ~~the incubations of A1 and A2 most likely led to the higher Chl *a*:POC ratios at the end of incubations (i.e., average~~
834 ~~over all treatments 0.008 ± 0.002 and 0.003 ± 0.003 for the Amundsen and Weddell Sea bioassays). Enhanced~~
835 ~~Chl *a*:POC ratios are a known acclimation to low light~~ (Laws & Bannister, 1980; Geider, 1987; Geider et al.,
836 1998; Wang et al., 2009). Despite the low light intensities in Amundsen Sea bioassays, Chl *a* concentrations and
837 phytoplankton abundances in the control treatment increased over time in the Amundsen Sea bioassays (especially
838 in A1, net growth rate based on total abundances of 0.253 ± 0.032 d⁻¹), which indicates that the phytoplankton
839 communities were low light adapted. Low light conditions are common for Amundsen Sea phytoplankton
840 (Schofield et al., 2015; Park et al., 2017) but still, the very low irradiance in A2 seemed to have limited growth
841 (0.09 ± 0.01 d⁻¹) as also illustrated by incomplete depletion of the dFe added (after 6 days of incubation). The high
842 initial F_v/F_m values suggest that the phytoplankton may not have been limited by dFe (under these low light
843 conditions) and would only require more dFe once light intensities increased again (Strzepek et al.; 2019, Vives
844 et al.; 2022, Latour et al.; 2024). The small increase in F_v/F_m in the Fe addition treatments may suggest growth
845 became dFe limited during the incubation (Fe-addition did show a significant effect on F_v/F_m at the last day of the
846 incubations), despite the light conditions remaining low. Considering diatoms being the taxonomic group
847 responding strongest to Fe additions (Noiri et al., 2005; Feng et al., 2010; Hinz et al., 2012; Mills et al., 2012; Zhu
848 et al., 2016), the low proportion of diatoms at the start of A2 may also have delayed a measurable effect of Fe
849 addition.

850 Although earlier studies reported positive responses of phytoplankton to Fe addition also under low light
851 conditions (Viljoen et al., 2018; Alderkamp et al., 2019), the light intensities used for the low light treatment in
852 those studies were still relatively high (i.e., 15 and 30 $\mu\text{mol quanta m}^{-2} \text{s}^{-1}$) and well above those in A1 and A2
853 (average of 3.4 and 1.5 $\mu\text{mol quanta m}^{-2} \text{s}^{-1}$). In addition to higher light levels, the lower initial dFe concentrations
854 in the Ross Sea study (Alderkamp et al. 2019) compared to our study indicate a stronger Fe limitation and
855 subsequently a stronger response to Fe addition. A recent study on Southern Ocean deep chlorophyll maximum
856 phytoplankton responses to Fe addition (Latour et al., 2024) reported a Chl *a* increase at low light intensities
857 (similar to our Amundsen Sea bioassays) and no change of POC (similar to bioassay A2) until light levels

858 increased. This supports our suggestion that the low light condition in A2 was a determining factor for the lack of
859 a response to Fe addition.

860 ~~Since both Weddell Sea and Amundsen Sea bioassays were initiated at times corresponding to the peak~~
861 ~~phytoplankton growth periods in each region, it is unlikely that the sampling time had a major effect on our results.~~

862 Future light conditions in the Southern Ocean will vary for the different regions, e.g., lower sea ice coverage may
863 enhance light availability (Leung et al., 2015; Petrou et al., 2016; Krumhardt et al., 2022), whereas increased cloud
864 coverage in the Antarctic Circumpolar Current region would reduce it (Grise et al., 2013; Kelleher and Grise,
865 2022; Krumhardt et al., 2022). Moreover, there are conflicting reports about whether mixed layer depths will
866 increase (Leung et al., 2015) or decrease (Krumhardt et al., 2022), which directly impacts light conditions for the
867 phytoplankton. Our results from the low light bioassay A2, showing only a small effect of Fe on phytoplankton,
868 suggest that in regions or periods with low light, Fe increase will not drastically stimulate phytoplankton growth.
869 This highlights the importance of including light availability in Southern Ocean ecosystem (modelling)
870 predictions.

871 ~~Nevertheless, Fe addition also had a positive effect on F_v/F_m in Amundsen Sea bioassays, matching earlier reports~~
872 ~~that F_v/F_m of ASP phytoplankton is partly controlled by Fe (Alderkamp et al., 2015).~~

873 Temperature alone showed a limited effect on phytoplankton, with only 3 phytoplankton groups (Phyto 3, Phyto
874 19 and diatom Phyto 22) increasing in abundances, and only Phyto 19 showing a consistent effect. Still, these
875 groups represent pico-sized as well as larger phytoplankton (2, 8.1 and 13.3 μm diameter). Earlier studies also
876 showed temperature to have only a limited effect on (natural) phytoplankton communities (Rose et al., 2009).
877 Indirect effects of warming (e.g., locally high ice-melt induced freshening, dFe increase) will likely have larger
878 impact on phytoplankton community compositions. Ice-melt induced freshening already led to a shift from diatom
879 to cryptophyte and flagellate dominated communities in the Western Antarctic Peninsula region (reviewed by
880 Deppeler and Davidson 2017), and increased dFe concentrations will affect phytoplankton community
881 composition even more so when combined with temperature increases (this study; Rose et al. 2009). Furthermore,
882 the availability of dFe is likely changing due changes in sources (see introduction) but is also influenced by
883 siderophore production (reviewed by Gledhill and Buck, 2012) but warming of the Southern Ocean does not seem
884 to have a direct effect (Sinha et al., 2019). Warming likely increases the growth rates of siderophore producing
885 bacteria (Sinha et. al. 2019), but this may be countered by reduced siderophore production due to ocean
886 acidification (Sinha et al. 2019). Overall, predictions about future conditions and their consequences are complex
887 and have large uncertainty, but it seems likely conditions will be temporally and spatially heterogenous with

888 varying changes in temperature and availability of Fe (and light). For example, while the warming of surface
889 water in the Amundsen Sea has already been observed, Weddell Sea surface temperatures for the deep basin seem
890 relatively stable at the moment with significant warming only below 700 m (Strass et al., 2020). However,
891 upwelling of this warm water leads to local temperature increases in notably coastal regions (Darelius et al., 2023),
892 potentially increasing future temperatures by over 2 °C warmer in troughs that connect the open ocean to ice shelves
893 (Teske et al., 2024), increasing not only temperatures but likely also glacial melt derived Fe supply. This makes
894 it prudent to assess not only individual, but also combined effects of increasing Fe and temperature as discussed
895 in the next section.

896

897 **4. 4 Enhanced responses to Fe with warming**

898 Fe addition led to an overall positive response of Chl *a* concentrations, phytoplankton photophysiology and
899 growth, but more so when combined with the ecologically relevant increase in temperature. The increase in
900 phytoplankton abundances was especially distinct for Weddell Sea bioassays. GLM analysis revealed that
901 temperature alone was a significant factor for total phytoplankton abundances, however more specifically, only
902 Phyto 3, Phyto 19 and Phyto 22 abundances displayed significant positive responses to temperature alone (T
903 treatment). The 2 °C warming alone was thus not a major driver of phytoplankton net growth in our bioassays,
904 but accelerated and enhanced Fe-addition responses (significant interaction effect for iron addition and
905 temperature increase on total phytoplankton abundances). The enhanced response to Fe with temperature was
906 especially distinct for bioassay W2 (average 1.61-fold change in total phytoplankton abundances in the TF
907 treatment compared to both F and T treatments; W1 showed a 1.48-fold average change). Despite low light levels,
908 this was also seen in Amundsen Sea bioassay A1, albeit to a lower extent (average 1.29-fold change in the TF
909 treatment compared to both F and T treatments). Larger-sized (> 20 µm) diatoms were mainly responsible for the
910 Chl *a* accumulation, which is consistent with previous studies (Noiri et al., 2005; Feng et al., 2010; Hinz et al.,
911 2012; Mills et al., 2012; Zhu et al., 2016) and supports the general consensus that especially large phytoplankton
912 show enhanced growth upon Fe addition due to their lower surface to volume ratio (Scharek et al., 1997). But also
913 (slightly) smaller diatoms Phyto 23 and 24 (average cell diameter of 15 and 19 µm, respectively) responded
914 positively to the combination of Fe and temperature. Diatom* Phyto 24 was even the main phytoplankton
915 population responsible for the increase in the < 20 µm Chl *a* fraction of the TF treatment in A1. The NMDS
916 analysis based on < 20 µm phytoplankton abundances showed clustering for W1 and W2 driven by Fe addition
917 and temperature, indicating that also smaller-sized phytoplankton display positive responses. This is supported by

918 increased < 20 µm Chl *a* concentrations and the 2.2 fold change in cellular carbon of < 20 µm phytoplankton in
919 F and TF treatments in the Weddell Sea bioassays (compared to the C and T treatments). Specifically, we recorded
920 distinct abundance increases of the small 7 µm Phyto 16 and Phyto 17, in the F and TF treatments of W2.
921 *Phaeocystis antarctica* (Phyto 8; 3.7 µm) showed higher net growth rates for Fe-addition treatments in both
922 bioassay W1 and also displayed higher abundances under the TF treatment for W2 but the effect was not very
923 apparent and overall, *P. antarctica* seems to handle the other treatments consistently well. Rose et al. (2009) and
924 Zhu et al. (2016) also found diatoms preferentially stimulated by Fe addition and/or temperature over *P.*
925 *antarctica*, which was also found in a broader context where *P. antarctica* dominated under Fe-low conditions,
926 whilst diatoms dominated in regions with higher Fe concentrations (Arrigo et al., 2017). In contrast, Andrew et
927 al. (2019) found comparable growth rates for *P. antarctica* and several diatom cultures (tested under Fe addition
928 and warming treatments). Similar to our study, they found highest growth for the combined Fe addition and
929 warming treatment for most species. Since diatoms tended to increase strongest with Fe addition, it can be
930 speculated that phytoplankton community compositions shift towards more diatoms with increases in Fe
931 concentrations, however other biogeochemical factors are also important to consider. The positive phytoplankton
932 growth responses were population specific and Phyto 13 (5.5. µm) in W2 even showed reduced abundances for
933 the F and TF treatments, underscoring the multifaceted factors controlling phytoplankton dynamics and
934 emphasizing the importance of understanding how trace metal concentrations and climate change together
935 influence the marine ecosystems in the Southern Ocean.

936 Alterations in phytoplankton community composition and cell size, as observed in our experiments, will directly
937 affect top-down control by (microzooplankton) grazers and viral infection and consequently trophic transfer
938 efficiency (Eich et al. 2022, Biggs et al. 2021). Not only will the flow of organic carbon through the food web be
939 affected by the different phytoplankton mortality, also the flux of organic carbon to deeper layers of the ocean
940 (biological carbon pump) depends on the phytoplankton community composition, cell size and type of loss factor.
941 Since the seawater was not filtered before distribution to the cubitainers to reduce contamination risk, there is a
942 chance (although small, Voronina et al., 1994) that large grazers were introduced to the incubations. We did not
943 specifically sample for large grazers but did not notice any on the filters for Chl *a* and POC. Large grazers can be
944 expected to graze on larger phytoplankton (Hansen et al. 1994), thereby reducing phytoplankton net growth. This
945 would be most noticeable for the F and TF treatments, given the positive response of larger phytoplankton to Fe
946 addition. Our results would then be underestimating the effect of Fe enrichment. Moreover, grazing would likely
947 enhance with temperature (e.g., Lewandowska and Sommer, 2010; Karakuş et al., 2022), further reducing (and

948 underestimating) net growth rates of larger phytoplankton specifically in the TF treatment. Also,
949 microzooplankton grazing rates are known to increase with temperature (Chen et al., 2012; Caron & Hutchins,
950 2013), and even viral lysis may occur faster at higher temperature (Maat et al., 2017). This may partially explain
951 the small effect of warming in the bioassays. Besides temperature, Fe availability has been reported to affect algal
952 virus production and infectivity (Slagter et al., 2016; Kranzler et al., 2021). Changes observed in our experiments
953 might thus also have been affected by temperature and/or dFe related changes in loss factors affecting specific
954 phytoplankton groups.

956 5. Conclusions

957 Our study stands out in that it combined trace metal chemistry and biology, Chl *a*, and population abundance to
958 examine co-effects using natural Antarctic phytoplankton communities at environmentally realistic Fe
959 concentrations (+ 2 nM) and a predicted (2 °C) temperature increase (Boyd et al., 2015; Jabre et al., 2021; Andrew
960 et al., 2022). ~~So far, studies investigating combined effects using natural Antarctic phytoplankton communities~~
961 ~~focussed on the Ross Sea and tested 3—6 °C warming (Rose et al., 2009; Jabre et al., 2021). Our bB~~bioassays
962 incubations were performed under trace metal clean conditions (the entire duration) and with temperature
963 remaining stable over the course of incubations (maximum fluctuation of temperature ± 0.3 °C). We stress the
964 importance of trace metal clean working conditions to avoid inadvertently assigning Fe addition effects on
965 phytoplankton to temperature when working in low Fe regions (i.e. Southern Ocean, but also open oceans in
966 general). The differences we found between the F and TF treatment may have been assigned to temperature alone
967 under non-trace metal clean working conditions (as Fe would inadvertently have been introduced), whilst our
968 results show that temperature alone did not have a (major) effect. Our data also shows the importance of
969 considering other regional and/or seasonal factors potentially limiting phytoplankton growth, such as e.g., light
970 availability (limiting light conditions in bioassay A2) and dMn availability (potentially limiting in W1), when
971 studying the effect of future climate on Southern Ocean phytoplankton. Additionally, our data indicates a trend of
972 increased uptake of trace metals under dFe limitation, suggesting there are many adaptive strategies employed by
973 phytoplankton in navigating nutrient scarcities under varying environmental conditions, with potential impact on
974 the stoichiometry of global (micro-) nutrient distributions due to the central role of the Southern Ocean.
975 In general, the addition of Fe was the primary factor for observed stimulatory effects, with temperature enhancing
976 the effects of dFe. ~~In Especially particular,~~ large diatoms benefitted from Fe addition, although several smaller-
977 sized phytoplankton populations showed enhanced abundances upon Fe addition. Climate change is predicted to

978 lead to a shift towards smaller phytoplankton (Deppeler & Davidson, 2017; Krumhardt et al., 2022). Our study
979 shows, however, that enhanced Fe input counteracts this warming-induced shift, assuming macronutrients will
980 not become limiting. Given that the intensity of the observed effects varied between the experiments with
981 distinctly different phytoplankton communities, this study emphasizes the need for studying diverse regions of
982 the Southern Ocean and performing multiple bioassays over the productive season to better understand and predict
983 potential future changes, especially as future changes in Fe availability are region-specific (Tagliabue et al., 2016;
984 Van Manen et al., 2022). ~~Alterations in phytoplankton community composition and cell size, as observed in our~~
985 ~~experiments, will directly affect top-down control by grazers and viral infection and consequently trophic transfer~~
986 ~~efficiency. Moreover, not only the flow of organic carbon through the food web will be affected, but also the flux~~
987 ~~of organic carbon to deeper layers of the ocean (biological carbon pump) depends on the phytoplankton~~
988 ~~community composition, cell size and type of loss factor. Factors such as the dFe concentrations, other trace metal~~
989 ~~concentrations which may potentially co-limit phytoplankton growth, and light availability, should also be~~
990 ~~considered when studying the effects of future climate on Antarctic phytoplankton. Moreover, the time of the year~~
991 ~~affects the starting composition of the phytoplankton community, and the sequence of the treatments in case of~~
992 ~~dual treatments (Fe addition and temperature increase) may affect the responses (Brooks and Crowe 2019), hence~~
993 ~~these factors should be considered.~~
994 ~~Depending on the geographical region and the time in the productive season (Thomalla et al., 2023), global~~
995 ~~warming is predicted to increase wind-induced mixing or strengthen vertical stratification (Bronse laer et al., 2020;~~
996 ~~De Lavergne et al., 2014; Hillenbrand & Cortese, 2006; Shi et al., 2020). Phytoplankton will bloom earlier in the~~
997 ~~productive season as a result of decreasing sea ice and consequently higher light (Krumhardt et al., 2022), rapidly~~
998 ~~drawing down available Fe, followed by stratification, and thus favourable conditions for smaller sized~~
999 ~~phytoplankton (Deppeler & Davidson, 2017; Krumhardt et al., 2022). Our study shows, however, that enhanced~~
1000 ~~Fe input in such regions may partly overturn this warming-induced shift, assuming macronutrients will not become~~
1001 ~~limiting.~~
1002 ~~We recommend that future bioassay studies consider phytoplankton gross growth, grazing, and viral lysis as well.~~
1003 ~~After all, the typically reported net changes in the bioassay phytoplankton community are the resultant of~~
1004 ~~production and losses. Both Fe as well as temperature can impact the extent of the loss factors. For example,~~
1005 ~~grazing rates are known to increase with temperature (Chen et al., 2012; Caron & Hutchins, 2013), viral lysis may~~
1006 ~~occur faster at higher temperature (Maat et al., 2017), and Fe availability can affect algal virus production and~~
1007 ~~infectivity (Slagter et al., 2016). Finally, potential region-specific differences in the share of grazing and lysis~~

1008 ~~(Mojica et al., 2016; Mojica et al., 2021; Eich et al., 2022) may influence net changes in phytoplankton biomass~~
1009 ~~or abundances in bioassays.~~The Southern Ocean biogeochemical cycling and ecosystems dynamics are complex
1010 and need to be better studied in field and modelling studies. The current study underlines the need for assessing
1011 consequences of near future temperature changes at environmentally relevant dFe concentrations.

1012

1013 *Data availability:* All data presented in this paper (nutrients, trace metals, phytoplankton abundances,
1014 photosynthetic efficiencies, Chl *a* concentrations, pigment based community composition, particulate organic
1015 carbon and particulate organic phosphate) are included in this published article and are available under
1016 <https://doi.org/10.25850/nioz/7b.b.hh>.

1017

1018 *Supplement:* The supplementary material related to this article is available online at XXX.

1019

1020 *Author contributions:* RM and CPDB conceptualized the study. CE, MvM, EB, SBEHP, HT, IA, JSPM and RM
1021 conducted the fieldwork under the lead of RM, JJ analysed the nutrient samples for Amundsen Sea bioassays,
1022 WvdP analysed the pigment samples and conducted the Chemtax analysis, CE, MvM, wrote the original draft,
1023 CPDB and RM edited the paper. EB, LJ and JSPM contributed to the discussion. All authors contributed to
1024 commenting on the paper.

1025

1026 *Competing interests:* The authors declare that they have no conflict of interest.

1027

1028 *Acknowledgements:* We would like to thank the captain and crew of both the R/V Araon and the R/V Polarstern,
1029 as well as the expedition leaders SangHoon Lee and Olaf Boebel and all other expedition participants. Our
1030 participation in R/V Polarstern expedition PS117 was funded by AWI under grant number AWI_PS117_02.
1031 Furthermore, we would like to thank John Seccombe from Aquahort for his support in conceiving and building
1032 the heatpumps as well as his remote support during the expeditions and Sharyn Ossebaar for nutrient
1033 measurements aboard R/V Polarstern. Sven Ober and all the colleagues from NIOZ national marine facilities
1034 (NMF) for the preparation of the Titan sampling system during the expeditions, as well as building the incubators
1035 and their help in the expedition preparation. We are also grateful to Bob Kusters (NIOZ) for his assistance with
1036 the incubators, ensuring they maintained the correct temperature throughout our study. Patrick Laan (NIOZ) for
1037 helping with the ICP-MS analyses, Flora Wille (NIOZ) for helping with the particulate metal analysis and Piet ter

1038 Schure and his team (DMT Marine Equipment) for supplying a winch system last minute for the Titan sampling
1039 system used on the R/V Araon.

1040

1041 *Financial support:* This work was part of the FePhyrus project (ALWPP.2016.020), which was supported by the
1042 Netherlands Polar Programme (NPP), with financial aid from the Dutch Research Council (NWO). Mathijs van
1043 Manen was supported by the Utrecht University-NIOZ collaboration. The ANA-08B expedition was supported
1044 by the Korea Polar Research Institute grant KOPRI PE24110. The PS117 expedition was supported by the
1045 auxiliary use proposal AWI_PS117_02. EMB was supported by an NSERC Canada Research Chair.

1046 **References**

- 1047 [Aflenzer, H., Hoffmann, L., Holmes, T., Wuttig, K., Genovese, C., and Bowie, A. R.: Effect of dissolved iron \(II\) and](#)
1048 [temperature on growth of the Southern Ocean phytoplankton species *Fragilariopsis cylindrus* and *Phaeocystis antarctica*,](#)
1049 [Polar Biol, 46, 1163–1173, <https://doi.org/10.1007/s00300-023-03191-z>, 2023.](#)
- 1050 [Alderkamp, A.-C., Van Dijken, G.-L., Lowry, K. E., Connelly, T. L., Lagerström, M., Sherrell, R. M., Haskins, C.,](#)
1051 [Rogalsky, E., Schofield, O., Stammerjohn, S. E., Yager, P. L., and Arrigo, K. R.: Fe availability drives phytoplankton](#)
1052 [photosynthesis rates during spring bloom in the Amundsen Sea Polynya, Antarctica, *Elementa*, 3,](#)
1053 [https://doi.org/10.12952/journal.elementa.000043, 2015.](#)
- 1054 [Alderkamp, A.-C., Van Dijken, G. L., Lowry, K. E., Lewis, K. M., Joy-Warren, H. L., Van De Poll, W., Laan, P., Gerringa,](#)
1055 [L., Delmont, T. O., Jenkins, B. D., and Arrigo, K. R.: Effects of iron and light availability on phytoplankton photosynthetic](#)
1056 [properties in the Ross Sea, *Marine Ecology Progress Series*, 621, 33–50, <https://doi.org/10.3354/meps13000>, 2019.](#)
- 1057 [Andrew, S. M., Morell, H. T., Strzepek, R. F., Boyd, P. W., and Ellwood, M. J.: Iron Availability Influences the Tolerance](#)
1058 [of Southern Ocean Phytoplankton to Warming and Elevated Irradiance, *Frontiers in Marine Science*, 6, 2019.](#)
- 1059 [Annett, A. L., Skiba, M., Henley, S. F., Venables, H. J., Meredith, M. P., Statham, P. J., and Ganeshram, R. S.: Comparative](#)
1060 [roles of upwelling and glacial iron sources in Ryder Bay, coastal western Antarctic Peninsula, *Marine Chemistry*, 176, 21–](#)
1061 [33, 2015.](#)
- 1062 [Arrigo, K. R.: Marine microorganisms and global nutrient cycles, *Nature*, 437, 349–355,](#)
1063 [https://doi.org/10.1038/nature04159, 2005.](#)
- 1064 [Arrigo, K. R. and Van Dijken, G. L.: Phytoplankton dynamics within 37 Antarctic coastal polynya systems, *Journal of*](#)
1065 [Geophysical Research: Oceans, 108, 2003.](#)
- 1066 [Arrigo, K. R., Lowry, K. E., and van Dijken, G. L.: Annual changes in sea ice and phytoplankton in polynyas of the](#)
1067 [Amundsen Sea, Antarctica, *Deep Sea Research Part II: Topical Studies in Oceanography*, 71, 5–15, 2012.](#)
- 1068 [Arrigo, K. R., Van Dijken, G. L., Alderkamp, A., Erickson, Z. K., Lewis, K. M., Lowry, K. E., Joy-Warren, H. L., Middag,](#)
1069 [R., Nash-Arrigo, J. E., Selz, V., and Van De Poll, W.: Early Spring Phytoplankton Dynamics in the Western Antarctic](#)
1070 [Peninsula, *JGR Oceans*, 122, 9350–9369, <https://doi.org/10.1002/2017JC013281>, 2017.](#)
- 1071 [Assmy, P., Smetacek, V., Montresor, M., Klaas, C., Henjes, J., Strass, V. H., Arrieta, J. M., Bathmann, U., Berg, G. M., and](#)
1072 [Breitbarth, E.: Thick-shelled, grazer-protected diatoms decouple ocean carbon and silicon cycles in the iron-limited](#)
1073 [Antarctic Circumpolar Current, *Proceedings of the National Academy of Sciences*, 110, 20633–20638, 2013.](#)
- 1074 [de Baar, H. J., Buma, A. G., Nolting, R. F., Cadée, G. C., Jacques, G., and Tréguer, P. J.: On iron limitation of the Southern](#)
1075 [Ocean: experimental observations in the Weddell and Scotia Seas, *Marine ecology progress series*, 105–122, 1990.](#)
- 1076 [Balaguer, J., Koch, F., Hassler, C., and Trimborn, S.: Iron and manganese co-limit the growth of two phytoplankton groups](#)
1077 [dominant at two locations of the Drake Passage, *Communications Biology*, 5, 207, 2022.](#)
- 1078 [Balaguer, J., Thoms, S., and Trimborn, S.: The physiological response of an Antarctic key phytoplankton species to low iron](#)
1079 [and manganese concentrations, *Limnology & Oceanography*, 68, 2153–2166, <https://doi.org/10.1002/lno.12412>, 2023.](#)
- 1080 [Basterretxea, G., Font-Muñoz, J. S., Hernández-Carrasco, I., and Sañudo-Wilhelmy, S. A.: Global variability of high-](#)
1081 [nutrient low-chlorophyll regions using neural networks and wavelet coherence analysis, *Ocean Sci.*, 19, 973–990,](#)
1082 [https://doi.org/10.5194/os-19-973-2023, 2023.](#)
- 1083 [Bazzani, E., Lauritano, C., and Saggiomo, M.: Southern Ocean Iron Limitation of Primary Production between Past](#)
1084 [Knowledge and Future Projections, *Journal of Marine Science and Engineering*, 11, 272, 2023.](#)
- 1085 [Biggs, T. E., Alvarez-Fernandez, S., Evans, C., Mojica, K. D., Rozema, P. D., Venables, H. J., Pond, D. W., and Brussaard,](#)
1086 [C. P.: Antarctic phytoplankton community composition and size structure: importance of ice type and temperature as](#)
1087 [regulatory factors, *Polar Biology*, 42, 1997–2015, 2019.](#)
- 1088 [Biggs, T. E., Huisman, J., and Brussaard, C. P.: Viral lysis modifies seasonal phytoplankton dynamics and carbon flow in the](#)
1089 [Southern Ocean, *The ISME journal*, 15, 3615–3622, 2021.](#)
- 1090 [Boyd, P. W.: The role of iron in the biogeochemistry of the Southern Ocean and equatorial Pacific: a comparison of in situ](#)
1091 [iron enrichments, *Deep Sea Research Part II: Topical Studies in Oceanography*, 49, 1803–1821, 2002.](#)

1092 [Boyd, P. W., Arrigo, K. R., Strzepek, R., and Van Dijken, G. L.: Mapping phytoplankton iron utilization: Insights into](#)
1093 [Southern Ocean supply mechanisms, *Journal of Geophysical Research: Oceans*, 117, 2012.](#)

1094 [Boyd, P. W., Strzepek, R. F., Ellwood, M. J., Hutchins, D. A., Nodder, S. D., Twining, B. S., and Wilhelm, S. W.: Why are](#)
1095 [biotic iron pools uniform across high- and low-iron pelagic ecosystems?, *Global Biogeochemical Cycles*, 29, 1028–1043,](#)
1096 <https://doi.org/10.1002/2014GB005014>, 2015.

1097 [Bronse laer, B., Russell, J. L., Winton, M., Williams, N. L., Key, R. M., Dunne, J. P., Feely, R. A., Johnson, K. S., and](#)
1098 [Sarmiento, J. L.: Importance of wind and meltwater for observed chemical and physical changes in the Southern Ocean, *Nat.*](#)
1099 [Geosci., 13, 35–42, <https://doi.org/10.1038/s41561-019-0502-8>, 2020.](#)

1100 [Browning, T. J., Achterberg, E. P., Engel, A., and Mawji, E.: Manganese co-limitation of phytoplankton growth and major](#)
1101 [nutrient drawdown in the Southern Ocean, *Nature communications*, 12, 884, 2021.](#)

1102 [Buesseler, K. O., Boyd, P. W., Black, E. E., and Siegel, D. A.: Metrics that matter for assessing the ocean biological carbon](#)
1103 [pump, *Proc. Natl. Acad. Sci. U.S.A.*, 117, 9679–9687, <https://doi.org/10.1073/pnas.1918114117>, 2020.](#)

1104 [Burns, S. M., Bundy, R. M., Abbott, W., Abdala, Z., Sterling, A. R., Chappell, P. D., Jenkins, B. D., and Buck, K. N.:](#)
1105 [Interactions of bioactive trace metals in shipboard Southern Ocean incubation experiments, *Limnology and Oceanography*,](#)
1106 [68, 525–543, <https://doi.org/10.1002/lno.12290>, 2023.](#)

1107 [Caron, D. A. and Hutchins, D. A.: The effects of changing climate on microzooplankton grazing and community structure:](#)
1108 [drivers, predictions and knowledge gaps, *Journal of Plankton Research*, 35, 235–252, <https://doi.org/10.1093/plankt/fbs091>,](#)
1109 [2013.](#)

1110 [Chen, B., Landry, M. R., Huang, B., and Liu, H.: Does warming enhance the effect of microzooplankton grazing on marine](#)
1111 [phytoplankton in the ocean?, *Limnology and oceanography*, 57, 519–526, 2012.](#)

1112 [Cullen, J. T., Chase, Z., Coale, K. H., Fitzwater, S. E., and Sherrell, R. M.: Effect of iron limitation on the cadmium to](#)
1113 [phosphorus ratio of natural phytoplankton assemblages from the Southern Ocean, *Limnology and Oceanography*, 48, 1079–](#)
1114 [1087, <https://doi.org/10.4319/lno.2003.48.3.1079>, 2003.](#)

1115 [Cunningham, B. R. and John, S. G.: The effect of iron limitation on cyanobacteria major nutrient and trace element](#)
1116 [stoichiometry, *Limnology and Oceanography*, 62, 846–858, <https://doi.org/10.1002/lno.10484>, 2017.](#)

1117 [Cutter, G., Casciotti, K., Croot, P., Geibert, W., Heimbürger, L.-E., Lohan, M., Planquette, H., and van de Fliedert, T.:](#)
1118 [Sampling and Sample-handling Protocols for GEOTRACES Cruises. Version 3, August 2017., 2017.](#)

1119 [Darelius, E., Daae, K., Dundas, V., Fer, I., Hellmer, H. H., Janout, M., Nicholls, K. W., Sallée, J.-B., and Østerhus, S.:](#)
1120 [Observational evidence for on-shelf heat transport driven by dense water export in the Weddell Sea, *Nature*](#)
1121 [Communications, 14, 1022, 2023.](#)

1122 [De Baar, H. J. W., Boyd, P. W., Coale, K. H., Landry, M. R., Tsuda, A., Assmy, P., Bakker, D. C. E., Bozec, Y., Barber, R.](#)
1123 [T., Brzezinski, M. A., Buesseler, K. O., Boyé, M., Croot, P. L., Gervais, F., Gorbunov, M. Y., Harrison, P. J., Hiscock, W.](#)
1124 [T., Laan, P., Lancelot, C., Law, C. S., Levasseur, M., Marchetti, A., Millero, F. J., Nishioka, J., Nojiri, Y., Van Oijen, T.,](#)
1125 [Riebesell, U., Rijkenberg, M. J. A., Saito, H., Takeda, S., Timmermans, K. R., Veldhuis, M. J. W., Waite, A. M., and Wong,](#)
1126 [C.: Synthesis of iron fertilization experiments: From the Iron Age in the Age of Enlightenment, *J. Geophys. Res.*, 110,](#)
1127 [2004JC002601, <https://doi.org/10.1029/2004JC002601>, 2005.](#)

1128 [De Baar, H. J. W., Timmermans, K. R., Laan, P., De Porto, H. H., Ober, S., Blom, J. J., Bakker, M. C., Schilling, J., Sarthou,](#)
1129 [G., and Smit, M. G.: Titan: A new facility for ultraclean sampling of trace elements and isotopes in the deep oceans in the](#)
1130 [international Geotraces program, *Marine Chemistry*, 111, 4–21, 2008.](#)

1131 [De Lavergne, C., Palter, J. B., Galbraith, E. D., Bernardello, R., and Marinov, I.: Cessation of deep convection in the open](#)
1132 [Southern Ocean under anthropogenic climate change, *Nature Climate Change*, 4, 278–282, 2014.](#)

1133 [Deppeler, S. L. and Davidson, A. T.: Southern Ocean phytoplankton in a changing climate, *Frontiers in Marine Science*, 4,](#)
1134 [40, 2017.](#)

1135 [Drijfhout, S. S., Bull, C. Y. S., Hewitt, H., Holland, P. R., Jenkins, A., Mathiot, P., and Garabato, A. N.: An Amundsen Sea](#)
1136 [source of decadal temperature changes on the Antarctic continental shelf, *Ocean Dynamics*, 74, 37–52,](#)
1137 <https://doi.org/10.1007/s10236-023-01587-3>, 2024.

1138 [Eich, C., Pont, S. B., and Brussaard, C. P.: Effects of UV radiation on the chlorophyte *Micromonas polaris* host–virus](#)

1139 [interactions and MpoV-45T virus infectivity, *Microorganisms*, 9, 2429, 2021.](#)

1140 [Eich, C., Biggs, T. E., van de Poll, W. H., van Manen, M., Tian, H.-A., Jung, J., Lee, Y., Middag, R., and Brussaard, C. P.: Ecological importance of viral lysis as a loss factor of phytoplankton in the Amundsen Sea, *Microorganisms*, 10, 1967, 2022.](#)

1141

1142 [Fahrbach, E., Hoppema, M., Rohardt, G., Schröder, M., and Wisotzki, A.: Decadal-scale variations of water mass properties](#)

1143 [in the deep Weddell Sea, *Ocean Dynamics*, 54, 77–91, 2004.](#)

1144 [Feng, Y., Hare, C. E., Rose, J. M., Handy, S. M., DiTullio, G. R., Lee, P. A., Smith Jr., W. O., Peloquin, J., Tozzi, S., Sun,](#)

1145 [J., Zhang, Y., Dunbar, R. B., Long, M. C., Sohst, B., Lohan, M., and Hutchins, D. A.: Interactive effects of iron, irradiance](#)

1146 [and CO₂ on Ross Sea phytoplankton, *Deep-Sea Research Part I: Oceanographic Research Papers*, 57, 368–383,](#)

1147 <https://doi.org/10.1016/j.dsr.2009.10.013>, 2010.

1148 [Fisher, B. J., Poulton, A. J., Meredith, M. P., Baldry, K., Schofield, O., and Henley, S. F.: Biogeochemistry of climate driven](#)

1149 [shifts in Southern Ocean primary producers, *Biogeosciences Discussions*, 1–29, 2023.](#)

1150 [Fourquez, M., Janssen, D. J., Conway, T. M., Cabanes, D., Ellwood, M. J., Sieber, M., Trimborn, S., and Hassler, C.:](#)

1151 [Chasing iron bioavailability in the Southern Ocean: Insights from *Phaeocystis antarctica* and iron speciation, *Sci. Adv.*, 9,](#)

1152 [eadf9696](https://doi.org/10.1126/sciadv.adf9696), <https://doi.org/10.1126/sciadv.adf9696>, 2023.

1153 [Friedlingstein, P., O’sullivan, M., Jones, M. W., Andrew, R. M., Gregor, L., Hauck, J., Le Quéré, C., Luijckx, I. T., Olsen, A.,](#)

1154 [and Peters, G. P.: Global carbon budget 2022, *Earth System Science Data Discussions*, 2022, 1–159, 2022.](#)

1155 [Fukuda, R., Ogawa, H., Nagata, T., and Koike, I.: Direct Determination of Carbon and Nitrogen Contents of Natural](#)

1156 [Bacterial Assemblages in Marine Environments, *Appl Environ Microbiol*, 64, 3352–3358,](#)

1157 <https://doi.org/10.1128/AEM.64.9.3352-3358.1998>, 1998.

1158 [Garrison, D. L., Gowing, M. M., Hughes, M. P., Campbell, L., Caron, D. A., Dennett, M. R., Shalapyonok, A., Olson, R. J.,](#)

1159 [Landry, M. R., Brown, S. L., Liu, H.-B., Azam, F., Steward, G. F., Ducklow, H. W., and Smith, D. C.: Microbial food web](#)

1160 [structure in the Arabian Sea: a US JGOFS study, *Deep Sea Research Part II: Topical Studies in Oceanography*, 47, 1387–](#)

1161 [1422](https://doi.org/10.1016/S0967-0645(99)00148-4), [https://doi.org/10.1016/S0967-0645\(99\)00148-4](https://doi.org/10.1016/S0967-0645(99)00148-4), 2000.

1162 [Geider, R. J.: Light and temperature dependence of the carbon to chlorophyll a ratio in microalgae and cyanobacteria:](#)

1163 [implications for physiology and growth of phytoplankton, *New Phytologist*, 1–34, 1987.](#)

1164 [Geider, R. J. and La Roche, J.: The role of iron in phytoplankton photosynthesis, and the potential for iron-limitation of](#)

1165 [primary productivity in the sea, *Photosynthesis research*, 39, 275–301, 1994.](#)

1166 [Gerringa, L. J., Alderkamp, A.-C., Laan, P., Thuróczy, C.-E., De Baar, H. J., Mills, M. M., van Dijken, G. L., van Haren, H.,](#)

1167 [and Arrigo, K. R.: Iron from melting glaciers fuels the phytoplankton blooms in Amundsen Sea \(Southern Ocean\): Iron](#)

1168 [biogeochemistry, *Deep Sea Research Part II: Topical Studies in Oceanography*, 71, 16–31, 2012.](#)

1169 [Gerringa, L. J. A., Alderkamp, A.-C., Laan, P., Thuróczy, C.-E., De Baar, H. J. W., Mills, M. M., van Dijken, G. L., van](#)

1170 [Haren, H., and Arrigo, K. R.: Corrigendum to "Iron from melting glaciers fuels the phytoplankton blooms in Amundsen Sea](#)

1171 [\(Southern Ocean\): iron biogeochemistry"\(Gerringa et al., 2012\), *Deep Sea Research Part II: Topical Studies in*](#)

1172 [Oceanography](#), 177, 104843, 2020.

1173 [Gledhill, M. and Buck, K. N.: The organic complexation of iron in the marine environment: a review, *Frontiers in*](#)

1174 [microbiology](#), 3, 69, 2012.

1175 [Gómez-Valdivia, F., Holland, P. R., Siahayan, A., Dutrieux, P., and Young, E.: Projected West Antarctic Ocean Warming](#)

1176 [Caused by an Expansion of the Ross Gyre, *Geophysical Research Letters*, 50, e2023GL102978,](#)

1177 <https://doi.org/10.1029/2023GL102978>, 2023.

1178 [Gordon, L. I., Jennings Jr, J. C., Ross, A. A., and Krest, J. M.: A suggested protocol for continuous flow automated analysis](#)

1179 [of seawater nutrients \(phosphate, nitrate, nitrite and silicic acid\) in the WOCE Hydrographic Program and the Joint Global](#)

1180 [Ocean Fluxes Study, WOCE hydrographic program office, methods manual WHPO, 1–52, 1993.](#)

1181 [Greene, R. M., Geider, R. J., Kolber, Z., and Falkowski, P. G.: Iron-Induced Changes in Light Harvesting and](#)

1182 [Photochemical Energy Conversion Processes in Eukaryotic Marine Algae I, *Plant Physiol*, 100, 565–575, 1992.](#)

1183 [Grise, K. M., Polvani, L. M., Tselioudis, G., Wu, Y., and Zelinka, M. D.: The ozone hole indirect effect: Cloud-radiative](#)

1184 [anomalies accompanying the poleward shift of the eddy-driven jet in the Southern Hemisphere, *Geophysical Research*](#)

1185 [Letters](#), 40, 3688–3692, <https://doi.org/10.1002/grl.50675>, 2013.

- 1186 [van Haren, H., Brussaard, C. P., Gerringa, L. J., van Manen, M. H., Middag, R., and Groenewegen, R.: Diapycnal mixing](#)
1187 [across the photic zone of the NE-Atlantic, Ocean Science Discussions, 2020, 1–31, 2020.](#)
- 1188 [Hassler, C. S. and Schoemann, V.: Bioavailability of organically bound Fe to model phytoplankton of the Southern Ocean,](#)
1189 [Biogeosciences, 6, 2281–2296, 2009.](#)
- 1190 [Hawco, N. J., Tagliabue, A., and Twining, B. S.: Manganese Limitation of Phytoplankton Physiology and Productivity in the](#)
1191 [Southern Ocean, Global Biogeochemical Cycles, 36, e2022GB007382, <https://doi.org/10.1029/2022GB007382>, 2022.](#)
- 1192 [Hillenbrand, C.-D. and Cortese, G.: Polar stratification: A critical view from the Southern Ocean, Palaeogeography,](#)
1193 [Palaeoclimatology, Palaeoecology, 242, 240–252, 2006.](#)
- 1194 [Hinz, D. J., Nielsdóttir, M. C., Korb, R. E., Whitehouse, M. J., Poulton, A. J., Moore, C. M., Achterberg, E. P., and Bibby, T.](#)
1195 [S.: Responses of microplankton community structure to iron addition in the Scotia Sea, Deep-Sea Research Part II: Topical](#)
1196 [Studies in Oceanography, 59–60, 36–46, <https://doi.org/10.1016/j.dsr2.2011.08.006>, 2012.](#)
- 1197 [Hoppema, M., Middag, R., de Baar, H. J., Fahrbach, E., van Weerlee, E. M., and Thomas, H.: Whole season net community](#)
1198 [production in the Weddell Sea, Polar Biology, 31, 101–111, 2007.](#)
- 1199 [Hopwood, M. J., Carroll, D., Höfer, J., Achterberg, E. P., Meire, L., Le Moigne, F. A., Bach, L. T., Eich, C., Sutherland, D.](#)
1200 [A., and González, H. E.: Highly variable iron content modulates iceberg-ocean fertilisation and potential carbon export,](#)
1201 [Nature Communications, 10, 5261, 2019.](#)
- 1202 [Huang, Y., Fassbender, A. J., and Bushinsky, S. M.: Biogenic carbon pool production maintains the Southern Ocean carbon](#)
1203 [sink, Proc. Natl. Acad. Sci. U.S.A., 120, e2217909120, <https://doi.org/10.1073/pnas.2217909120>, 2023.](#)
- 1204 [Hutchins, D. A. and Boyd, P. W.: Marine phytoplankton and the changing ocean iron cycle, Nature Climate Change, 6,](#)
1205 [1072–1079, 2016.](#)
- 1206 [Hutchins, D. A. and Bruland, K. W.: Iron-limited diatom growth and Si:N uptake ratios in a coastal upwelling regime,](#)
1207 [Nature, 393, 561–564, <https://doi.org/10.1038/31203>, 1998.](#)
- 1208 [Jabre, L. and Bertrand, E. M.: Interactive effects of iron and temperature on the growth of *Fragilariopsis cylindrus*,](#)
1209 [Limnology and Oceanography Letters, 5, 363–370, 2020.](#)
- 1210 [Jabre, L. J., Allen, A. E., McCain, J. S. P., McCrow, J. P., Tenenbaum, N., Spackeen, J. L., Sipler, R. E., Green, B. R.,](#)
1211 [Bronk, D. A., Hutchins, D. A., and Bertrand, E. M.: Molecular underpinnings and biogeochemical consequences of](#)
1212 [enhanced diatom growth in a warming Southern Ocean, Proceedings of the National Academy of Sciences, 118,](#)
1213 [e2107238118, <https://doi.org/10.1073/pnas.2107238118>, 2021.](#)
- 1214 [Jensen, L. T., Wyatt, N. J., Landing, W. M., and Fitzsimmons, J. N.: Assessment of the stability, sorption, and](#)
1215 [exchangeability of marine dissolved and colloidal metals, Marine Chemistry, 220, 103754,](#)
1216 [<https://doi.org/10.1016/j.marchem.2020.103754>, 2020.](#)
- 1217 [Karakuş, O., Völker, C., Iversen, M., Hagen, W., and Hauck, J.: The Role of Zooplankton Grazing and Nutrient Recycling](#)
1218 [for Global Ocean Biogeochemistry and Phytoplankton Phenology, JGR Biogeosciences, 127, e2022JG006798,](#)
1219 [<https://doi.org/10.1029/2022JG006798>, 2022.](#)
- 1220 [Kelleher, M. K. and Grise, K. M.: Varied midlatitude shortwave cloud radiative responses to Southern Hemisphere](#)
1221 [circulation shifts, Atmospheric Science Letters, 23, e1068, <https://doi.org/10.1002/asl.1068>, 2022.](#)
- 1222 [Klunder, M. B., Laan, P., Middag, R., De Baar, H. J. W., and Van Ooijen, J. C.: Dissolved iron in the Southern Ocean](#)
1223 [\(Atlantic sector\), Deep Sea Research Part II: Topical Studies in Oceanography, 58, 2678–2694, 2011.](#)
- 1224 [Klunder, M. B., Laan, P., De Baar, H. J. W., Middag, R., Neven, I., and Van Ooijen, J.: Dissolved Fe across the Weddell Sea](#)
1225 [and Drake Passage: impact of DFe on nutrient uptake, Biogeosciences, 11, 651–669, 2014.](#)
- 1226 [Knust, R.: Polar research and supply vessel POLARSTERN operated by the Alfred-Wegener-Institute, Journal of large-scale](#)
1227 [research facilities JLSRF, 3, A119–A119, 2017.](#)
- 1228 [Kranzler, C. F., Brzezinski, M. A., Cohen, N. R., Lampe, R. H., Maniscalco, M., Till, C. P., Mack, J., Latham, J. R.,](#)
1229 [Bruland, K. W., and Twining, B. S.: Impaired viral infection and reduced mortality of diatoms in iron-limited oceanic](#)
1230 [regions, Nature Geoscience, 14, 231–237, 2021.](#)

1231 [Kroh, G. E. and Pilon, M.: Regulation of iron homeostasis and use in chloroplasts, *International Journal of Molecular Sciences*, 21, 3395, 2020.](#)

1232

1233 [Krumhardt, K. M., Long, M. C., Sylvester, Z. T., and Petrik, C. M.: Climate drivers of Southern Ocean phytoplankton community composition and potential impacts on higher trophic levels, *Frontiers in Marine Science*, 9, 916140, 2022a.](#)

1234

1235 [Krumhardt, K. M., Long, M. C., Sylvester, Z. T., and Petrik, C. M.: Climate drivers of Southern Ocean phytoplankton community composition and potential impacts on higher trophic levels, *Frontiers in Marine Science*, 9, 916140, 2022b.](#)

1236

1237 [Kustka, A. B., Allen, A. E., and Morel, F. M.: Sequence analysis and transcriptional regulation of iron acquisition genes in two marine diatoms 1, *Journal of Phycology*, 43, 715–729, 2007.](#)

1238

1239 [Lampe, R. H., Mann, E. L., Cohen, N. R., Till, C. P., Thamatrakoln, K., Brzezinski, M. A., Bruland, K. W., Twining, B. S., and Marchetti, A.: Different iron storage strategies among bloom-forming diatoms, *Proceedings of the National Academy of Sciences*, 115, E12275–E12284, <https://doi.org/10.1073/pnas.1805243115>, 2018.](#)

1240

1241

1242 [Lane, E. S., Jang, K., Cullen, J. T., and Maldonado, M. T.: The interaction between inorganic iron and cadmium uptake in the marine diatom *Thalassiosira oceanica*, *Limnology and oceanography*, 53, 1784–1789, 2008.](#)

1243

1244 [Lannuzel, D., Vancoppenolle, M., van Der Merwe, P., De Jong, J., Meiners, K. M., Grotti, M., Nishioka, J., and Schoemann, V.: Iron in sea ice: Review and new insights, *Elementa*, 4, 000130, 2016.](#)

1245

1246 [Latour, P., Strzepek, R. F., Wuttig, K., van der Merwe, P., Bach, L. T., Eggins, S., Boyd, P. W., Ellwood, M. J., Pinfold, T. L., and Bowie, A. R.: Seasonality of phytoplankton growth limitation by iron and manganese in subantarctic waters, *Elementa: Science of the Anthropocene*, 11, 2023.](#)

1247

1248

1249 [Latour, P., Eggins, S., Van Der Merwe, P., Bach, L. T., Boyd, P. W., Ellwood, M. J., Bowie, A. R., Wuttig, K., and Strzepek, R. F.: Characterization of a Southern Ocean deep chlorophyll maximum: Response of phytoplankton to light, iron, and manganese enrichment, *Limnol Oceanogr Letters*, 9, 145–154, <https://doi.org/10.1002/lol2.10366>, 2024.](#)

1250

1251

1252 [Laufkötter, C., Vogt, M., Gruber, N., Aita-Noguchi, M., Aumont, O., Bopp, L., Buitenhuis, E., Doney, S. C., Dunne, J., and Hashioka, T.: Drivers and uncertainties of future global marine primary production in marine ecosystem models, *Biogeosciences*, 12, 6955–6984, 2015.](#)

1253

1254

1255 [Laws, E. A. and Bannister, T. T.: Nutrient-and light-limited growth of *Thalassiosira fluviatilis* in continuous culture, with implications for phytoplankton growth in the ocean 1, *Limnology and Oceanography*, 25, 457–473, 1980.](#)

1256

1257 [Lewandowska, A. and Sommer, U.: Climate change and the spring bloom: a mesocosm study on the influence of light and temperature on phytoplankton and mesozooplankton, *Marine Ecology Progress Series*, 405, 101–111, 2010.](#)

1258

1259 [Maat, D. S., Biggs, T., Evans, C., Van Bleijswijk, J. D. L., Van der Wel, N. N., Dutilh, B. E., and Brussaard, C. P. D.: Characterization and Temperature Dependence of Arctic *Micromonas polaris* Viruses, *Viruses*, 9, 134, <https://doi.org/10.3390/v9060134>, 2017.](#)

1260

1261

1262 [Mackey, M. D., Mackey, D. J., Higgins, H. W., and Wright, S. W.: CHEMTAX—a program for estimating class abundances from chemical markers: application to HPLC measurements of phytoplankton, *Marine Ecology Progress Series*, 144, 265–283, 1996.](#)

1263

1264

1265 [Marie, D., Partensky, F., Vaulot, D., and Brussaard, C.: Enumeration of Phytoplankton, Bacteria, and Viruses in Marine Samples, *CP Cytometry*, 10, <https://doi.org/10.1002/0471142956.cy1111s10>, 1999.](#)

1266

1267 [Martin, J. H., Fitzwater, S. E., and Gordon, R. M.: Iron deficiency limits phytoplankton growth in Antarctic waters, *Global Biogeochemical Cycles*, 4, 5–12, 1990.](#)

1268

1269 [McCain, J. S. P., Tagliabue, A., Susko, E., Achterberg, E. P., Allen, A. E., and Bertrand, E. M.: Cellular costs underpin micronutrient limitation in phytoplankton, *Science Advances*, 7, eabg6501, <https://doi.org/10.1126/sciadv.abg6501>, 2021.](#)

1270

1271 [Meredith, M., M. Sommerkorn, S. Cassotta, C. Derksen, A. Ekaykin, A. Hollowed, G. Kofinas, A. Mackintosh, J. Melbourne-Thomas, M.M.C. Muelbert, G. Ottersen, H. Pritchard, and E.A.G. Schuur: Chapter 3: IPCC Polar regions — Special Report on the Ocean and Cryosphere in a Changing Climate, 2019.](#)

1272

1273

1274 [Meyerink, S. W., Ellwood, M. J., Maher, W. A., Dean Price, G., and Strzepek, R. F.: Effects of iron limitation on silicon uptake kinetics and elemental stoichiometry in two Southern Ocean diatoms, *Eucampia antarctica* and *Proboscia inermis*, and the temperate diatom *Thalassiosira pseudonana*, *Limnology & Oceanography*, 62, 2445–2462.](#)

1275

1276

- 1277 <https://doi.org/10.1002/Ino.10578>, 2017.
- 1278 [Middag, R., De Baar, H. J., Bruland, K. W., and Van Heuven, S. M.: The distribution of nickel in the West-Atlantic Ocean, its relationship with phosphate and a comparison to cadmium and zinc. *Frontiers in Marine Science*, 7, 105, 2020.](#)
- 1279
- 1280 [Middag, R., Zitoun, R., and Conway, T.: Trace Metals, in: *Marine Analytical Chemistry*, edited by: Blasco, J. and Tovar-Sánchez, A., Springer International Publishing, Cham, 103–198, \[https://doi.org/10.1007/978-3-031-14486-8_3\]\(https://doi.org/10.1007/978-3-031-14486-8_3\), 2023.](#)
- 1281
- 1282 [Millero, F. J., Sotolongo, S., and Izaguirre, M.: The oxidation kinetics of Fe \(II\) in seawater, *Geochimica et Cosmochimica Acta*, 51, 793–801, 1987.](#)
- 1283
- 1284 [Milligan, A. J. and Harrison, P. J.: Effects of non-steady-state iron limitation on nitrogen assimilatory enzymes in the marine diatom *thalassiosira weissflogii* \(BACILLARIOPHYCEAE\), *Journal of Phycology*, 36, 78–86, <https://doi.org/10.1046/j.1529-8817.2000.99013.x>, 2000.](#)
- 1285
- 1286
- 1287 [Mills, M. M., Alderkamp, A.-C., Thuróczy, C.-E., van Dijken, G. L., Laan, P., de Baar, H. J., and Arrigo, K. R.: Phytoplankton biomass and pigment responses to Fe amendments in the Pine Island and Amundsen polynyas, *Deep Sea Research Part II: Topical Studies in Oceanography*, 71, 61–76, 2012.](#)
- 1288
- 1289
- 1290 [Minas, H. J. and Minas, M.: Net community production in High nutrient-low chlorophyll waters of the tropical and Antarctic oceans-grazing vs iron hypothesis, *Oceanologica Acta*, 15, 145–162, 1992.](#)
- 1291
- 1292 [Misumi, K., Lindsay, K., Bryan, F. O., Moore, J. K., Doney, S. C., Tsumune, D., and Yoshida, Y.: The iron budget in ocean surface waters in the 20th and 21st centuries: Projections by the Community Earth System Model version 1, *Biogeosci. Discuss.*, 10, 8505–8559, 2013.](#)
- 1293
- 1294
- 1295 [Moore, C. M., Seeyave, S., Hickman, A. E., Allen, J. T., Lucas, M. I., Planquette, H., Pollard, R. T., and Poulton, A. J.: Iron-light interactions during the CROZet natural iron bloom and EXport experiment \(CROZEX\) I: Phytoplankton growth and photophysiology, *Deep-Sea Research Part II: Topical Studies in Oceanography*, 54, 2045–2065, <https://doi.org/10.1016/j.dsr2.2007.06.011>, 2007.](#)
- 1296
- 1297
- 1298
- 1299 [Moore, C. M., Mills, M. M., Arrigo, K. R., Berman-Frank, I., Bopp, L., Boyd, P. W., Galbraith, E. D., Geider, R. J., Guieu, C., Jaccard, S. L., Jickells, T. D., La Roche, J., Lenton, T. M., Mahowald, N. M., Marañón, E., Marinov, I., Moore, J. K., Nakatsuka, T., Oschlies, A., Saito, M. A., Thingstad, T. F., Tsuda, A., and Ulloa, O.: Processes and patterns of oceanic nutrient limitation, *Nature Geosci.*, 6, 701–710, <https://doi.org/10.1038/ngeo1765>, 2013.](#)
- 1300
- 1301
- 1302
- 1303 [Moore, J. K., Fu, W., Primeau, F., Britten, G. L., Lindsay, K., Long, M., Doney, S. C., Mahowald, N., Hoffman, F., and Randerson, J. T.: Sustained climate warming drives declining marine biological productivity, *Science*, 359, 1139–1143, <https://doi.org/10.1126/science.aao6379>, 2018.](#)
- 1304
- 1305
- 1306 [Morán, X. A. G., Sebastián, M., Pedrís-Alif, C., and Estrada, M.: Response of Southern Ocean phytoplankton and bacterioplankton production to short-term experimental warming, *Limnology & Oceanography*, 51, 1791–1800, <https://doi.org/10.4319/lo.2006.51.4.1791>, 2006.](#)
- 1307
- 1308
- 1309 [Moreau, S., Hattermann, T., de Steur, L., Kauko, H. M., Ahonen, H., Ardelan, M., Assmy, P., Chierici, M., Descamps, S., Dinter, T., Falkenhaus, T., Fransson, A., Grønningsæter, E., Hallfredsson, E. H., Huhn, O., Lebrun, A., Lowther, A., Lübcker, N., Monteiro, P., Peeken, I., Roychoudhury, A., Rózańska, M., Ryan-Keogh, T., Sanchez, N., Singh, A., Simonsen, J. H., Steiger, N., Thomalla, S. J., van Tonder, A., Wiktor, J. M., and Steen, H.: Wind-driven upwelling of iron sustains dense blooms and food webs in the eastern Weddell Gyre, *Nat Commun.*, 14, 1303, <https://doi.org/10.1038/s41467-023-36992-1>, 2023.](#)
- 1310
- 1311
- 1312
- 1313
- 1314
- 1315 [Noiri, Y., Kudo, I., Kiyosawa, H., Nishioka, J., and Tsuda, A.: Influence of iron and temperature on growth, nutrient utilization ratios and phytoplankton species composition in the western subarctic Pacific Ocean during the SEEDS experiment, *Progress in Oceanography*, 64, 149–166, 2005.](#)
- 1316
- 1317
- 1318 [Ohnemus, D. C., Auro, M. E., Sherrell, R. M., Lagerström, M., Morton, P. L., Twining, B. S., Rauschenberg, S., and Lam, P. J.: Laboratory intercomparison of marine particulate digestions including Piranha: a novel chemical method for dissolution of polyethersulfone filters, *Limnology & Ocean Methods*, 12, 530–547, <https://doi.org/10.4319/lom.2014.12.530>, 2014.](#)
- 1319
- 1320
- 1321 [Olson, R. J., Sosik, H. M., Chekalyuk, A. M., and Shalapyonok, A.: Effects of iron enrichment on phytoplankton in the Southern Ocean during late summer: Active fluorescence and flow cytometric analyses, *Deep-Sea Research Part II: Topical Studies in Oceanography*, 47, 3181–3200, \[https://doi.org/10.1016/S0967-0645\\(00\\)00064-3\]\(https://doi.org/10.1016/S0967-0645\(00\)00064-3\), 2000.](#)
- 1322
- 1323
- 1324 [Park, J., Kuzminov, F. I., Bailleul, B., Yang, E. J., Lee, S., Falkowski, P. G., and Gorbunov, M. Y.: Light availability rather than Fe controls the magnitude of massive phytoplankton bloom in the Amundsen Sea polynyas, *Antarctica, Limnology and*](#)
- 1325

- 1326 [Oceanography](https://doi.org/10.1002/lno.10565), 62, 2260–2276, <https://doi.org/10.1002/lno.10565>, 2017.
- 1327 [Pausch, F., Bischof, K., and Trimborn, S.: Iron and manganese co-limit growth of the Southern Ocean diatom *Chaetoceros debilis*. PLOS ONE, 14, e0221959, <https://doi.org/10.1371/journal.pone.0221959>, 2019.](https://doi.org/10.1371/journal.pone.0221959)
- 1329 [Peers, G. and Price, N. M.: A role for manganese in superoxide dismutases and growth of iron-deficient diatoms. Limnology & Oceanography, 49, 1774–1783, <https://doi.org/10.4319/lo.2004.49.5.1774>, 2004.](https://doi.org/10.4319/lo.2004.49.5.1774)
- 1331 [Petrou, K., Kranz, S. A., Trimborn, S., Hassler, C. S., Ameijeiras, S. B., Sackett, O., Ralph, P. J., and Davidson, A. T.: Southern Ocean phytoplankton physiology in a changing climate. Journal of Plant Physiology, 203, 135–150, 2016.](https://doi.org/10.1111/j.1365-3113.2016.04611.x)
- 1333 [Pinkerton, M. H., Boyd, P. W., Deppeler, S., Hayward, A., Höfer, J., and Moreau, S.: Evidence for the impact of climate change on primary producers in the Southern Ocean. Frontiers in Ecology and Evolution, 9, 592027, 2021.](https://doi.org/10.3389/fecol.2021.692027)
- 1335 [Planquette, H. and Sherrell, R. M.: Sampling for particulate trace element determination using water sampling bottles: methodology and comparison to in situ pumps. Limnology and Oceanography: Methods, 10, 367–388, 2012.](https://doi.org/10.3389/fmets.2012.00038)
- 1337 [Primeau, F. W., Holzer, M., and DeVries, T.: Southern Ocean nutrient trapping and the efficiency of the biological pump. J. Geophys. Res. Oceans, 118, 2547–2564, <https://doi.org/10.1002/jgrc.20181>, 2013.](https://doi.org/10.1002/jgrc.20181)
- 1339 [Raiswell, R., Benning, L. G., Tranter, M., and Tulaczyk, S.: Bioavailable iron in the Southern Ocean: the significance of the iceberg conveyor belt. Geochem Trans, 9, 7, <https://doi.org/10.1186/1467-4866-9-7>, 2008.](https://doi.org/10.1186/1467-4866-9-7)
- 1341 [Raiswell, R., Hawkings, J. R., Benning, L. G., Baker, A. R., Death, R., Albani, S., Mahowald, N., Krom, M. D., Poulton, S. W., and Wadham, J.: Potentially bioavailable iron delivery by iceberg-hosted sediments and atmospheric dust to the polar oceans. Biogeosciences, 13, 3887–3900, 2016.](https://doi.org/10.1016/j.bioge.2016.07.001)
- 1344 [Raven, J. A.: Predictions of Mn and Fe use efficiencies of phototrophic growth as a function of light availability for growth and of C assimilation pathway. New Phytologist, 116, 1–18, <https://doi.org/10.1111/j.1469-8137.1990.tb00505.x>, 1990.](https://doi.org/10.1111/j.1469-8137.1990.tb00505.x)
- 1346 [Reay, D. S., Priddle, J., Nedwell, D. B., Whitehouse, M. J., Ellis-Evans, J. C., Deubert, C., and Connelly, D. P.: Regulation by low temperature of phytoplankton growth and nutrient uptake in the Southern Ocean. Marine Ecology Progress Series, 219, 51–64, 2001.](https://doi.org/10.1002/mec.1001)
- 1349 [Rignot, E., Jacobs, S., Mouginot, J., and Scheuchl, B.: Ice-Shelf Melting Around Antarctica. Science, 341, 266–270, <https://doi.org/10.1126/science.1235798>, 2013.](https://doi.org/10.1126/science.1235798)
- 1351 [Rijkenberg, M. J., de Baar, H. J., Bakker, K., Gerringa, L. J., Keijzer, E., Laan, M., Laan, P., Middag, R., Ober, S., and van Ooijen, J.: “PRISTINE”: a new high volume sampler for ultraclean sampling of trace metals and isotopes. Marine Chemistry, 177, 501–509, 2015.](https://doi.org/10.1016/j.marchem.2015.07.001)
- 1354 [Rose, J. M., Feng, Y., DiTullio, G. R., Dunbar, R. B., Hare, C. E., Lee, P. A., Lohan, M., Long, M., Smith Jr, W. O., and Sohst, B.: Synergistic effects of iron and temperature on Antarctic phytoplankton and microzooplankton assemblages. Biogeosciences, 6, 3131–3147, 2009.](https://doi.org/10.1016/j.bioge.2009.07.001)
- 1357 [Ryan-Keogh, T. J., Thomalla, S. J., Monteiro, P. M., and Tagliabue, A.: Multidecadal trend of increasing iron stress in Southern Ocean phytoplankton. Science, 379, 834–840, 2023.](https://doi.org/10.1126/science.1235798)
- 1359 [Ryderheim, F., Grønning, J., and Kiørboe, T.: Thicker shells reduce copepod grazing on diatoms. Limnology and Oceanography Letters, 7, 435–442, 2022.](https://doi.org/10.1002/lno.10565)
- 1361 [Sarmiento, J. L., Gruber, N., Brzezinski, M. A., and Dunne, J. P.: High-latitude controls of thermocline nutrients and low latitude biological productivity. Nature, 427, 56–60, <https://doi.org/10.1038/nature02127>, 2004.](https://doi.org/10.1038/nature02127)
- 1363 [Schoffman, H., Lis, H., Shaked, Y., and Keren, N.: Iron–Nutrient Interactions within Phytoplankton. Frontiers in Plant Science, 7, 2016.](https://doi.org/10.3389/fpls.2016.00073)
- 1365 [Schofield, O., Miles, T., Alderkamp, A.-C., Lee, S., Haskins, C., Rogalsky, E., Sipler, R., Sherrell, R. M., and Yager, P. L.: In situ phytoplankton distributions in the Amundsen Sea Polynya measured by autonomous gliders. Elementa, 3, 000073, 2015.](https://doi.org/10.3389/fmets.2015.00073)
- 1368 [Selz, V., Lowry, K. E., Lewis, K. M., Joy-Warren, H. L., van de Poll, W., Nirmel, S., Tong, A., and Arrigo, K. R.: Distribution of *Phaeocystis antarctica*-dominated sea ice algal communities and their potential to seed phytoplankton across the western Antarctic Peninsula in spring. Marine Ecology Progress Series, 586, 91–112, 2018.](https://doi.org/10.1002/mec.1001)
- 1370

- 1371 [Seytimammedov, K., Stirling, C. H., Reid, M. R., van Hale, R., Laan, P., Arrigo, K. R., van Dijken, G., Alderkamp, A.-C.,](#)
1372 [and Middag, R.: The distribution of Fe across the shelf of the Western Antarctic Peninsula at the start of the phytoplankton](#)
1373 [growing season, *Marine Chemistry*, 238, 104066, 2022.](#)
- 1374 [Shaw, T. J., Smith Jr, K. L., Hexel, C. R., Dudgeon, R., Sherman, A. D., Vernet, M., and Kaufmann, R. S.: 234Th-based](#)
1375 [carbon export around free-drifting icebergs in the Southern Ocean, *Deep Sea Research Part II: Topical Studies in*](#)
1376 [Oceanography](#), 58, 1384–1391, 2011.
- 1377 [Sherrell, R. M., Lagerström, M. E., Forsch, K. O., Stammerjohn, S. E., and Yager, P. L.: Dynamics of dissolved iron and](#)
1378 [other bioactive trace metals \(Mn, Ni, Cu, Zn\) in the Amundsen Sea Polynya, Antarctica, *Elementa: Science of the*](#)
1379 [Anthropocene](#), 3, 000071, <https://doi.org/10.12952/journal.elementa.000071>, 2015.
- 1380 [Shi, J.-R., Talley, L. D., Xie, S.-P., Liu, W., and Gille, S. T.: Effects of buoyancy and wind forcing on Southern Ocean](#)
1381 [climate change, *Journal of Climate*](#), 33, 10003–10020, 2020.
- 1382 [Sieber, M., Conway, T. M., de Souza, G. F., Hassler, C. S., Ellwood, M. J., and Vance, D.: Isotopic fingerprinting of](#)
1383 [biogeochemical processes and iron sources in the iron-limited surface Southern Ocean, *Earth and Planetary Science Letters*](#),
1384 [567, 116967, 2021.](#)
- 1385 [Sinha, A. K., Parli Venkateswaran, B., Tripathy, S. C., Sarkar, A., and Prabhakaran, S.: Effects of growth conditions on](#)
1386 [siderophore producing bacteria and siderophore production from Indian Ocean sector of Southern Ocean, *J Basic Microbiol*](#),
1387 [59, 412–424, <https://doi.org/10.1002/jobm.201800537>, 2019.](#)
- 1388 [Slagter, H. A., Gerringa, L. J. A., and Brussaard, C. P. D.: Phytoplankton Virus Production Negatively Affected by Iron](#)
1389 [Limitation, *Frontiers in Marine Science*](#), 3, 2016.
- 1390 [Stapleford, L. S. and Smith, R. E.: The interactive effects of temperature and silicon limitation on the psychrophilic ice](#)
1391 [diatom *Pseudonitzschia seriata*, *Polar Biology*](#), 16, 589–594, 1996.
- 1392 [Strass, V. H., Rohardt, G., Kanzow, T., Hoppema, M., and Boebel, O.: Multidecadal Warming and Density Loss in the Deep](#)
1393 [Weddell Sea, Antarctica, *Journal of Climate*](#), 33, 9863–9881, <https://doi.org/10.1175/JCLI-D-20-0271.1>, 2020.
- 1394 [Strzepek, R. F., Boyd, P. W., and Sunda, W. G.: Photosynthetic adaptation to low iron, light, and temperature in Southern](#)
1395 [Ocean phytoplankton, *Proceedings of the National Academy of Sciences*](#), 116, 4388–4393, 2019.
- 1396 [Tagliabue, A., Aumont, O., DeAth, R., Dunne, J. P., Dutkiewicz, S., Galbraith, E., Misumi, K., Moore, J. K., Ridgwell, A.,](#)
1397 [Sherman, E., Stock, C., Vichi, M., Völker, C., and Yool, A.: How well do global ocean biogeochemistry models simulate](#)
1398 [dissolved iron distributions?, *Global Biogeochemical Cycles*](#), 30, 149–174, <https://doi.org/10.1002/2015GB005289>, 2016.
- 1399 [Takahashi, T., Sweeney, C., Hales, B., Chipman, D. W., Newberger, T., Goddard, J. G., Iannuzzi, R. A., and Sutherland, S.](#)
1400 [C.: The changing carbon cycle in the Southern Ocean, *Oceanography*](#), 25, 26–37, 2012.
- 1401 [Taylor, S. R. and McLennan, S. M.: The continental crust: its composition and evolution, 1985.](#)
- 1402 [Teske, V., Timmermann, R., and Semmler, T.: Subsurface warming in the Antarctica’s Weddell Sea can be avoided by](#)
1403 [reaching the 2° C warming target, *Communications Earth & Environment*](#), 5, 93, 2024.
- 1404 [Thomalla, S. J., Nicholson, S.-A., Ryan-Keogh, T. J., and Smith, M. E.: Widespread changes in Southern Ocean](#)
1405 [phytoplankton blooms linked to climate drivers, *Nature Climate Change*](#), 13, 975–984, 2023.
- 1406 [Turner, J., Colwell, S. R., Marshall, G. J., Lachlan-Cope, T. A., Carleton, A. M., Jones, P. D., Lagun, V., Reid, P. A., and](#)
1407 [Iagovkina, S.: Antarctic climate change during the last 50 years, *International journal of Climatology*](#), 25, 279–294, 2005.
- 1408 [Twining, B. S. and Baines, S. B.: The trace metal composition of marine phytoplankton, *Annual review of marine science*](#), 5,
1409 [191–215, 2013.](#)
- 1410 [Twining, B. S., Baines, S. B., and Fisher, N. S.: Element stoichiometries of individual plankton cells collected during the](#)
1411 [Southern Ocean Iron Experiment \(SOFEX\), *Limnology and oceanography*](#), 49, 2115–2128, 2004.
- 1412 [Van der Merwe, P., Wuttig, K., Holmes, T., Trull, T. W., Chase, Z., Townsend, A. T., Goemann, K., and Bowie, A. R.: High](#)
1413 [lability Fe particles sourced from glacial erosion can meet previously unaccounted biological demand: Heard Island,](#)
1414 [Southern Ocean, *Frontiers in Marine Science*](#), 6, 332, 2019.
- 1415 [Van Heukelem, L. and Thomas, C. S.: Computer-assisted high-performance liquid chromatography method development](#)

1416 [with applications to the isolation and analysis of phytoplankton pigments, *Journal of Chromatography A*, 910, 31–49, 2001.](#)

1417 [Van Leeuwe, M. A., Villerius, L. A., Roggeveld, J., Visser, R. J. W., and Stefels, J.: An optimized method for automated](#)
1418 [analysis of algal pigments by HPLC, *Marine chemistry*, 102, 267–275, 2006.](#)

1419 [Van Manen, M., Aoki, S., Brussaard, C. P., Conway, T. M., Eich, C., Gerringa, L. J., Jung, J., Kim, T.-W., Lee, S., and Lee,](#)
1420 [Y.: The role of the Dotson Ice Shelf and Circumpolar Deep Water as driver and source of dissolved and particulate iron and](#)
1421 [manganese in the Amundsen Sea polynya, *Southern Ocean, Marine Chemistry*, 246, 104161, 2022.](#)

1422 [Van Oijen, T., Van Leeuwe, M. A., Granum, E., Weissing, F. J., Bellerby, R. G. J., Gieskes, W. W. C., and De Baar, H. J.](#)
1423 [W.: Light rather than iron controls photosynthate production and allocation in Southern Ocean phytoplankton populations](#)
1424 [during austral autumn, *Journal of Plankton Research*, 26, 885–900, 2004.](#)

1425 [Veldhuis, M. J. and Kraay, G. W.: Phytoplankton in the subtropical Atlantic Ocean: towards a better assessment of biomass](#)
1426 [and composition, *Deep Sea Research Part I: Oceanographic Research Papers*, 51, 507–530, 2004.](#)

1427 [Venables, H. and Moore, C. M.: Phytoplankton and light limitation in the Southern Ocean: Learning from high-nutrient,](#)
1428 [high-chlorophyll areas, *Journal of Geophysical Research: Oceans*, 115, <https://doi.org/10.1029/2009JC005361>, 2010.](#)

1429 [Verardo, D. J., Froelich, P. N., and McIntyre, A.: Determination of organic carbon and nitrogen in marine sediments using](#)
1430 [the Carlo Erba NA-1500 Analyzer, *Deep Sea Research Part A. Oceanographic Research Papers*, 37, 157–165, 1990.](#)

1431 [Viljoen, J. J., Philibert, R., Van Horsten, N., Mtshali, T., Roychoudhury, A. N., Thomalla, S., and Fietz, S.: Phytoplankton](#)
1432 [response in growth, photophysiology and community structure to iron and light in the Polar Frontal Zone and Antarctic](#)
1433 [waters, *Deep-Sea Research Part I: Oceanographic Research Papers*, 141, 118–129, <https://doi.org/10.1016/j.dsr.2018.09.006>,](#)
1434 [2018.](#)

1435 [Vives, C. R., Schallenberg, C., Strutton, P. G., and Westwood, K. J.: Iron and light limitation of phytoplankton growth off](#)
1436 [East Antarctica, *Journal of Marine Systems*, 234, <https://doi.org/10.1016/j.jmarsys.2022.103774>, 2022.](#)

1437 [Von Berg, L., Prend, C. J., Campbell, E. C., Mazloff, M. R., Talley, L. D., and Gille, S. T.: Weddell Sea Phytoplankton](#)
1438 [Blooms Modulated by Sea Ice Variability and Polynya Formation, *Geophysical Research Letters*, 47, e2020GL087954,](#)
1439 [<https://doi.org/10.1029/2020GL087954>, 2020.](#)

1440 [Voronina, N. M., Kosobokova, K. N., and Pakhomov, E. A.: Composition and biomass of summer metazoan plankton in the](#)
1441 [0–200 m layer of the Atlantic sector of the Antarctic, *Polar Biol*, 14, <https://doi.org/10.1007/BF00234970>, 1994.](#)

1442 [Waite, A. M. and Nodder, S. D.: The effect of in situ iron addition on the sinking rates and export flux of Southern Ocean](#)
1443 [diatoms, *Deep Sea Research Part II: Topical Studies in Oceanography*, 48, 2635–2654, 2001.](#)

1444 [Wang, X. J., Behrenfeld, M., Le Borgne, R., Murtugudde, R., and Boss, E.: Regulation of phytoplankton carbon to](#)
1445 [chlorophyll ratio by light, nutrients and temperature in the Equatorial Pacific Ocean: a basin-scale model, *Biogeosciences*, 6,](#)
1446 [391–404, 2009.](#)

1447 [Wolfe-Simon, F., Grzebyk, D., Schofield, O., and Falkowski, P. G.: The role and evolution of superoxide dismutases in](#)
1448 [algae, *Journal of Phycology*, 41, 453–465, <https://doi.org/10.1111/j.1529-8817.2005.00086.x>, 2005.](#)

1449 [Worden, A. Z., Nolan, J. K., and Palenik, B.: Assessing the dynamics and ecology of marine picophytoplankton: The](#)
1450 [importance of the eukaryotic component, *Limnology and Oceanography*, 49, 168–179,](#)
1451 [<https://doi.org/10.4319/lo.2004.49.1.0168>, 2004.](#)

1452 [Wu, M., McCain, J. S. P., Rowland, E., Middag, R., Sandgren, M., Allen, A. E., and Bertrand, E. M.: Manganese and iron](#)
1453 [deficiency in Southern Ocean *Phaeocystis antarctica* populations revealed through taxon-specific protein indicators, *Nature*](#)
1454 [Communications, 10, 3582, <https://doi.org/10.1038/s41467-019-11426-z>, 2019.](#)

1455 [Yoon, J.-E., Yoo, K.-C., Macdonald, A. M., Yoon, H.-I., Park, K.-T., Yang, E. J., Kim, H.-C., Lee, J. I., Lee, M. K., Jung, J.,](#)
1456 [Park, J., Lee, J., Kim, S., Kim, S.-S., Kim, K., and Kim, I.-N.: Reviews and syntheses: Ocean iron fertilization experiments –](#)
1457 [past, present, and future looking to a future Korean Iron Fertilization Experiment in the Southern Ocean \(KIFES\) project,](#)
1458 [Biogeosciences, 15, 5847–5889, <https://doi.org/10.5194/bg-15-5847-2018>, 2018.](#)

1459 [Zhu, Z., Xu, K., Fu, F., Spackeen, J. L., Bronk, D. A., and Hutchins, D. A.: A comparative study of iron and temperature](#)
1460 [interactive effects on diatoms and *Phaeocystis antarctica* from the Ross Sea, Antarctica, *Marine Ecology Progress Series*,](#)
1461 [550, 39–51, 2016.](#)

1462 Aflenzer, H., Hoffmann, L., Holmes, T., Wuttig, K., Genovese, C., & Bowie, A. R. (2023). Effect of dissolved
1463 iron (II) and temperature on growth of the Southern Ocean phytoplankton species *Fragilariopsis*
1464 *cylindrus* and *Phaeocystis antarctica*. *Polar Biology*, *46*(11), 1163–1173.
1465 <https://doi.org/10.1007/s00300-023-03191-z>

1466 Alderkamp, A. C., van Dijken, G. L., Lowry, K. E., Connelly, T. L., Lagerström, M., Sherrell, R. M., Haskins,
1467 C., Rogalsky, E., Schofield, O., Stammerjohn, S. E., Yager, P. L., & Arrigo, K. R. (2015). Fe
1468 availability drives phytoplankton photosynthesis rates during spring bloom in the Amundsen Sea
1469 Polynya, Antarctica. *Elementa: Science of the Anthropocene*, *3*(C), 000043.
1470 <https://doi.org/10.12952/journal.elementa.000043>

1471 Alderkamp, A. C., Van Dijken, G. L., Lowry, K. E., Lewis, K. M., Joy Warren, H. L., Van De Poll, W., Laan,
1472 P., Gerringa, L., Delmont, T. O., Jenkins, B. D., & Arrigo, K. R. (2019). Effects of iron and light
1473 availability on phytoplankton photosynthetic properties in the Ross Sea. *Marine Ecology Progress*
1474 *Series*, *621*, 33–50. Scopus. <https://doi.org/10.3354/meps13000>

1475 Alfred Wegener Institut Helmholtz Zentrum für Polar und Meeresforschung. (2017). Polar Research and
1476 Supply Vessel POLARSTERN Operated by the Alfred Wegener Institute. *Journal of large scale*
1477 *research facilities*, *3*, A119. <http://dx.doi.org/10.17815/jlsrf-3-163>

1478 Andrew, S. M., Morell, H. T., Strzepek, R. F., Boyd, P. W., & Ellwood, M. J. (2019). Iron availability
1479 influences the tolerance of southern ocean phytoplankton to warming and elevated irradiance. *Frontiers*
1480 *in Marine Science*, *6*, 681.

1481 Andrew, S. M., Strzepek, R. F., M. Whitney, S., Chow, W. S., & Ellwood, M. J. (2022). Divergent
1482 physiological and molecular responses of light and iron limited Southern Ocean phytoplankton.
1483 *Limnology and Oceanography Letters*, *7*(2), 150–158. <https://doi.org/10.1002/lol2.10223>

1484 Annett, A. L., Skiba, M., Henley, S. F., Venables, H. J., Meredith, M. P., Statham, P. J., & Ganeshram, R. S.
1485 (2015). Comparative roles of upwelling and glacial iron sources in Ryder Bay, coastal western
1486 Antarctic Peninsula. *Marine Chemistry*, *176*, 21–33.

1487 Arrigo, K. R., & van Dijken, G. L. (2003). Phytoplankton dynamics within 37 Antarctic coastal polynya
1488 systems. *Journal of Geophysical Research: Oceans*, *108*(8), 27 1–27 18.
1489 <https://doi.org/10.1029/2002jc001739>

1490 Arrigo, K. R., van Dijken, G. L., Alderkamp, A. C., Erickson, Z. K., Lewis, K. M., Lowry, K. E., Joy Warren,
1491 H. L., Middag, R., Nash Arrigo, J. E., Selz, V., & van de Poll, W. (2017). Early Spring Phytoplankton

1492 Dynamics in the Western Antarctic Peninsula. *Journal of Geophysical Research: Oceans*, 122(12),
1493 9350–9369. <https://doi.org/10.1002/2017JC013281>

1494 Assmy, P., Smetacek, V., Montresor, M., Klaas, C., Henjes, J., Strass, V. H., Arrieta, J. M., Bathmann, U., Berg,
1495 G. M., & Breitbarth, E. (2013). Thick-shelled, grazer-protected diatoms decouple ocean carbon and
1496 silicon cycles in the iron-limited Antarctic Circumpolar Current. *Proceedings of the National Academy
1497 of Sciences*, 110(51), 20633–20638.

1498 Balaguer, J., Koch, F., Hassler, C., & Trimborn, S. (2022). Iron and manganese co-limit the growth of two
1499 phytoplankton groups dominant at two locations of the Drake Passage. *Communications Biology*, 5(1),
1500 Article 1. <https://doi.org/10.1038/s42003-022-03148-8>

1501 Basterretxea, G., Font Muñoz, J. S., Hernández-Carrasco, I., & Sañudo-Wilhelmy, S. A. (2023). Global
1502 variability of high-nutrient low-chlorophyll regions using neural networks and wavelet coherence
1503 analysis. *Ocean Science*, 19(4), 973–990. <https://doi.org/10.5194/os-19-973-2023>

1504 Bazzani, E., Lauritano, C., & Saggiomo, M. (2023). Southern Ocean Iron Limitation of Primary Production
1505 between Past Knowledge and Future Projections. *Journal of Marine Science and Engineering*, 11(2),
1506 272.

1507 Bertrand, E. M., Saito, M. A., Lee, P. A., Dunbar, R. B., Sedwick, P. N., & Ditullio, G. R. (2011). Iron
1508 limitation of a springtime bacterial and phytoplankton community in the Ross Sea: Implications for
1509 vitamin B12 nutrition. *Frontiers in Microbiology*, 2(AUG). Scopus.
1510 <https://doi.org/10.3389/fmicb.2011.00160>

1511 Bertrand, E. M., Saito, M. A., Rose, J. M., Riesselman, C. R., Lohan, M. C., Noble, A. E., Lee, P. A., &
1512 DiTullio, G. R. (2007). Vitamin B12 and iron colimitation of phytoplankton growth in the Ross Sea.
1513 *Limnology and Oceanography*, 52(3), 1079–1093.

1514 Biggs, T. E., Alvarez-Fernandez, S., Evans, C., Mojica, K. D., Rozema, P. D., Venables, H. J., Pond, D. W., &
1515 Brussaard, C. P. (2019). Antarctic phytoplankton community composition and size structure:
1516 Importance of ice type and temperature as regulatory factors. *Polar Biology*, 42, 1997–2015.

1517 Boyd, P. W. (2002). The role of iron in the biogeochemistry of the Southern Ocean and equatorial Pacific: A
1518 comparison of in situ iron enrichments. *Deep Sea Research Part II: Topical Studies in Oceanography*,
1519 49(9–10), 1803–1821.

1520 Boyd, P. W., Arrigo, K. R., Strzeppek, R., & Van Dijken, G. L. (2012). Mapping phytoplankton iron utilization:
1521 Insights into Southern Ocean supply mechanisms. *Journal of Geophysical Research: Oceans*, 117(C6).

1522 Boyd, P. W., Rynearson, T. A., Armstrong, E. A., Fu, F., Hayashi, K., Hu, Z., Hutchins, D. A., Kudela, R. M.,
1523 Litchman, E., & Mulholland, M. R. (2013). Marine phytoplankton temperature-versus-growth
1524 responses from polar to tropical waters—outcome of a scientific community-wide study. *PloS One*, *8*(5),
1525 e63091.

1526 Boyd, P. W., Strzepek, R. F., Ellwood, M. J., Hutchins, D. A., Nodder, S. D., Twining, B. S., & Wilhelm, S. W.
1527 (2015). Why are biotic iron pools uniform across high- and low-iron pelagic ecosystems? *Global*
1528 *Biogeochemical Cycles*, *29*(7), 1028–1043. <https://doi.org/10.1002/2014GB005014>

1529 Brooks, P. R., & Crowe, T. P. (2019). Combined effects of multiple stressors: New insights into the influence of
1530 ——— timing and sequence. *Frontiers in Ecology and Evolution*, *7*, 387.

1531 Bronselaer, B., Russell, J. L., Winton, M., Williams, N. L., Key, R. M., Dunne, J. P., Feely, R. A., Johnson, K.
1532 S., & Sarmiento, J. L. (2020). Importance of wind and meltwater for observed chemical and physical
1533 changes in the Southern Ocean. *Nature Geoscience*, *13*(1), 35–42. [https://doi.org/10.1038/s41561-019-](https://doi.org/10.1038/s41561-019-0502-8)
1534 [0502-8](https://doi.org/10.1038/s41561-019-0502-8)

1535 Browning, T. J., Achterberg, E. P., Engel, A., & Mawji, E. (2021). Manganese co-limitation of phytoplankton
1536 growth and major nutrient drawdown in the Southern Ocean. *Nature Communications*, *12*(1), Article 1.
1537 <https://doi.org/10.1038/s41467-021-21122-6>

1538 Buesseler, K. O., Boyd, P. W., Black, E. E., & Siegel, D. A. (2020). Metrics that matter for assessing the ocean
1539 biological carbon pump. *Proceedings of the National Academy of Sciences*, *117*(18), 9679–9687.
1540 <https://doi.org/10.1073/pnas.1918114117>

1541 Burns, S. M., Bundy, R. M., Abbott, W., Abdala, Z., Sterling, A. R., Chappell, P. D., Jenkins, B. D., & Buck, K.
1542 N. (2023). Interactions of bioactive trace metals in shipboard Southern Ocean incubation experiments.
1543 *Limnology and Oceanography*, *68*(3), 525–543. <https://doi.org/10.1002/lno.12290>

1544 Caron, D. A., & Hutchins, D. A. (2013). The effects of changing climate on microzooplankton grazing and
1545 community structure: Drivers, predictions and knowledge gaps. *Journal of Plankton Research*, *35*(2),
1546 235–252. <https://doi.org/10.1093/plankt/fbs091>

1547 Chen, B., Landry, M. R., Huang, B., & Liu, H. (2012). Does warming enhance the effect of microzooplankton
1548 grazing on marine phytoplankton in the ocean? *Limnology and Oceanography*, *57*(2), 519–526.

1549 Cullen, J. T., & Sherrell, R. M. (1999). Techniques for determination of trace metals in small samples of size-
1550 fractionated particulate matter: Phytoplankton metals off central California. *Marine Chemistry*, *67*(3–
1551 4), 233–247.

1552 Cunningham, B. R., & John, S. G. (2017). The effect of iron limitation on cyanobacteria major nutrient and
1553 trace element stoichiometry. *Limnology and Oceanography*, *62*(2), 846–858.
1554 <https://doi.org/10.1002/lno.10484>

1555 Cutter, G. A., Andersson, P., Codispoti, L., Croot, P., Place, P., Hoe, T., Kingdom, U., Francois, R., Sciences,
1556 O., Lohan, M., Circus, D., & Obata, H. (2017). *Sampling and Sample handling Protocols for*
1557 *GEOTRACES Cruises*. *3.0*(August).

1558 Darelhus, E., Daae, K., Dundas, V., Fer, I., Hellmer, H. H., Janout, M., Nicholls, K. W., Sallée, J. B., &
1559 Østerhus, S. (2023). Observational evidence for on-shelf heat transport driven by dense water export in
1560 the Weddell Sea. *Nature Communications*, *14*(1), 1022.

1561 De Baar, H. J. W., Boyd, P. W., Coale, K. H., Landry, M. R., Tsuda, A., Assmy, P., Bakker, D. C. E., Bozec, Y.,
1562 Barber, R. T., Brzezinski, M. A., Buesseler, K. O., Boyé, M., Croot, P. L., Gervais, F., Gorbunov, M.
1563 Y., Harrison, P. J., Hiscock, W. T., Laan, P., Lancelot, C., ... Wong, C. (2005). Synthesis of iron
1564 fertilization experiments: From the Iron Age in the Age of Enlightenment. *Journal of Geophysical*
1565 *Research: Oceans*, *110*(C9), 2004JC002601. <https://doi.org/10.1029/2004JC002601>

1566 De Baar, H. J. W., Timmermans, K. R., Laan, P., De Porto, H. H., Ober, S., Blom, J. J., Bakker, M. C.,
1567 Schilling, J., Sarthou, G., Smit, M. G., & Klunder, M. (2008). Titan: A new facility for ultraclean
1568 sampling of trace elements and isotopes in the deep oceans in the international Geotraces program.
1569 *Marine Chemistry*, *111*(1–2), 4–21. <https://doi.org/10.1016/j.marchem.2007.07.009>

1570 De Lavergne, C., Palter, J. B., Galbraith, E. D., Bernardello, R., & Marinov, I. (2014). Cessation of deep
1571 convection in the open Southern Ocean under anthropogenic climate change. *Nature Climate Change*,
1572 *4*(4), 278–282.

1573 Deppeler, S. L., & Davidson, A. T. (2017). Southern Ocean Phytoplankton in a Changing Climate. *Frontiers in*
1574 *Marine Science*, *4*. <https://www.frontiersin.org/articles/10.3389/fmars.2017.00040>

1575 Drijfhout, S. S., Bull, C. Y. S., Hewitt, H., Holland, P. R., Jenkins, A., Mathiot, P., & Garabato, A. N. (2024).
1576 An Amundsen Sea source of decadal temperature changes on the Antarctic continental shelf. *Ocean*
1577 *Dynamics*, *74*(1), 37–52. <https://doi.org/10.1007/s10236-023-01587-3>

1578 Eich, C., Biggs, T. E., van de Poll, W. H., van Manen, M., Tian, H. A., Jung, J., Lee, Y., Middag, R., &
1579 Brussaard, C. P. (2022). Ecological importance of viral lysis as a loss factor of phytoplankton in the
1580 Amundsen Sea. *Microorganisms*, *10*(10), 1967.

1581 Eich, C., Pont, S. B., & Brussaard, C. P. (2021). Effects of UV radiation on the chlorophyte *Micromonas polaris*
1582 host–virus interactions and MpoV-45T virus infectivity. *Microorganisms*, *9*(12), 2429.

1583 Fahrbach, E., Hoppema, M., Rohardt, G., Schröder, M., & Wisotzki, A. (2004). Decadal scale variations of
1584 water mass properties in the deep Weddell Sea. *Ocean Dynamics*, *54*(1), 77–91.
1585 <https://doi.org/10.1007/s10236-003-0082-3>

1586 Feng, Y., Hare, C. E., Rose, J. M., Handy, S. M., DiTullio, G. R., Lee, P. A., Smith, W. O., Peloquin, J., Tozzi,
1587 S., Sun, J., Zhang, Y., Dunbar, R. B., Long, M. C., Sohst, B., Lohan, M., & Hutchins, D. A. (2010).
1588 Interactive effects of iron, irradiance and CO₂ on Ross Sea phytoplankton. *Deep Sea Research Part I:
1589 Oceanographic Research Papers*, *57*(3), 368–383. <https://doi.org/10.1016/j.dsr.2009.10.013>

1590 Fisher, B. J., Poulton, A. J., Meredith, M. P., Baldry, K., Schofield, O., & Henley, S. F. (2023).
1591 Biogeochemistry of climate driven shifts in Southern Ocean primary producers. *Biogeosciences
1592 Discussions*, 1–29.

1593 Fourquez, M., Janssen, D. J., Conway, T. M., Cabanes, D., Ellwood, M. J., Sieber, M., Trimborn, S., & Hassler,
1594 C. (2023). Chasing iron bioavailability in the Southern Ocean: Insights from *Phaeocystis antarctica*
1595 and iron speciation. *Science Advances*, *9*(26), eadf9696. <https://doi.org/10.1126/sciadv.adf9696>

1596 Friedlingstein, P., O'sullivan, M., Jones, M. W., Andrew, R. M., Gregor, L., Hauck, J., Le Quéré, C., Luijkx, I.,
1597 T., Olsen, A., & Peters, G. P. (2022). Global carbon budget 2022. *Earth System Science Data
1598 Discussions*, 2022, 1–159.

1599 From, N., Richardson, K., Mousing, E. A., & Jensen, P. E. (2014). Removing the light history signal from
1600 normalized variable fluorescence (F_v/F_m) measurements on marine phytoplankton. *Limnology and
1601 Oceanography: Methods*, *12*(11), 776–783. <https://doi.org/10.4319/lom.2014.12.776>

1602 Garrison, D. L., Gowing, M. M., Hughes, M. P., Campbell, L., Caron, D. A., Dennett, M. R., Shalapyonok, A.,
1603 Olson, R. J., Landry, M. R., Brown, S. L., Liu, H. B., Azam, F., Steward, G. F., Ducklow, H. W., &
1604 Smith, D. C. (2000). Microbial food web structure in the Arabian Sea: A US JGOFS study. *Deep Sea
1605 Research Part II: Topical Studies in Oceanography*, *47*(7), 1387–1422. [https://doi.org/10.1016/S0967-
1606 0645\(99\)00148-4](https://doi.org/10.1016/S0967-0645(99)00148-4)

1607 Geider, R. J. (1987). Light and temperature dependence of the carbon to chlorophyll a ratio in microalgae and
1608 cyanobacteria: Implications for physiology and growth of phytoplankton. *New Phytologist*, 1–34.

1609 Geider, R. J., & La Roche, J. (1994). The role of iron in phytoplankton photosynthesis, and the potential for
1610 iron-limitation of primary productivity in the sea. *Photosynthesis Research*, *39*, 275–301.

1611 Geider, R. J., MacIntyre, H. L., & Kana, T. M. (1998). A dynamic regulatory model of phytoplanktonic
1612 acclimation to light, nutrients, and temperature. *Limnology and Oceanography*, 43(4), 679–694.

1613 Gerringa, L. J. A., Alderkamp, A. C., Laan, P., Thuróczy, C. E., De Baar, H. J. W., Mills, M. M., van Dijken,
1614 G. L., van Haren, H., & Arrigo, K. R. (2020). Corrigendum to "Iron from melting glaciers fuels the
1615 phytoplankton blooms in Amundsen Sea (Southern Ocean): Iron biogeochemistry" (Gerringa et al.,
1616 2012). *Deep Sea Research Part II: Topical Studies in Oceanography*, 177, 104843.

1617 Gerringa, L. J. A., Laan, P., Arrigo, K. R., van Dijken, G. L., & Alderkamp, A. C. (2019). The organic
1618 complexation of iron in the Ross sea. *Marine Chemistry*, 215, 103672.
1619 <https://doi.org/10.1016/j.marchem.2019.103672>

1620 Gerringa, L. J., Alderkamp, A. C., Laan, P., Thuróczy, C. E., De Baar, H. J., Mills, M. M., van Dijken, G. L.,
1621 van Haren, H., & Arrigo, K. R. (2012). Iron from melting glaciers fuels the phytoplankton blooms in
1622 Amundsen Sea (Southern Ocean): Iron biogeochemistry. *Deep Sea Research Part II: Topical Studies in
1623 Oceanography*, 71, 16–31.

1624 Gómez Valdivia, F., Holland, P. R., Siahaan, A., Dutrieux, P., & Young, E. (2023). Projected West Antarctic
1625 Ocean Warming Caused by an Expansion of the Ross Gyre. *Geophysical Research Letters*, 50(6),
1626 e2023GL102978. <https://doi.org/10.1029/2023GL102978>

1627 Gordon, L. I., Jennings Jr, J. C., Ross, A. A., & Krest, J. M. (1993). A suggested protocol for continuous flow
1628 automated analysis of seawater nutrients (phosphate, nitrate, nitrite and silicic acid) in the WOCE
1629 Hydrographic Program and the Joint Global Ocean Fluxes Study. *WOCE Hydrographic Program
1630 Office, Methods Manual WHPO*, 68/91, 1–52.

1631 Greene, R. M., Geider, R. J., Kolber, Z., & Falkowski, P. G. (1992). Iron induced changes in light harvesting
1632 and photochemical energy conversion processes in eukaryotic marine algae. *Plant Physiology*, 100(2),
1633 565–575.

1634 Hassler, C. S., & Schoemann, V. (2009). Bioavailability of organically bound Fe to model phytoplankton of the
1635 Southern Ocean. *Biogeosciences*, 6(10), 2281–2296.

1636 Hawco, N. J., Tagliabue, A., & Twining, B. S. (2022). Manganese Limitation of Phytoplankton Physiology and
1637 Productivity in the Southern Ocean. *Global Biogeochemical Cycles*, 36(11), e2022GB007382.
1638 <https://doi.org/10.1029/2022GB007382>

1639 Hillenbrand, C. D., & Cortese, G. (2006). Polar stratification: A critical view from the Southern Ocean.
1640 *Palaeogeography, Palaeoclimatology, Palaeoecology*, 242(3–4), 240–252.

1641 [Hinz, D. J., Nielsdóttir, M. C., Korb, R. E., Whitehouse, M. J., Poulton, A. J., Moore, C. M., Achterberg, E. P.,](#)
1642 [& Bibby, T. S. \(2012\). Responses of microplankton community structure to iron addition in the Scotia](#)
1643 [Sea. *Deep-Sea Research Part II: Topical Studies in Oceanography*, 59–60, 36–46.](#)
1644 <https://doi.org/10.1016/j.dsr2.2011.08.006>

1645 [Hopwood, M. J., Carroll, D., Höfer, J., Achterberg, E. P., Meire, L., Le Moigne, F. A., Bach, L. T., Eich, C.,](#)
1646 [Sutherland, D. A., & González, H. E. \(2019\). Highly variable iron content modulates iceberg–ocean](#)
1647 [fertilisation and potential carbon export. *Nature Communications*, 10\(1\), 5261.](#)

1648 [Huang, Y., Fassbender, A. J., & Bushinsky, S. M. \(2023\). Biogenic carbon pool production maintains the](#)
1649 [Southern Ocean carbon sink. *Proceedings of the National Academy of Sciences*, 120\(18\),](#)
1650 [e2217909120. <https://doi.org/10.1073/pnas.2217909120>](#)

1651 [Hutchins, D. A., & Boyd, P. W. \(2016\). Marine phytoplankton and the changing ocean iron cycle. *Nature*](#)
1652 [*Climate Change*, 6\(12\), 1072–1079.](#)

1653 [Hutchins, D. A., & Bruland, K. W. \(1998\). Iron limited diatom growth and Si:N uptake ratios in a coastal](#)
1654 [upwelling regime. *Nature*, 393\(6685\), 561–564. Scopus. <https://doi.org/10.1038/31203>](#)

1655 [Jabre, L., & Bertrand, E. M. \(2020\). Interactive effects of iron and temperature on the growth of *Fragilariopsis*](#)
1656 [*cylindrus*. *Limnology and Oceanography Letters*, 5\(5\), 363–370.](#)

1657 [Jabre, L. J., Allen, A. E., McCain, J. S. P., McCrow, J. P., Tenenbaum, N., Spackeen, J. L., Sipler, R. E., Green,](#)
1658 [B. R., Bronk, D. A., Hutchins, D. A., & Bertrand, E. M. \(2021\). Molecular underpinnings and](#)
1659 [biogeochemical consequences of enhanced diatom growth in a warming Southern Ocean. *Proceedings*](#)
1660 [*of the National Academy of Sciences*, 118\(30\), e2107238118. <https://doi.org/10.1073/pnas.2107238118>](#)

1661 [Jensen, L. T., Wyatt, N. J., Landing, W. M., & Fitzsimmons, J. N. \(2020\). Assessment of the stability, sorption,](#)
1662 [and exchangeability of marine dissolved and colloidal metals. *Marine Chemistry*, 220, 103754.](#)
1663 <https://doi.org/10.1016/j.marchem.2020.103754>

1664 [Jeon, M. H., Jung, J., Park, M. O., Aoki, S., Kim, T. W., & Kim, S. K. \(2021\). Tracing Circumpolar Deep](#)
1665 [Water and glacial meltwater using humic-like fluorescent dissolved organic matter in the Amundsen](#)
1666 [Sea, Antarctica. *Marine Chemistry*, 235, 104008. <https://doi.org/10.1016/j.marchem.2021.104008>](#)

1667 [Kroh, G. E., & Pilon, M. \(2020\). Regulation of iron homeostasis and use in chloroplasts. *International Journal*](#)
1668 [*of Molecular Sciences*, 21\(9\), 3395.](#)

1669 Krumhardt, K. M., Long, M. C., Sylvester, Z. T., & Petrik, C. M. (2022). Climate drivers of Southern Ocean
1670 phytoplankton community composition and potential impacts on higher trophic levels. *Frontiers in*
1671 *Marine Science*, *9*, 916140.

1672 Kustka, A. B., Allen, A. E., & Morel, F. M. (2007). Sequence analysis and transcriptional regulation of iron
1673 acquisition genes in two marine diatoms 1. *Journal of Phycology*, *43*(4), 715–729.

1674 Lampe, R. H., Mann, E. L., Cohen, N. R., Till, C. P., Thamatrakoln, K., Brzezinski, M. A., Bruland, K. W.,
1675 Twining, B. S., & Marchetti, A. (2018). Different iron storage strategies among bloom-forming
1676 diatoms. *Proceedings of the National Academy of Sciences*, *115*(52), E12275–E12284.
1677 <https://doi.org/10.1073/pnas.1805243115>

1678 Lane, E. S., Jang, K., Cullen, J. T., & Maldonado, M. T. (2008). The interaction between inorganic iron and
1679 cadmium uptake in the marine diatom *Thalassiosira oceanica*. *Limnology and Oceanography*, *53*(5),
1680 1784–1789.

1681 Lannuzel, D., Vancoppenolle, M., van Der Merwe, P., De Jong, J., Meiners, K. M., Grotti, M., Nishioka, J., &
1682 Schoemann, V. (2016). Iron in sea ice: Review and new insights. *Elementa*, *4*, 000130.

1683 Laws, E. A., & Bannister, T. T. (1980). Nutrient and light limited growth of *Thalassiosira fluviatilis* in
1684 continuous culture, with implications for phytoplankton growth in the ocean 1. *Limnology and*
1685 *Oceanography*, *25*(3), 457–473.

1686 Maat, D. S., Biggs, T., Evans, C., Van Bleijswijk, J. D. L., Van der Wel, N. N., Dutilh, B. E., & Brussaard, C. P.
1687 D. (2017). Characterization and Temperature Dependence of Arctic *Micromonas polaris* Viruses.
1688 *Viruses*, *9*(6), Article 6. <https://doi.org/10.3390/v9060134>

1689 Mackey, M. D., Mackey, D. J., Higgins, H. W., & Wright, S. W. (1996). CHEMTAX—a program for estimating
1690 class abundances from chemical markers: Application to HPLC measurements of phytoplankton.
1691 *Marine Ecology Progress Series*, *144*, 265–283.

1692 Marie, D., Partensky, F., Vaultot, D., & Brussaard, C. P. D. (1999). Enumeration of phytoplankton, bacteria, and
1693 viruses in marine samples. *Current Protocols in Cytometry*. <https://doi.org/10.1002/0471142956>

1694 Martin, J. H., Fitzwater, S. E., & Gordon, R. M. (1990). Iron deficiency limits phytoplankton growth in
1695 Antarctic waters. *Global Biogeochemical Cycles*, *4*(1), 5–12.

1696 McCain, J. S. P., Tagliabue, A., Susko, E., Achterberg, E. P., Allen, A. E., & Bertrand, E. M. (2021). Cellular
1697 costs underpin micronutrient limitation in phytoplankton. *Science Advances*, *7*(32), eabg6501.
1698 <https://doi.org/10.1126/sciadv.abg6501>

1699 Meredith, M., M. Sommerkorn, S. Cassotta, C. Derksen, A. Ekaykin, A. Hollowed, G. Kofinas, A. Mackintosh,
1700 J. Melbourne-Thomas, M.M.C. Muelbert, G. Ottosen, H. Pritchard, and E.A.G. Schuur. (2019).
1701 *Chapter 3: IPCC Polar regions — Special Report on the Ocean and Cryosphere in a Changing*
1702 *Climate*. https://www.ipcc.ch/srocc/chapter/chapter_3_2/

1703 Meyerink, S. W., Ellwood, M. J., Maher, W. A., Dean Price, G., & Strzepek, R. F. (2017). Effects of iron
1704 limitation on silicon uptake kinetics and elemental stoichiometry in two Southern Ocean diatoms,
1705 *Eucampia antarctica* and *Proboscia inermis*, and the temperate diatom *Thalassiosira pseudonana*.
1706 *Limnology and Oceanography*, 62(6), 2445–2462.

1707 Middag, R., De Baar, H. J., Bruland, K. W., & Van Heuven, S. M. (2020). The distribution of nickel in the
1708 West Atlantic Ocean, its relationship with phosphate and a comparison to cadmium and zinc. *Frontiers*
1709 *in Marine Science*, 7, 105.

1710 Middag, R., Zitoun, R., & Conway, T. (2023). Trace Metals. In J. Blasco & A. Tovar Sánchez (Eds.), *Marine*
1711 *Analytical Chemistry* (pp. 103–198). Springer International Publishing. [https://doi.org/10.1007/978-3-](https://doi.org/10.1007/978-3-031-14486-8_3)
1712 [031-14486-8_3](https://doi.org/10.1007/978-3-031-14486-8_3)

1713 Mills, M. M., Alderkamp, A. C., Thuróczy, C. E., van Dijken, G. L., Laan, P., de Baar, H. J. W., & Arrigo, K.
1714 R. (2012). Phytoplankton biomass and pigment responses to Fe amendments in the Pine Island and
1715 Amundsen polynyas. *Deep Sea Research Part II: Topical Studies in Oceanography*, 71–76(3), 61–76.
1716 <https://doi.org/10.1016/j.dsr2.2012.03.008>

1717 Minas, H. J., & Minas, M. (1992). Net community production in High nutrient low chlorophyll waters of the
1718 tropical and Antarctic oceans: grazing vs iron hypothesis. *Oceanologica Acta*, 15(2), 145–162.

1719 Moore, J. K., Fu, W., Primeau, F., Britten, G. L., Lindsay, K., Long, M., Doney, S. C., Mahowald, N., Hoffman,
1720 F., & Randerson, J. T. (2018). Sustained climate warming drives declining marine biological
1721 productivity. *Science*, 359(6380), 1139–1143. <https://doi.org/10.1126/science.aaa6379>

1722 Morán, X. A. G., Sebastián, M., Pedrís Alió, C., & Estrada, M. (2006). Response of Southern Ocean
1723 phytoplankton and bacterioplankton production to short term experimental warming. *Limnology and*
1724 *Oceanography*, 51(4), 1791–1800. <https://doi.org/10.4319/lo.2006.51.4.1791>

1725 Morrison, A. K., England, M. H., Hogg, A. McC., & Kiss, A. E. (2023). Weddell Sea Control of Ocean
1726 Temperature Variability on the Western Antarctic Peninsula. *Geophysical Research Letters*, 50(15),
1727 e2023GL103018. <https://doi.org/10.1029/2023GL103018>

1728 Noiri, Y., Kudo, I., Kiyosawa, H., Nishioka, J., & Tsuda, A. (2005). Influence of iron and temperature on
1729 growth, nutrient utilization ratios and phytoplankton species composition in the western subarctic
1730 Pacific Ocean during the SEEDS experiment. *Progress in Oceanography*, *64*(2–4), 149–166.
1731 <https://doi.org/10.1016/j.pocean.2005.02.006>

1732 Ohnemus, D. C., Auro, M. E., Sherrell, R. M., Lagerström, M., Morton, P. L., Twining, B. S., Rauschenberg, S.,
1733 & Lam, P. J. (2014). Laboratory intercomparison of marine particulate digestions including Piranha: A
1734 novel chemical method for dissolution of polyethersulfone filters. *Limnology and Oceanography: Methods*,
1735 *12*(8), 530–547.

1736 Olson, R. J., Sosik, H. M., Chekalyuk, A. M., & Shalapyonok, A. (2000). Effects of iron enrichment on
1737 phytoplankton in the Southern Ocean during late summer: Active fluorescence and flow cytometric
1738 analyses. *Deep Sea Research Part II: Topical Studies in Oceanography*, *47*(15–16), 3181–3200.
1739 Scopus. [https://doi.org/10.1016/S0967-0645\(00\)00064-3](https://doi.org/10.1016/S0967-0645(00)00064-3)

1740 Pausch, F., Bischof, K., & Trimborn, S. (2019). Iron and manganese co-limit growth of the Southern Ocean
1741 diatom *Chaetoceros debilis*. *PLOS ONE*, *14*(9), e0221959.
1742 <https://doi.org/10.1371/journal.pone.0221959>

1743 Peers, G., & Prie, N. M. (2004). A role for manganese in superoxide dismutases and growth of iron-deficient
1744 diatoms. *Limnology and Oceanography*, *49*(5), 1774–1783. <https://doi.org/10.4319/lo.2004.49.5.1774>

1745 Planquette, H., & Sherrell, R. M. (2012). Sampling for particulate trace element determination using water
1746 sampling bottles: Methodology and comparison to in situ pumps. *Limnology and Oceanography: Methods*,
1747 *10*(5), 367–388.

1748 Primeau, F. W., Holzer, M., & DeVries, T. (2013). Southern Ocean nutrient trapping and the efficiency of the
1749 biological pump. *Journal of Geophysical Research: Oceans*, *118*(5), 2547–2564.
1750 <https://doi.org/10.1002/jgre.20181>

1751 R-Core Team. (2021). *R: A language and environment for statistical computing*. (4.1.0). R Foundation for
1752 Statistical Computing.

1753 Reay, D. S., Priddle, J., Nedwell, D. B., Whitehouse, M. J., Ellis-Evans, J. C., Deubert, C., & Connelly, D. P.
1754 (2001). Regulation by low temperature of phytoplankton growth and nutrient uptake in the Southern
1755 Ocean. *Marine Ecology Progress Series*, *219*, 51–64.

1756 Rignot, E., Jacobs, S., Mouginot, J., & Scheuchl, B. (2013). Ice Shelf Melting Around Antarctica. *Science*,
1757 *341*(6143), 266–270. <https://doi.org/10.1126/science.1235798>

1758 Rijkenberg, M. J. A., de Baar, H. J. W., Bakker, K., Gerringa, L. J. A., Keijzer, E., Laan, M., Laan, P., Middag,
1759 R., Ober, S., van Ooijen, J., Ossebaar, S., van Weerlee, E. M., & Smit, M. G. (2015). ‘PRISTINE’, a
1760 new high volume sampler for ultraclean sampling of trace metals and isotopes. *Marine Chemistry*,
1761 177(October 2017), 501–509. <https://doi.org/10.1016/j.marchem.2015.07.001>

1762 Rose, J. M., Feng, Y., DiTullio, G. R., Dunbar, R. B., Hare, C. E., Lee, P. A., Lohan, M., Long, M., Smith Jr,
1763 W. O., & Sohst, B. (2009). Synergistic effects of iron and temperature on Antarctic phytoplankton and
1764 microzooplankton assemblages. *Biogeosciences*, 6(12), 3131–3147.

1765 Ryan-Keogh, T. J., Thomalla, S. J., Monteiro, P. M., & Tagliabue, A. (2023). Multidecadal trend of increasing
1766 iron stress in Southern Ocean phytoplankton. *Science*, 379(6634), 834–840.

1767 Ryderheim, F., Grønning, J., & Kjørboe, T. (2022). Thicker shells reduce copepod grazing on diatoms.
1768 *Limnology and Oceanography Letters*, 7(5), 435–442.

1769 Sarmiento, J. L., Gruber, N., Brzezinski, M. A., & Dunne, J. P. (2004). High latitude controls of thermocline
1770 nutrients and low latitude biological productivity. *Nature*, 427(6969), Article 6969.
1771 <https://doi.org/10.1038/nature02127>

1772 Scharek, R., Van Leeuwe, M. A., & De Baar, H. J. W. (1997). Responses of Southern Ocean phytoplankton to
1773 the addition of trace metals. *Deep-Sea Research Part II: Topical Studies in Oceanography*, 44(1–2),
1774 209–227. [https://doi.org/10.1016/S0967-0645\(96\)00074-4](https://doi.org/10.1016/S0967-0645(96)00074-4)

1775 Schoffman, H., Lis, H., Shaked, Y., & Keren, N. (2016). Iron–Nutrient Interactions within Phytoplankton.
1776 *Frontiers in Plant Science*, 7. <https://www.frontiersin.org/articles/10.3389/fpls.2016.01223>

1777 Selz, V., Lowry, K. E., Lewis, K. M., Joy-Warren, H. L., van de Poll, W., Nirmel, S., Tong, A., & Arrigo, K. R.
1778 (2018). Distribution of *Phaeocystis antarctica* dominated sea ice algal communities and their potential
1779 to seed phytoplankton across the western Antarctic Peninsula in spring. *Marine Ecology Progress
1780 Series*, 586, 91–112.

1781 Seyitmuhammedov, K., Stirling, C. H., Reid, M. R., van Hale, R., Laan, P., Arrigo, K. R., van Dijken, G.,
1782 Alderkamp, A. C., & Middag, R. (2022). The distribution of Fe across the shelf of the Western
1783 Antarctic Peninsula at the start of the phytoplankton growing season. *Marine Chemistry*, 238, 104066.

1784 Sherrell, R. M., Lagerström, M. E., Forsch, K. O., Stammerjohn, S. E., & Yager, P. L. (2015). Dynamics of
1785 dissolved iron and other bioactive trace metals (Mn, Ni, Cu, Zn) in the Amundsen Sea Polynya,
1786 Antarctica. *Elementa: Science of the Anthropocene*, 3, 000071.
1787 <https://doi.org/10.12952/journal.elementa.000071>

1788 Shi, J. R., Talley, L. D., Xie, S. P., Liu, W., & Gille, S. T. (2020). Effects of buoyancy and wind forcing on
1789 Southern Ocean climate change. *Journal of Climate*, *33*(23), 10003–10020.

1790 Slagter, H. A., Gerringa, L. J. A., & Brussaard, C. P. D. (2016). Phytoplankton Virus Production Negatively
1791 Affected by Iron Limitation. *Frontiers in Marine Science*, *3*.
1792 <https://www.frontiersin.org/articles/10.3389/fmars.2016.00156>

1793 Stapleford, L. S., & Smith, R. E. (1996). The interactive effects of temperature and silicon limitation on the
1794 psychrophilic ice diatom *Pseudonitzschia seriata*. *Polar Biology*, *16*, 589–594.

1795 Tagliabue, A., Aumont, O., DeAth, R., Dunne, J. P., Dutkiewicz, S., Galbraith, E., Misumi, K., Moore, J. K.,
1796 Ridgwell, A., Sherman, E., Stock, C., Vichi, M., Völker, C., & Yool, A. (2016). How well do global
1797 ocean biogeochemistry models simulate dissolved iron distributions? *Global Biogeochemical Cycles*,
1798 *30*(2), 149–174. <https://doi.org/10.1002/2015GB005289>

1799 Tagliabue, A., Sallée, J. B., Bowie, A. R., Lévy, M., Swart, S., & Boyd, P. W. (2014). Surface water iron
1800 supplies in the Southern Ocean sustained by deep winter mixing. *Nature Geoscience*, *7*(4), 314–320.

1801 Takahashi, T., Sweeney, C., Hales, B., Chipman, D. W., Newberger, T., Goddard, J. G., Iannuzzi, R. A., &
1802 Sutherland, S. C. (2012). The changing carbon cycle in the Southern Ocean. *Oceanography*, *25*(3), 26–
1803 37.

1804 Teske, V., Timmermann, R., & Semmler, T. (2024). Subsurface warming in the Antarctica's Weddell Sea can
1805 be avoided by reaching the 2°C warming target. *Communications Earth & Environment*, *5*(1), 93.

1806 Thomalla, S. J., Nicholson, S. A., Ryan-Keogh, T. J., & Smith, M. E. (2023). Widespread changes in Southern
1807 Ocean phytoplankton blooms linked to climate drivers. *Nature Climate Change*, *13*(9), 975–984.

1808 Twining, B. S., Baines, S. B., & Fisher, N. S. (2004). Element stoichiometries of individual plankton cells
1809 collected during the Southern Ocean Iron Experiment (SOFEX). *Limnology and Oceanography*, *49*(6),
1810 2115–2128. <https://doi.org/10.4319/lo.2004.49.6.2115>

1811 Van der Merwe, P., Wuttig, K., Holmes, T., Trull, T. W., Chase, Z., Townsend, A. T., Goemann, K., & Bowie,
1812 A. R. (2019). High lability Fe particles sourced from glacial erosion can meet previously unaccounted
1813 biological demand: Heard Island, Southern Ocean. *Frontiers in Marine Science*, *6*, 332.

1814 Van Heukelem, L., & Thomas, C. S. (2001). Computer assisted high performance liquid chromatography
1815 method development with applications to the isolation and analysis of phytoplankton pigments. *Journal*
1816 *of Chromatography A*, *910*(1), 31–49. [https://doi.org/10.1016/S0378-4347\(00\)00603-4](https://doi.org/10.1016/S0378-4347(00)00603-4)

1817 Van Manen, M., Aoki, S., Brussaard, C. P., Conway, T. M., Eich, C., Gerringa, L. J., Jung, J., Kim, T. W., Lee,
1818 S., & Lee, Y. (2022). The role of the Dotson Ice Shelf and Circumpolar Deep Water as driver and
1819 source of dissolved and particulate iron and manganese in the Amundsen Sea polynya, Southern
1820 Ocean. *Marine Chemistry*, 246, 104161.

1821 Veldhuis, M. J., & Kraay, G. W. (2004). Phytoplankton in the subtropical Atlantic Ocean: Towards a better
1822 assessment of biomass and composition. *Deep Sea Research Part I: Oceanographic Research Papers*,
1823 51(4), 507–530.

1824 Venables, H., & Moore, C. M. (2010). Phytoplankton and light limitation in the Southern Ocean: Learning from
1825 high nutrient, high-chlorophyll areas. *Journal of Geophysical Research: Oceans*, 115(C2).

1826 Verardo, D. J., Froelich, P. N., & McIntyre, A. (1990). Determination of organic carbon and nitrogen in marine
1827 sediments using the Carlo Erba NA-1500 Analyzer. *Deep Sea Research Part A: Oceanographic
1828 Research Papers*, 37(1), 157–165.

1829 Viljoen, J. J., Philibert, R., Van Horsten, N., Mtshali, T., Roychoudhury, A. N., Thomalla, S., & Fietz, S.
1830 (2018). Phytoplankton response in growth, photophysiology and community structure to iron and light
1831 in the Polar Frontal Zone and Antarctic waters. *Deep Sea Research Part I: Oceanographic Research
1832 Papers*, 141, 118–129. Scopus. <https://doi.org/10.1016/j.dsr.2018.09.006>

1833 Waite, A. M., & Nodder, S. D. (2001). The effect of in situ iron addition on the sinking rates and export flux of
1834 Southern Ocean diatoms. *Deep Sea Research Part II: Topical Studies in Oceanography*, 48(11–12),
1835 2635–2654.

1836 Wang, X. J., Behrenfeld, M., Le Borgne, R., Murtugudde, R., & Boss, E. (2009). Regulation of phytoplankton
1837 carbon to chlorophyll ratio by light, nutrients and temperature in the Equatorial Pacific Ocean: A basin-
1838 scale model. *Biogeosciences*, 6(3), 391–404.

1839 Worden, A. Z., Nolan, J. K., & Palenik, B. (2004). Assessing the dynamics and ecology of marine
1840 picophytoplankton: The importance of the eukaryotic component. *Limnology and Oceanography*,
1841 49(1), 168–179. <https://doi.org/10.4319/lo.2004.49.1.0168>

1842 Wu, M., McCain, J. S. P., Rowland, E., Middag, R., Sandgren, M., Allen, A. E., & Bertrand, E. M. (2019a).
1843 Manganese and iron deficiency in Southern Ocean *Phaeocystis antarctica* populations revealed through
1844 taxon-specific protein indicators. *Nature Communications*, 10(1), 3582.
1845 <https://doi.org/10.1038/s41467-019-11426-z>

1846 ~~Yoon, J. E., Yoo, K. C., Macdonald, A. M., Yoon, H. I., Park, K. T., Yang, E. J., Kim, H. C., Lee, J. I., Lee, M.~~
1847 ~~K., Jung, J., Park, J., Lee, J., Kim, S., Kim, S.-S., Kim, K., & Kim, I.-N. (2018). Reviews and~~
1848 ~~syntheses: Ocean iron fertilization experiments—past, present, and future looking to a future Korean~~
1849 ~~Iron Fertilization Experiment in the Southern Ocean (KIFES) project. *Biogeosciences*, 15(19), 5847–~~
1850 ~~5889. <https://doi.org/10.5194/bg-15-5847-2018>~~
1851 ~~Zhu, Z., Xu, K., Fu, F., Spackeen, J. L., Bronk, D. A., & Hutchins, D. A. (2016). A comparative study of iron~~
1852 ~~and temperature interactive effects on diatoms and *Phaeocystis antarctica* from the Ross Sea,~~
1853 ~~Antarctica. *Marine Ecology Progress Series*, 550, 39–51.~~
1854